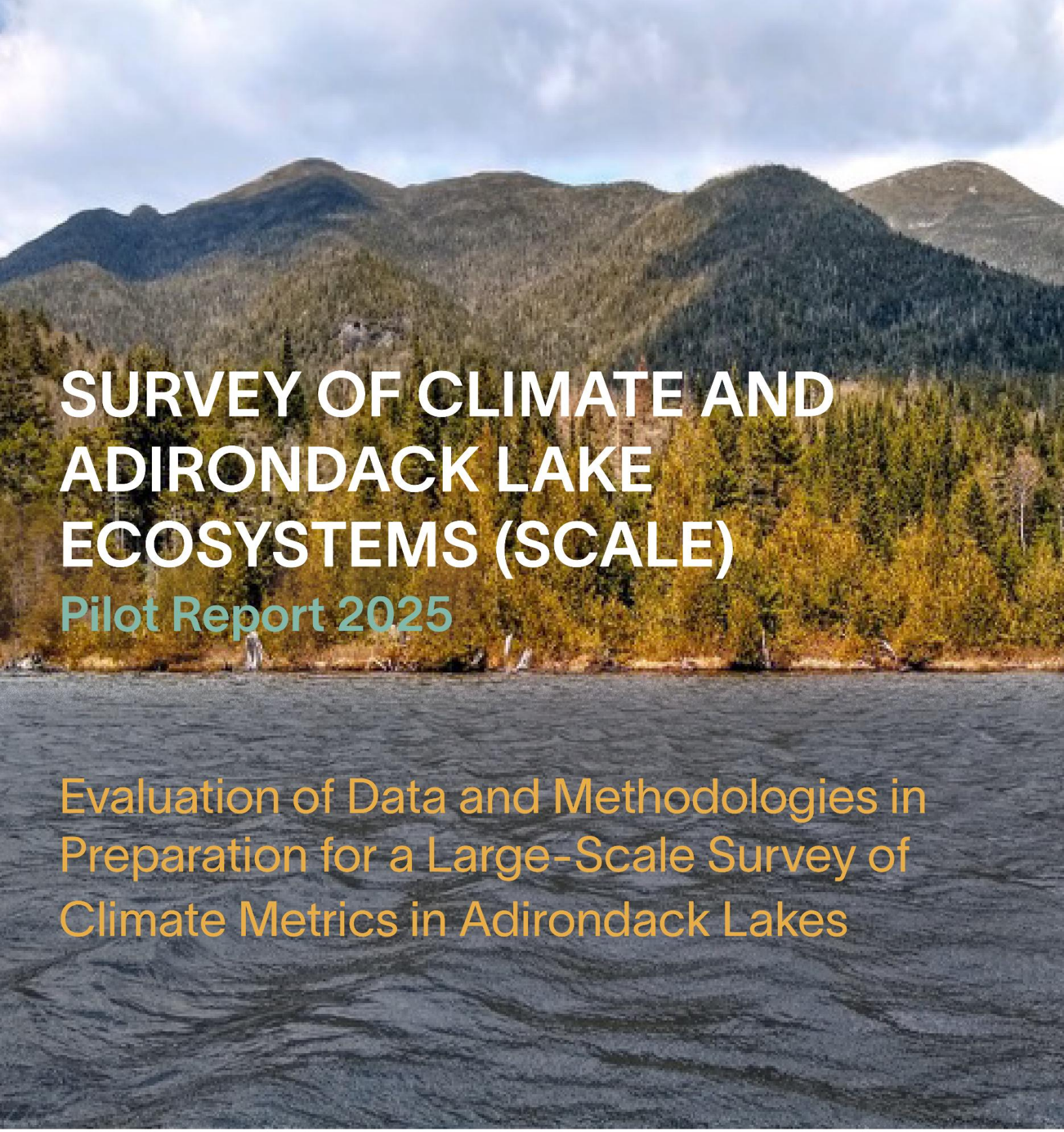

SURVEY OF CLIMATE AND ADIRONDACK LAKE ECOSYSTEMS (SCALE)

Pilot Report 2025

Evaluation of Data and Methodologies in Preparation for a Large-Scale Survey of Climate Metrics in Adirondack Lakes

NEW YORK STATE | Department of Environmental Conservation

AUSABLE Freshwater Center

Rensselaer

Syracuse University

CUNY | NEW YORK CITY COLLEGE OF TECHNOLOGY CITY TECH

Cornell CALS College of Agriculture and Life Sciences

Acknowledgements

Funding for this work was provided largely through the New York State Aid to Localities. We would like to acknowledge the New York State Department of Environmental Conservation for their administration of these funds and support of this project. Carbon characterization was supported by the New York State Energy Research and Development Authority (NYSERDA) under Award No. 216244 and Ausable Freshwater Center under Award No. 2023-DEC/SCALE #1:4. Dr. Teng Zeng is also supported by the National Science Foundation under Grant No. 2145214. Funding for the Environmental DNA and Isotope studies were subsidized by personnel support from Cornell University's Adirondack Fishery Research Program and USGS Northeast Climate Adaptation Science Center. We gratefully acknowledge the contributions of the staff of the Cornell Stable Isotope Lab and the Cornell Environmental DNA & Genomics Core Facility.

We would like to acknowledge NYSERDA for their support and funding of the 2021 workshop which helped to lay the groundwork for this project, as well as the Adirondack Council for their support and advocacy.

We would also like to acknowledge the state of New York State and the NYSDEC for the preservation and conservation of the public lands and lakes of the Adirondack Park, many of which were included in this study.

Finally, we would like to thank the Adirondack Mountain Club, Great Camp Sagamore, and YMCA Gorham for generously providing access to their respective lakes.

Authors and Affiliations

Authors are listed in alphabetical order

Primary Authors

Montana Airey, Cornell University

Jose Andres, Cornell University

Marzieh Azarderakhsh, New York City College of Technology, City University of New York (CUNY)

Jonathan J. Borrelli, Rensselaer Polytechnic Institute

Charles T. Driscoll, Syracuse University

Isabella Errigo, Cornell University

Nicolas Locatelli, Cornell University

Peter B. McIntyre, Cornell University

Hamid Norouzi, New York City College of Technology, City University of New York (CUNY)

Kevin C Rose, Rensselaer Polytechnic Institute

Teng Zeng, Syracuse University

Contributing Authors

Krista L. Kennedy, Ausable Freshwater Center

Philip K. Snyder, Ausable Freshwater Center

Kelley Tucker, Ausable Freshwater Center

Table of Contents

Table of Figures and Tables

SCALE Pilot Project Overview

Waterbodies in New York State are affected by climate change, including increasing air temperatures, shorter winters, less ice cover, warmer and longer summers, more heatwaves, more precipitation, and more severe storms. Lakes in the Adirondacks serve as particularly sensitive sentinel indicators of climate change impacts on freshwater quality due to the quality of historical monitoring programs, large geographic diversity across the Park, and relatively limited impacts from other stressors, such as human land use. As lakes lie in the lowest point in the landscape, they integrate changes that occur around them and accumulate records of change over centuries time scales in their sediments, enabling the ability to measure and understand climate change impacts.

Measuring the impacts of climate change on Adirondack lakes is critical to understanding and forecasting future changes in freshwater quality. However, existing monitoring programs are ill-equipped to quantify and track future climate change impacts. A new survey of current ecological conditions is needed that leverages modern tools and technologies applied to a statistically robust distribution of Adirondack waterbodies.

Efficiently and effectively conducting a Survey of Climate and Adirondack Lake Ecosystems (SCALE) requires several antecedent steps. First, sampling a broad representative suite of lakes and avoiding biased sampling requires understanding the distribution of lakes across the Adirondacks. In turn, this necessitates creating a comprehensive compilation of historical data sets and complementing this compilation with remote sensing and hydrodynamic modeling to understand lake dynamics in areas with limited or no historical sampling. Second, there are several tools and technologies that provide tremendous capability to collect large amounts of data with single samples. However, these tools and technologies need some method development to ensure quality data are produced applicable to biota and water chemistry in the region.

Through this SCALE Pilot effort, researchers and field crews from the Ausable Freshwater Center, City University of New York, Cornell University, Rensselaer Polytechnic Institute, and Syracuse University collaborated to (1) conduct hydrodynamic modeling, remote sensing, and data mining to identify and select lakes for SCALE field operations, and (2) develop and refine methods, including field sampling plans, for carbon characterization, eDNA, and stable isotope analyses to ensure quality data are collected. This SCALE Pilot report summarizes each of these component efforts. In sum, these efforts have formed the foundation for a successful SCALE field program that is slated to begin in summer, 2025.

Hydrodynamic Modeling

Overview and motivation

We completed hydrodynamic modeling of hundreds of Adirondack lakes to assess trends in modeled lake thermal attributes, including lake summer surface water temperature, summer bottom water temperature, and stratification onset, duration, strength, and breakdown. This also includes assessment of how these thermal attributes vary with factors such as lake surface area, depth, and clarity. We completed this work because these physical characteristics regulate many important ecosystem properties in lakes, such as phytoplankton growth, dissolved oxygen availability, carbon cycling attributes, and phosphorus release from sediments that are SCALE priority topics. However, long-term data on temperatures at multiple depths in Adirondack lakes are limited. Without such data it is difficult to assess how the changing climate has, and will, impact lake warming and the resulting ecological effects. Through this effort, we used hydrodynamic modeling to complement and extend long-term data sets to understand how lake temperatures have likely changed in unmonitored lakes over time, how lakes are likely to respond to future climate change scenarios, and what lakes are most sensitive to warming. Understanding the hydrodynamic attributes and trends through time helps identify lakes for the survey selection process by ensuring that we sample a lake population that contains a wide range of temperature, mixing depths, and mixing durations.

Model description

We used Simstrat (Gaudard et al. 2019), a common, well-validated, open-source, process-based hydrodynamic model, to simulate daily lake temperature profiles over a 42-year period (1980-2022). Initially, we applied the Simstrat model using default parameterization options available through the LakeEnsemblR R package (Moore et al. 2021). For each lake that we simulated (n = 443, **Figure 1**) we used lake-specific data for latitude and longitude, surface area, maximum and mean depth. Modelled lakes ranged from 5.2 to 46.6 m maximum depth (1.1 – 15.4 m mean depth). The surface area of the lakes ranged from 4 to 831 ha, and were at elevations between 137 and 877 m.

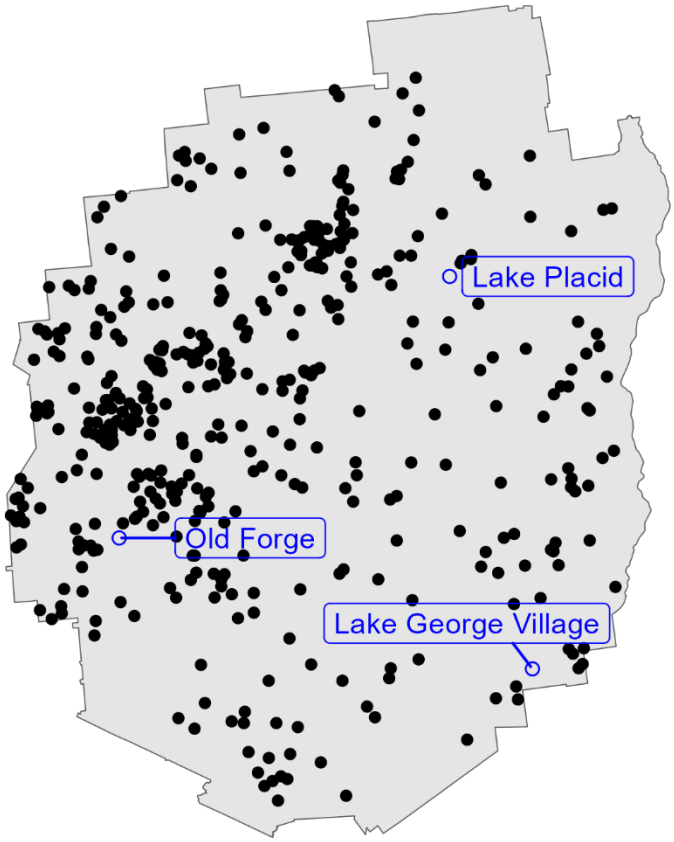

Figure 1: Map of the Adirondack State Park (blueline) with points for the locations for 443 modelled lakes. Three towns are identified as points of reference in labelled blue open circles.

We further incorporated a time-varying light attenuation parameter based on either observed Secchi depth, or a combination of Secchi depth and remote-sensing based water clarity trend. For lakes in the Adirondack Effects Assessment Program (AEAP; n=23), water clarity (Secchi depth) was available approximately annually over a period of ~20 years from the *adklakedata* R package (Leach et al. 2018). The AEAP sampled 28 lakes approximately twice a summer from 1994 through 2012 for water chemistry and plankton communities. For other lakes, we combined Secchi depth observed in the 1980s and applied a linear change based on the trend estimated by remote sensing. We next converted Secchi depths to diffuse attenuation coefficients (K_d) using the equation K_d = 1.7/Secchi depth. Secchi depth, as well as surface area and max/mean depth were obtained from the Adirondack Lake Survey Corporation records (Kretzer et al https://doi.org/10.6084/m9.figshare.22312732.v1). We also approximated the bathymetry using the *rLakeAnalyzer* package with the Voldev method parameterized with maximum depth, mean depth, and surface area (Winslow et al. 2019). Each lake model was driven by hourly meteorology data obtained from ERA5 reanalysis (Hersbach et al. 2020). ERA5

weather data are available at a 0.25° x 0.25° grid, and we used the grid cell whose centroid was closest to each modelled lake.

From each lake model's output, we used the temperature profile to compute mean epilimnetic temperature, mean hypolimnetic temperature, thermocline depth (as the center of buoyancy), and the strength of stratification (as Schmidt stability). Each of these values were calculated using functions from the rLakeAnalyzer R package.

Model performance

Using temperature profile data from AEAP lakes we validated the method of using primarily default parameters by comparing observed temperatures against modelled temperatures. We did this by calculating the root mean square error (RMSE). We were able to simulate temperature profiles for 23 of the 28 AEAP lakes, because we restricted modelling to lakes that were at least 5 m deep. Ten of the 23 lakes had a RMSE ≤ 2.5 °C which represents a reasonable fit to observed data. For comparison, a larger study of 1137 lakes using similar methods for the General Lake Model (GLM) resulted in an RMSE of 2.7 across all depths (224,812 measurements). Overall RMSE in our simulations ranged from 1.5 to 8.8 for each lake, with a larger range in error values in shallower lakes (**Figure 2**). This shows that the model performs well in larger, deeper lakes, but there is greater uncertainty in modeling temperature in shallow lakes.

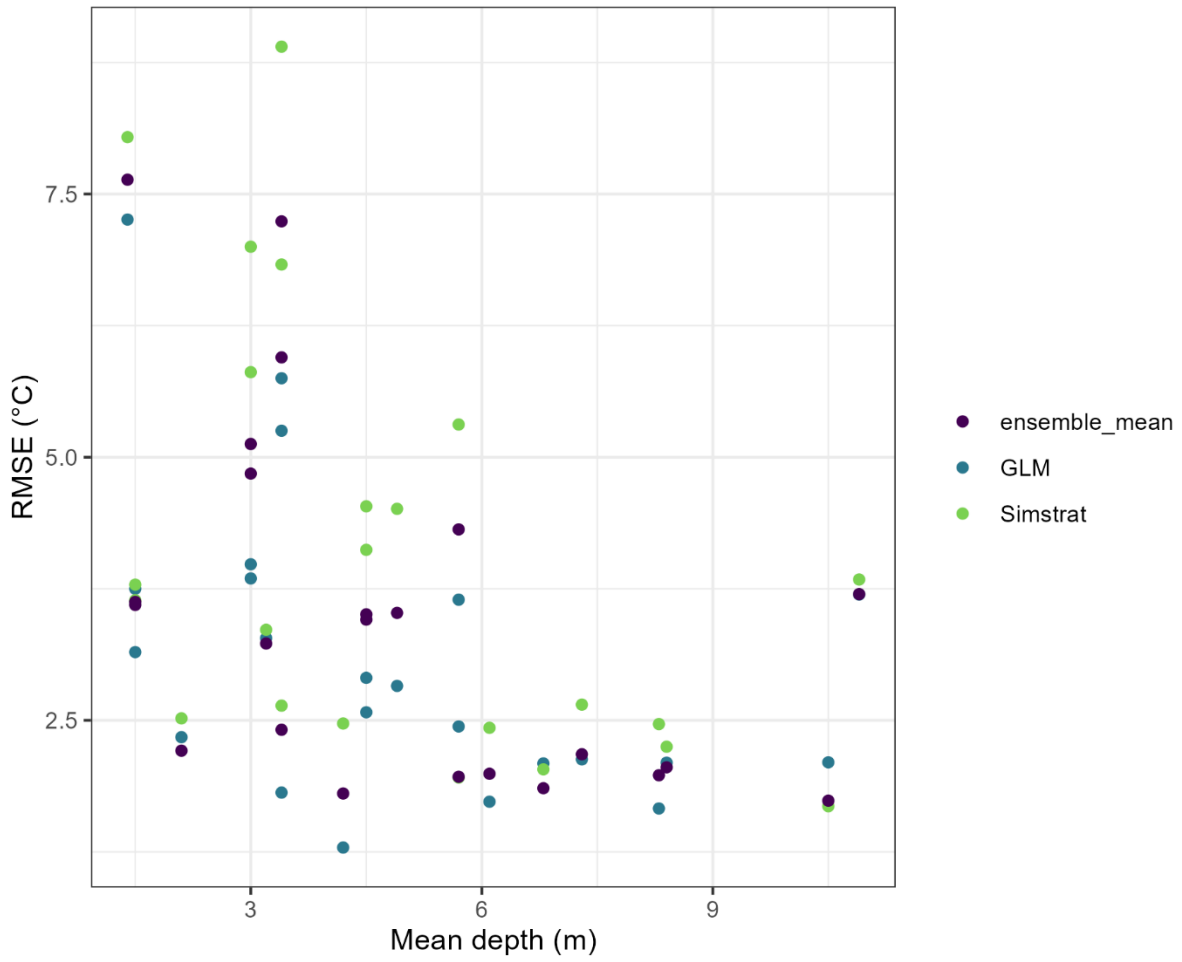

Figure 2: Error in modelled temperature for AEAP lakes by mean depth using default parameterization of the General Lake Model (GLM), Simstrat, and the mean prediction of both models (ensemble_mean).

Modeling Results

Our model results show that summer surface water temperatures are significantly increasing throughout the park (**Figure 3**). A mixed effects model with a fixed effect of year and random effect of lake showed that on average summer epilimnetic temperatures increased by 0.04 °C per year. In many deeper lakes, particularly those greater than eight meters, hypolimnetic water is getting colder (**Figure 4**). Changing water clarity also had an apparent effect on epilimnetic temperature and thermocline depth measured as center of buoyancy (**Figure 5**). Reduced water clarity resulted in warmer surface water, and shallower thermoclines. We did not find an impact of water clarity trend on Schmidt stability.

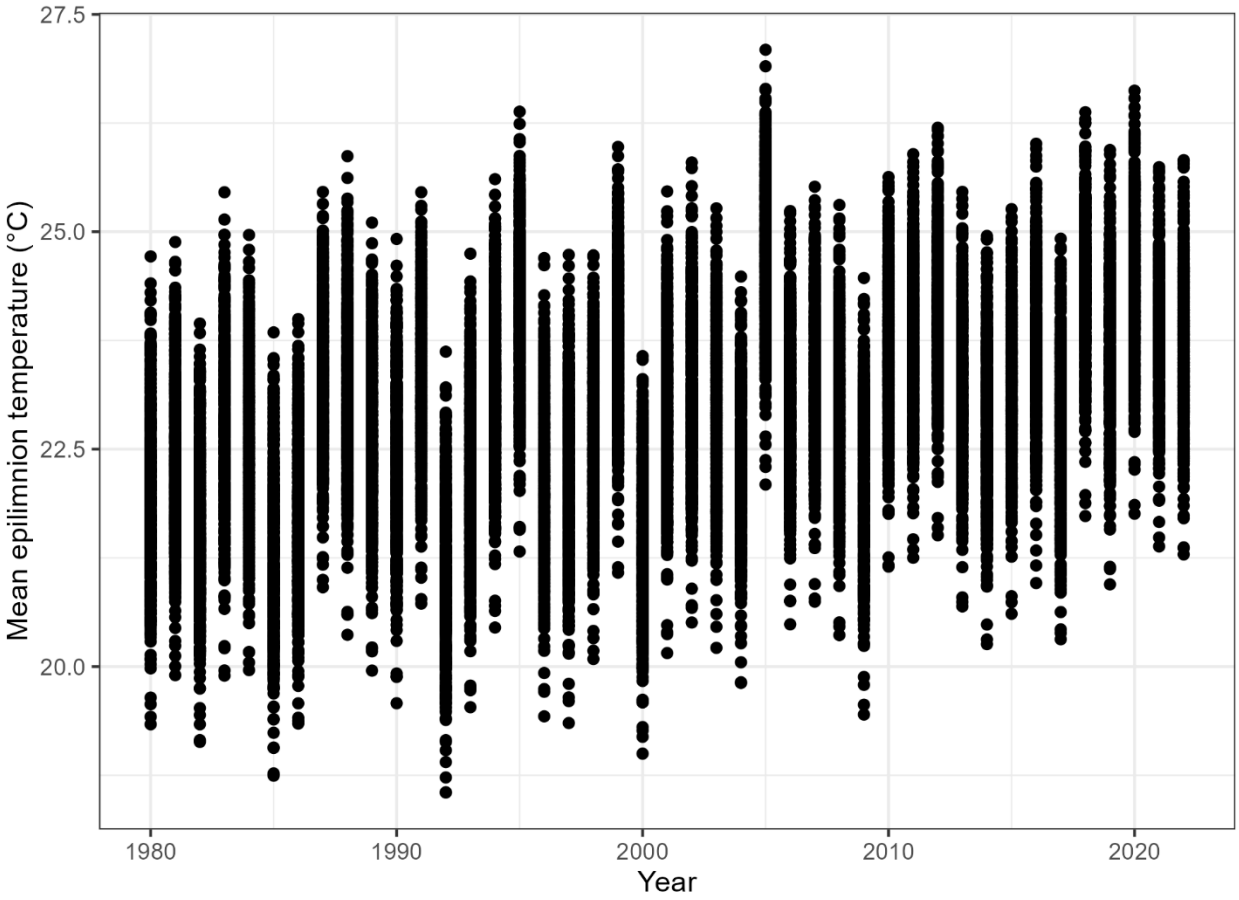

Figure 3: Mean summer epilimnetic water temperature across 443 Adirondack lakes.

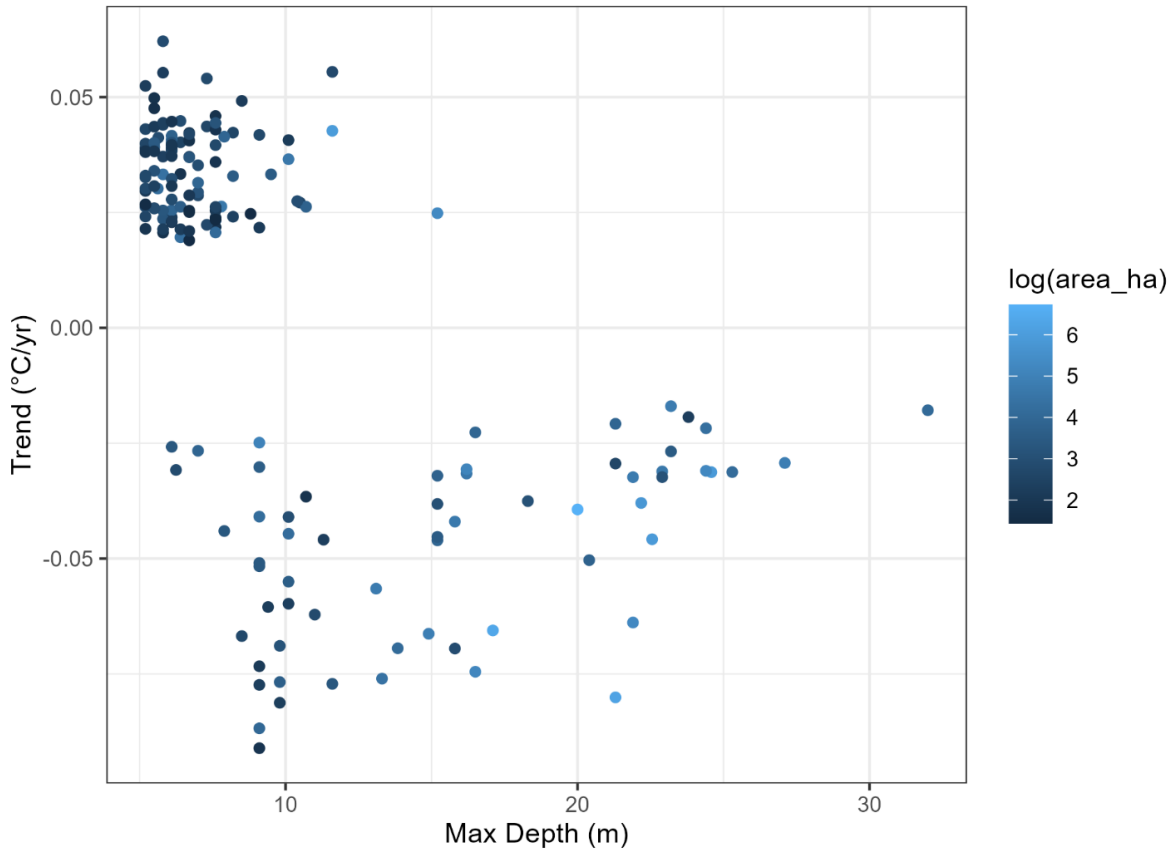

Figure 4: Significant trends in summer hypolimnetic water temperature by lake maximum depth and surface area.

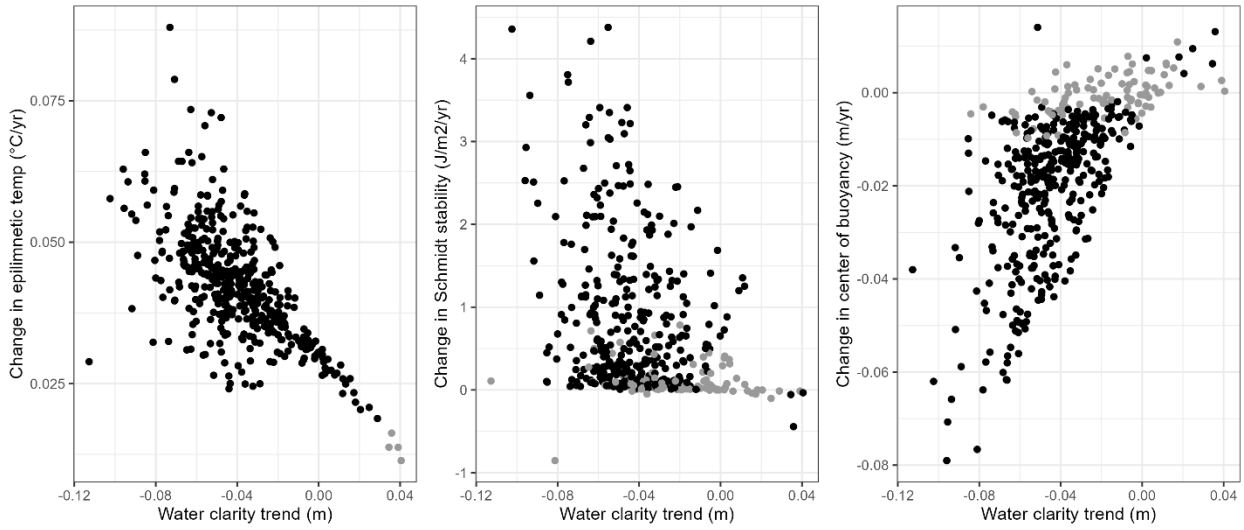

Figure 5: Relationship between the trend in water clarity and modeled change in epilimnetic temperature, Schmidt stability, and center of buoyancy. Black points represent significant trends in epilimnetic temperature, Schmidt stability, or center of buoyancy, while grey points indicate no significant trend.

Next steps

Lake temperature modeling will provide context to the survey results we find and complement the manually collected data from the survey to better understand the factors shaping the physical, chemical, and biological attributes of Adirondack Lakes. We anticipate updating the models when new calibration and validation data are obtained (i.e. following the first year of high intensity sampling) to improve modeling accuracy and extend survey results to other unsampled lakes across the Adirondacks. We plan to write up the results of our modeling and submit them to a peer-review journal.

Data availability

All data used in hydrodynamic modeling is from publicly available sources. Code and data used to generate the hydrodynamic modeling simulations are available on GitHub at: https://github.com/ADK-SCALE/lake_hydrodynamics.

Remote Sensing

Overview and motivation

We used satellite remote sensing data to analyze and understand changes that have occurred in Adirondack lakes over the past four decades, particularly for lakes where monitoring data does not exist. The remote sensing data comprises spectral responses from the Earth's surface and the atmosphere, captured across various spectral bands that differ in radiometric, spatial, temporal, and spectral resolutions. The primary use of these datasets has been to predict lake surface temperature and lake chlorophyll concentrations. Lake surface temperature is a primary regulator of many ecological attributes, and chlorophyll concentrations are an often managed-for water quality criterion. High chlorophyll can also be related to the presence of harmful algal blooms. Understanding seasonal, spatial, and long-term patterns in lake temperature and chlorophyll across the park informs SCALE lake selection for field work and helps generalize findings from field work to the broader region, and ultimately across all of New York State.

Lake temperature overview

The main purpose of conducting remote sensing research on Adirondack lakes temperature is to assess warming rates in small lakes, many of which are undergoing browning. Lake browning refers to the process where lakes and other freshwater bodies become progressively darker in color over time. This phenomenon is mainly due to an increase in dissolved organic matter (DOM), especially dissolved organic carbon (DOC), often originating

from soils, wetlands, and decaying vegetation in surrounding catchments. Browning affects lake heat budgets and complicates the prediction of warming rates based on air temperature trends. The second purpose of this work was to evaluate seasonal heterogeneity in lake warming rates, which is poorly understood but has major biological and ecological implications.

Here, we investigate the capabilities and applications of multiple satellite platforms in understanding surface water temperature changes across 135 small lakes in the Adirondacks. By integrating these satellite observations with existing field data, we examined surface water temperature variability during ice-free seasons since 1984. Satellite-derived water surface temperature estimates were evaluated and validated by comparing them with near-surface water temperature measurements at selected lakes across the Adirondack Park. In addition, we assessed monthly temperature changes to identify trends and seasonal variations.

Data from the Landsat series of satellites, managed by the United States Geological Survey (USGS), and MODIS (Moderate Resolution Imaging Spectroradiometer) observations from NASA represent a comprehensive temporal record with extensive spatial coverage, vital for studying all lakes within the Adirondack region. Sentinel-2 data, provided by the European Space Agency (ESA), complements this with its high spatial resolution imagery. Landsat and Sentinel satellites offer a revisit time of 12 to 16 days, with spatial resolutions of 30 meters and 20 meters, respectively. MODIS provides coarser resolution imagery (1 kilometer) but has the advantage of daily observation frequency, allowing for more frequent monitoring. Analysis of these satellite data is critical to understand wide-spread environmental changes occurring across Adirondack lakes.

Lake temperature algorithm development overview

We employed multi-platform imagery with different spatiotemporal coverage to analyze land and lake surface parameters. We performed the analyses at the individual lake level as well as across the entire Adirondack Park region (including both lake and water areas). Although more advanced satellites are in orbit, the Landsat series and the MODIS satellite have the advantage of a multi-decadal record which partly coincides with the time-period of the field data.

MODIS onboard AQUA satellite provides regional scale, high temporal observations from 2002-present at 1 km spatial resolution (Wan, Hook and Hulley 2015). AQUA, deployed in May of 2002, overpasses a single tile of the MODIS sinusoidal tile grid at the equator twice daily at 1:30 AM and PM solar time. We extracted cloud-free MODIS daytime surface temperature within the boundary of the Adirondack Park. While nighttime temperatures were determined to be more reliable for climate studies (Zhang et al. 2018), we used daytime temperatures to better correspond with Landsat observations and field measurements. This choice may introduce higher uncertainty in trend detection compared to nighttime LST, which is generally considered

more reliable for climate studies, but ensures stronger consistency across datasets and facilitates direct validation of surface temperature observations. Cloud-free values from the MYD11A1 daily product (Wan, Hook and Hulley 2015) were used to eliminate anomalous results likely caused by clouds or atmospheric disturbances.

For each lake we extracted Landsat 5 (1984-2011) and Landsat 7 (1999-2024) data, taking only images with less than 15% of clouds, and then passing them through an additional cloud filter to remove all cloudy or shadowed pixels from the lake area. We used the USGS Collection 2, Level 2 Tier 1 Land Surface temperature product, as it is consistent over the Landsat series. We extracted satellite temperature estimates via the Google Earth Engine Python API, which maintains an extensive archive of Landsat data spanning over four decades. Our analysis leveraged Landsat surface temperature data derived from 30 m resolution products, targeting the deepest part of each lake with a 3x3 pixel area; a standard method in such studies (Ritchie, Cooper and Yongqing 1987; Dyba, et al. 2022). This technique helps reduce resampling errors and uncertainties, especially in areas with complex terrain. All nine temperature readings after excluding ice, cloudy, and shadow pixels from both Landsat 5 and 7 were averaged along with their timestamp information for each lake. We used the mean of the nine pixels for each lake, after testing confirmed negligible differences between mean and median values.

Lake temperature field data

We identified 135 lakes (**Figure 6**) to use for validation and calibration of satellite temperatures based on the availability of data collected through the Citizens Statewide Lake Assessment Program (CSLAP) (https://dec.ny.gov/environmental-protection/water/water-quality/sampling-activities) and the Adirondack Effects Assessment Program (AEAP). 113 lakes were selected from the CSLAP program for the study, the surface areas range from 0.1 to 115.6 km². In addition, 22 lakes from the AEAP over the period 1994-2012 were used. The surface areas for these lakes ranged from 0.06 to 0.9 km.

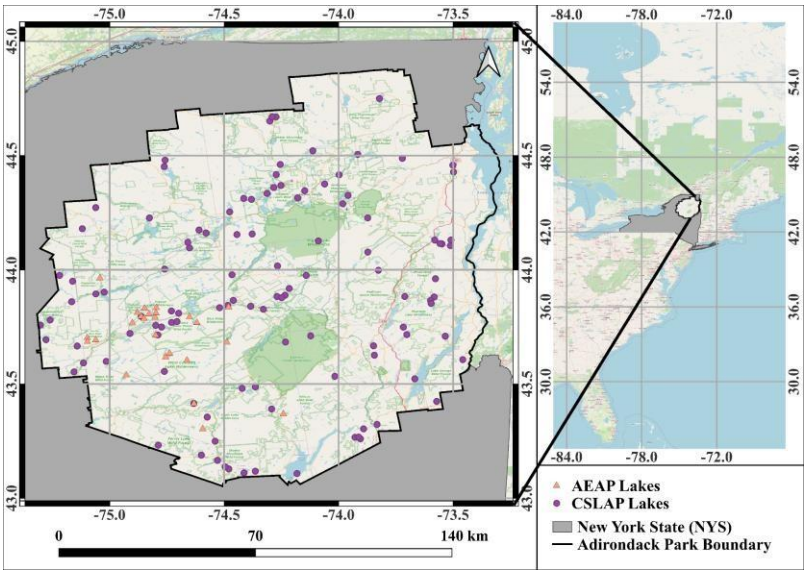

Figure 6. Map showing the boundary of Adirondack Park with the locations of AEAP and CSLAP lakes included in this study.

Satellite lake temperature estimate validation

One of the primary goals of this study is to validate satellite-derived water temperature data against in situ measurements of near-surface water temperature to ensure their accuracy for long-term monitoring of temperature trends. We conducted separate analyses for each satellite to evaluate the consistency of their performance over time. The time series from satellite data were compared to corresponding *in situ* observations to assess their reliability for climate studies in aquatic ecosystems. Due to the limited number of same-day measurements between Landsat 5 or 7 flyover dates and the existing field data, we allowed for a three-day window on either side of the field data date to find satellite matches. When calculating slopes for validation, only satellite images matching the specific dates were used, not all images within the month.

We compared satellite temperatures to field measurements in two ways: by comparing satellites to each other (harmonized) and by comparing satellite data with field data. First, we compared Landsat 5 and 7 to evaluate the continuity of the Landsat Temperature product.

There was reasonable agreement between measurements of the same lakes by both satellites, generally taken within a day or two of each other (**Figure 7**). To avoid the ice season, we only assessed data from March to November, though some measurements from both satellites still recorded temperatures below freezing. Measurements were strongly correlated (r = 0.95) with a bias of 0.52°C, indicating strong agreement with some discrepancies likely due to differences in observation dates.

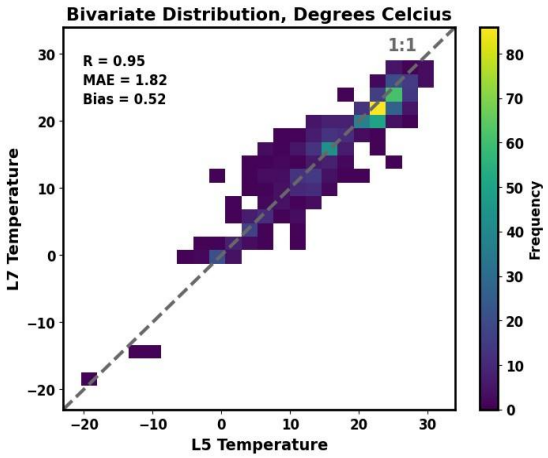

Figure 7. The Bivariate distribution of L5 and L7 lake scenes temperature estimates within 3 days of each other.

We also compared the field measurements of water temperature at depths close to the surface from CSLAP and AEAP with satellite-derived water surface temperatures from Landsat 5 and 7. Both Landsat 5 and 7 generally showed good agreement with the field measurements despite uncertainties related to location, date, and depth variations (**Figure 8**). Landsat 5 had a slightly better correlation (r = 0.77) with field measurements compared to Landsat 7 (r = 0.71). The RMSEs for Landsat 5 was 1.9°C and 1.7°C for Landsat 7 when compared to field measurements. We also observed a higher correlation (r = 0.9) between field and satellite temperature estimates when focusing on the 80 Lake Classification Inventory lakes (LCI, NYS DEC's professional lake monitoring program, https://dec.ny.gov/environmental-protection/water/water-quality/monitoring), with a better RMSE value of 1.1°C. This improved correlation may be due to the different methods of field data collection between the citizen scientist and professional monitoring lake programs. ~~Our findings suggest that rigorous field methods can enhance the accuracy and reliability of satellite-derived temperature estimates~~. The accuracy and reliability of satellite estimates can be enhanced by using advanced monitoring protocols such as in-situ probe data collection, which have more refined reporting than field thermometers.

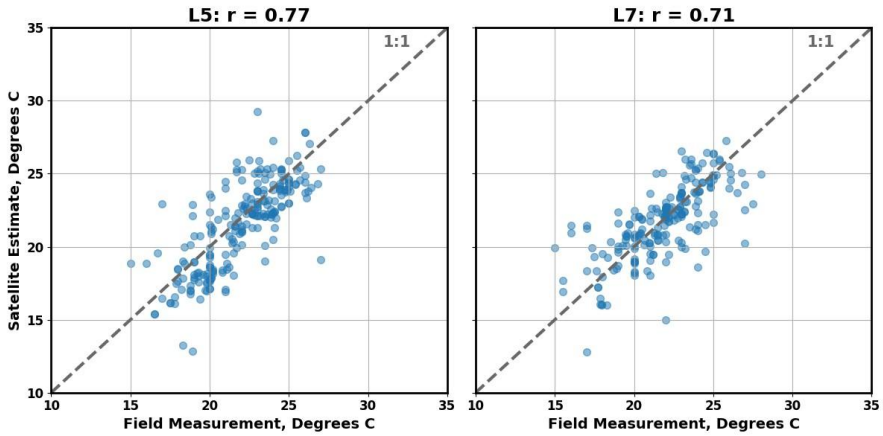

Figure 8. Scatter plot of lake water temperature from CSLAP and AEAP field measurements at depths close to the surface versus satellite-based water surface temperature from Landsat 5 (left) and Landsat 7 (right).

Field measurements were point surface temperature measurements while corresponding satellite temperatures were spatial averages over a 3x3 pixel area (8100 square meters). Additionally, differences between exact surface temperatures (sensed by satellites) and field measurements at depths up to 1 meter may contribute to uncertainties. CSLAP lake measurements often come from the deepest point, while AEAP samples are taken near lake outlets. We estimated lake temperatures from the 3x3 grid of the nine pixels closest to the deepest point to avoid land contamination. This may introduce uncertainties for AEAP lakes, but our statistical analyses showed minimal spatial variation in these lakes' temperatures.

Lake temperature trends

We analyzed the long-term temperature trend for each lake using Landsat 5 and 7 data, and field measurements. Trends were calculated separately using linear regression for monthly and seasonal data, with particular emphasis on the summer months and the transition period from spring to fall. For both the seasonal/monthly and annual analyses, we included all data points from March to November to capture the full range of temperature variability during the ice-free seasons. A similar methodology was applied to a broader study of the park using MODIS data, with the exception that trends were computed individually for each pixel. Trends for each month of the year were also determined for all pixels across the park.

Monthly temperature trends derived from Landsat 5 and 7 observations across 135 lakes in the Adirondack were often variable (**Figure 9**). December, January, and February were omitted due to their higher *p*-values, suggesting an absence of consistent trends, likely caused by limited ice-free observations and potential ice-related distortions in temperature measurements. The shoulder months of March and November had more prevalent cloud cover resulting in fewer data points available for trend analysis. The Landsat 5 trends, during 1984-

2012, were generally higher compared to Landsat 7's 1999-2023 period, except for May and November.

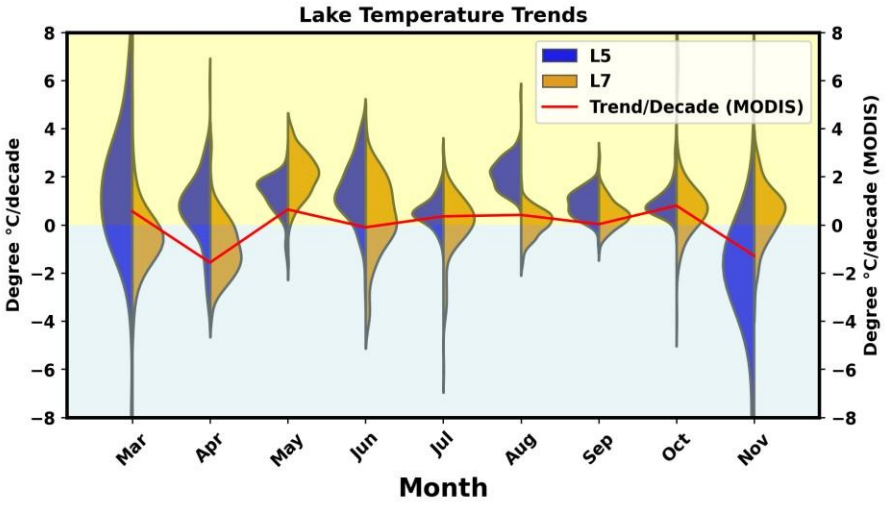

Figure 9. Distribution of temperature trends from Landsat 5 and 7 observations for each month across all lakes. The solid red line represents the average monthly trend for the entire Adirondack Park from 2002-2022, derived from MODIS LST estimates.

Park-wide trends in land surface temperature, derived from MODIS data across both land and water areas, showed positive tendencies consistent with those observed in Landsat 7 data over a similar time-period. These trends ranged from -1.57°C and 1.20°C for April and November and varied between -0.10 to 0.79°C for other months. The comprehensive trends for the park, represented by MODIS, were lower than those observed by Landsat, potentially due to the differences in spatial resolution, observation frequency, and that MODIS reflects all surfaces including top of the canopy temperature (not soil temperature) rather than the direct water surface temperatures measured by Landsat.

Data from all three satellites (Landsat 5, Landsat 7, and MODIS) showed faster warming in May and October compared to the core summer months, consistent with research suggesting a lengthening of the warm season in lakes globally (Woolway 2023). This trend may indicate an extension of the warm season, with earlier ice melt and the onset of lake stratification in May. The significant warming observed in October suggests that stratification may persist later into the season as well, reinforcing the idea of a prolonged warm period.

We assessed temperature trends of an extended summer (May – Oct), core summer (June – Aug), and annual (Mar – Nov) periods for 30 selected lakes with more than 2 km^2 area (**Figure 10**). Results based on Landsat 5 showed high and consistently warming trends for all periods. However, annual trends from Landsat 7 alone indicate both cooling and warming. Using data from both satellites, we found a warming trend for all seasons. It's important to consider potential biases arising from the differences between Landsat 5 and 7 including variations in

sensor configurations, spatial resolution, and radiometric resolutions. These factors may account for the distinct trend values observed from the two sensors.

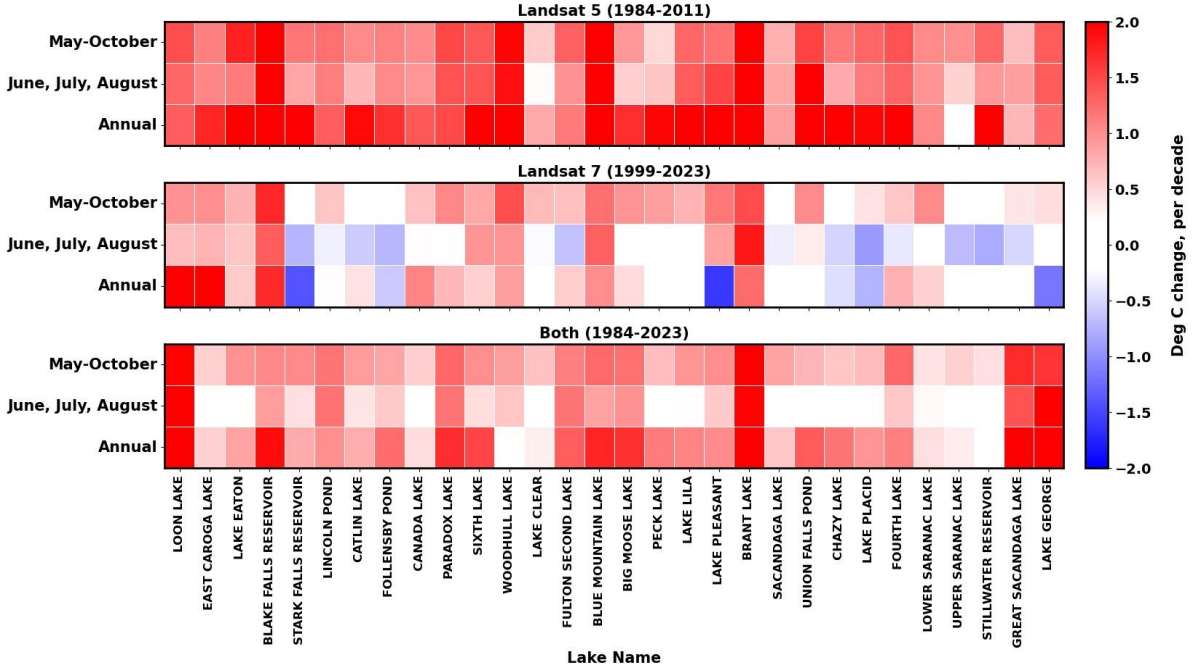

Figure 10. The slope of a linear regression of water surface temperature variability over specific seasons during the available time. Top panel) Landsat 5 only. Middle panel) Landsat 7 only. Bottom panel) Combined Landsat 5 and 7 to create an overall trend for the past 40 years. 30 lakes with an area of more than 2 km2 are selected. Lakes are in order from smallest to largest (left to right).

We further assessed the overall temperature trend for the ice-free season, typically the period from May 1st to November 30th. Based on combined Landsat 5 and 7 data from 1984 – 2023 we found an average increase of 1.11 °C per decade across the 135 study lakes (**Figure 11**). Our analysis included outliers, such as temperatures below zero degrees Celsius, that were likely because of unflagged ice pixels.

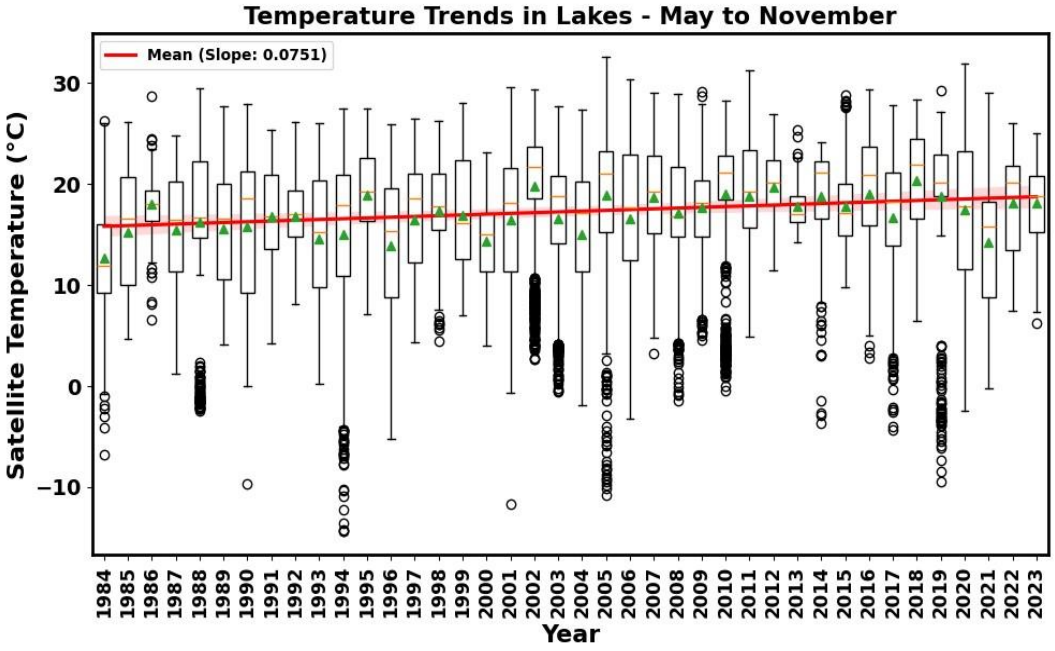

Figure 11. The Boxplot of lake water surface temperature of the selected 135 lakes for May to November from 1984 to 2023 using Landsat 5 and 7 and the overall trend line.

Most lakes had trends around 1 degree per decade, although some had negative trends. The park-wide trend, as indicated by MODIS data, showed an overall increase of less than 1 degree Celsius per decade. Notably, the southern part of the park demonstrated slightly higher warming trends compared to other regions (**Figure 12**). We also analyzed air temperature variations and trends using data from the Saratoga Lake station, provided by NOAA's National Centers for Environmental Information (National Centers for Environmental Information n.d.). The results showed that regional air temperatures increased by 0.44°C per decade. Interestingly, this suggests that lakes in the area are warming even faster than the surrounding air. The results of this work are under review for a journal publication (Azarderakhsh et al., Under Review).

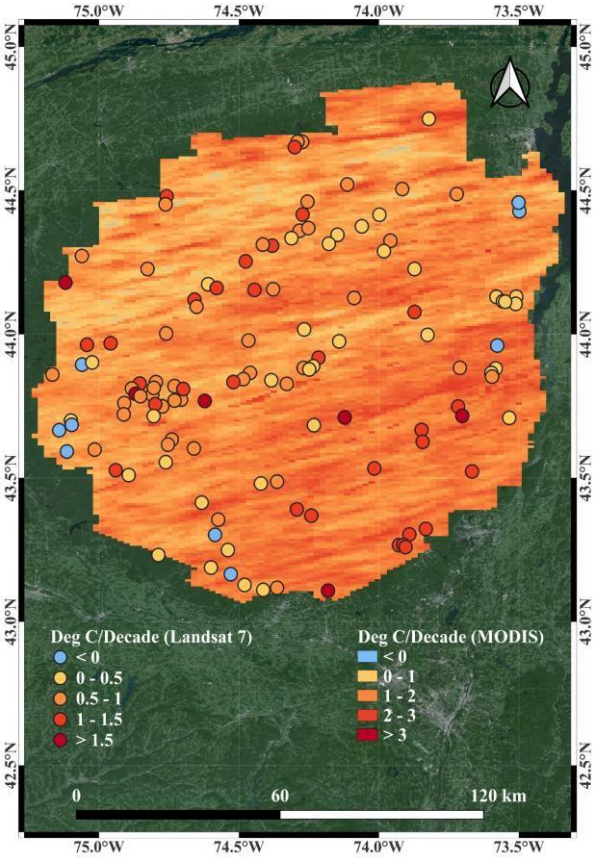

Figure 12. The May-October trend of Landsat 7 data overlaid on MODIS LST trend for the entire Adirondack Park Boundary and selected lakes.

Lake chlorophyll *a* concentrations overview

Chlorophyll *a* (chl-a) is an often-used proxy to characterize the productivity or algal biomass of a lake or other waterbody. There are existing empirical models to estimate chl-a based on satellite spectral bands. However, a key limitation of existing empirical models for chl-a retrieval is their lack of transferability across regions. Current empirical models are mainly developed for water bodies with high chl-a concentrations, while majority of the lakes in the Adirondacks have very low chl-a and appear very dark in optical satellite surface reflectance. As demonstrated by Boucher et al. (2019), empirical models developed for specific study areas often fail to perform effectively in other regions due to variations in optical properties and environmental conditions. This highlights the need for more robust and adaptable approaches, such as machine learning models, which can capture the complex dynamics of water quality parameters by incorporating a wider range of remote sensing bands and characteristics.

Machine learning models, primarily random forest regression, have shown promise in outperforming traditional band-ratio and spectral shape methods, offering greater flexibility and accuracy in chl-a estimation. While previous studies have made significant strides in remote

sensing of harmful algal blooms (HABs), several critical gaps remain. First, the focus on large lakes (>10 km²) and coarse-resolution imagery (e.g., Sentinel 3 at 300 m) limits the applicability of these methods to smaller water bodies, which constitute most of the lakes in the Adirondacks (Schröder et al., 2024). Second, existing approaches often rely on HAB-specific indicators like phycocyanin, which, while useful for identifying blooms, do not provide a comprehensive understanding of chl-a dynamics across the entire bloom season, including its development, peak, and decline.
Third, many studies lack the integration of multi-sensor data (e.g., combining Landsat and Sentinel 2), which could enhance temporal resolution and improve monitoring capabilities (Pahlevan et al., 2019). Additionally, the application of advanced atmospheric correction techniques to improve the accuracy of chl-a retrievals in small lakes remains underexplored.

We began to address these gaps by using Landsat 8 and 9, as well as Sentinel-2 fine-scale imagery, combined with non-optically active predictor variables, to create a statewide model of chl-a in New York's inland lakes. We then applied a robust atmospheric correction over aquatic surfaces on the raw satellite imagery above as the existing surface reflectance product, Land Surface Reflectance Code (LaSRC), available on USGS platform, are developed for land. By focusing on all lakes across the state, rather than just those in the Adirondacks, we were able to increase the amount of training data and thus develop a more robust algorithm that could later be applied to remote sensing observations in the Adirondack region. A constellation of satellites further improves the temporal resolution of our overall dataset. By using Landsat 8 and 9 and Sentinel-2 (30 m and 10 m, respectively), we could include lakes as small as 0.04 km² and increase the frequency of observations. Our primary goal was to explore machine learning methods suitable for estimating chl-a concentrations in Adirondack lakes.

Lake chlorophyll *a* field data

We used the LAGOS-NE dataset to select lakes in New York larger than 0.04 km^2 (Soranno, Bacon et al. 2017). Above 0.04 km^2, lakes will contain enough pixels (>45) from the Landsat 8 & 9 and Sentinel-2 satellites to execute algal bloom analysis. We compiled data from lakes in New York with in-*situ* chl-a data from open-source data repositories including the Citizens Statewide Lake Assessment Program (CSLAP), United States Geological Survey (USGS, 2016), observatory buoys in Lake Chautauqua (**Table 1**). Chl-a data was joined to the filtered lakes greater than 0.04 km^2 resulting in 347 unique sites on which to train the model (**Figure 13**).

Table 1. In situ data sources and their respective start/end dates, coverage, and citations.

Data Source	Date	Number of sites/lakes	Citation
NYSDEC monitoring programs	2011 - 2022	687 lakes	DOW, Bureau of Water Assessment and Management. URL accessed 2023: https://dec.ny.gov/environmentalhttps://dec.ny.gov/environmental-protection/water/water-quality/monitoringprotection/water/water-quality/monitoring
USGS National Water Quality Laboratory	2018 - 2021	338 sample sites	USGS, 2016. URL accessed 2023: https://www.usgs.gov/labs/national-water-qualityhttps://www.usgs.gov/labs/national-water-quality-laboratorylaboratory

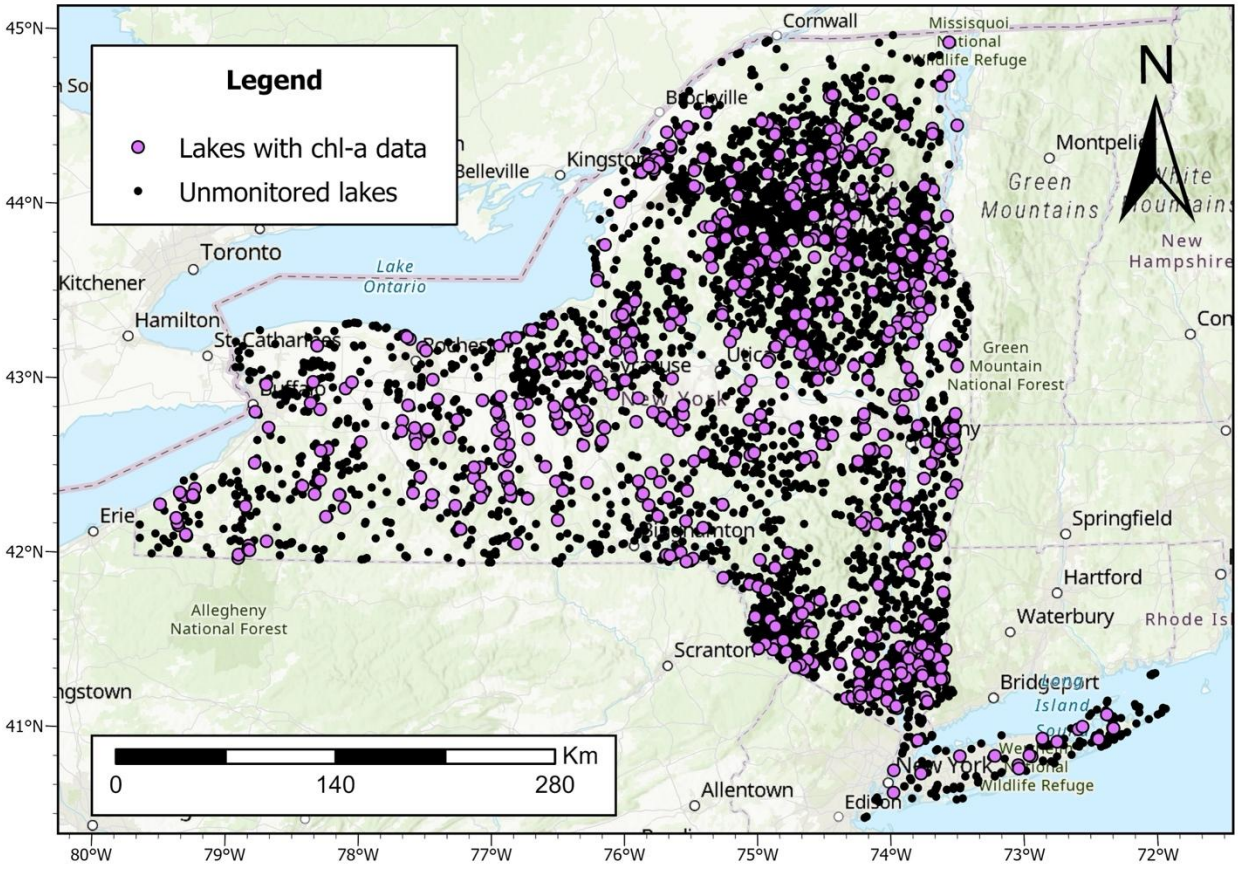

Figure 13. The New York lakes study region, depicting lakes with in-situ Chl-a data (pink, n = 349) and unmonitored lakes (black, n = 4461).

Satellite data processing for lake chlorophyll

The Landsat 8 & 9 Operational Land Imager (OLI) and Sentinel-2 Multispectral Instrument (MSI) imagery are accessible via Google Earth Engine image collections. The Landsat OLI satellites have a revisit period of 16 days and collect data on 8 spectral bands at 30 m spatial resolution, and we used the coastal aerosols, visible light, and near infrared (NIR) bands (1-5). We filtered the Landsat OLI raw image collections to summer months (May 1 - September 30) from 2013 – 2022 and included Landsat 9 imagery beginning in 2021. Sentinel-2 MSI has higher temporal, spatial, and spectral resolutions of 5 days, 10 m, and 13 spectral bands, respectively. Of the 13 bands, we used the first nine ranging from coastal aerosols to NIR. We compiled Sentinel-2 raw imageries for the summer months from 2019 – 2022 corresponding with data availability from the s2cloudless imagery in North America.

Due to inland water bodies' optically complex and dark features, utilizing a water-based atmospheric correction provides more accurate chl-a reflectance values than imagery corrected with standard land-based corrections. All three image collections were pre-processed with the Modified Atmospheric correction for INland waters (MAIN) (Page, Olmanson and Mishra 2019). This algorithm accounts for the complexity of small inland waters with high turbidity, chl-a, or other colored dissolved organic matter (CDOM).

We calculated median band values from buffered sample location points using zonal statistics and a 60 m buffer. Band statistics were matched with chl-a samples by lake name and sample date, and we allowed for a capture date matchup of ± 7 days to increase the size of our training dataset.

Machine Learning Modeling

We implemented nonlinear machine learning models that ranked highly including Extra Trees Regression (ETR), Support Vector Regression (SVR), Random Forest Regression (RFR), and Gradient Boosted Regression (GBR) to predict chl-a concentration over the lakes with existing training data. For all model iterations, we split the data for training and testing, with 80% of the data being randomly selected for training and the remaining 20% used for testing. For RFR, GBR, ETR, and SVR models, we used a 500-iteration random search to optimize the results.

We executed additional model optimization testing various combinations of input variables and subsetted chl-a. Input variables for each model included all Landsat 8 & 9 (bands 1-5), Sentinel 2 (bands 1-8a), and additional water characteristics variables such as percent of developed area and lake size. We used the National Land Cover Database (NLCD) 2019 to derive the percentage of inter-watershed agricultural and developed land (Dewitz, 2021). Furthermore, we ran each model with select variables (e.g. only Landsat bands, only Sentinel 2 and morphology, Landsat and Sentinel 2, etc.). Finally, we split the dataset into low and high concentrations, analyzing the performance of a low chl-a model versus high chl-a model (low

chl-a < 15 µg/l, high chl-a > 15 µg/l). Performance was assessed using coefficient of determination (R^2), root mean squared error (RMSE) and mean absolute error (MAE) to assess model strengths and weaknesses compared to statewide ground-based measurements.

Results – Lake chlorophyll

Model results indicated that ETR, RFR, and GBR performed similarly well, with $R^2 > 0.60$ (**Table 2**). Overall, we found that ETR, RFR, and GBR performed similarly, and they performed consistently better than the SVR model with R^2 values of 0.72, 0.68, 0.51, and 0.18, respectively. Additional testing of the ETR model indicated that the incorporation of non-optical features substantially boosted performance (R^2 0.48 to 0.72) with the best output including all tested variables.

Table 2. Model iteration results with satellite combinations and features; Km^2 = lake surface area, National Land Cover Database (NLCD) = percent of interwatershed agricultural and developed land.

Trial	R^2	RMSE	MAE
ETR L8/9 + S2	0.48	11.14	6.04
ETR L8/9 + S2 + Km^2	0.60	9.76	5.23
ETR L8/9 + S2 + NLCD	0.71	8.33	4.10
ETR L8/9 + Km^2 + NLCD	0.57	9.95	4.89
ETR S2 + Km^2 + NLCD	0.71	8.49	4.10
ETR All	0.72	8.19	3.97
RFR All	0.67	8.93	4.82
GBR All	0.51	10.80	6.16

We implemented a permutation importance analysis to determine which of the input variables are most influential in the ETR model's decision making (**Figure 14**). The results of this analysis indicate that the non-optically active input variables, morphology and percent developed land, hold the most weight in the model. The spectral bands with the most influence are the green (560 nm) band, red (665 nm) band, and NIR 703 nm. Variables noted to have a strong influence in previous studies, NIR 864 nm and NIR 740 nm, ranked lower, indicating that they are not significant influential indicators of chl-a concentrations. The results of this work are planned to be published in a journal manuscript (Greene et al., under preparation).

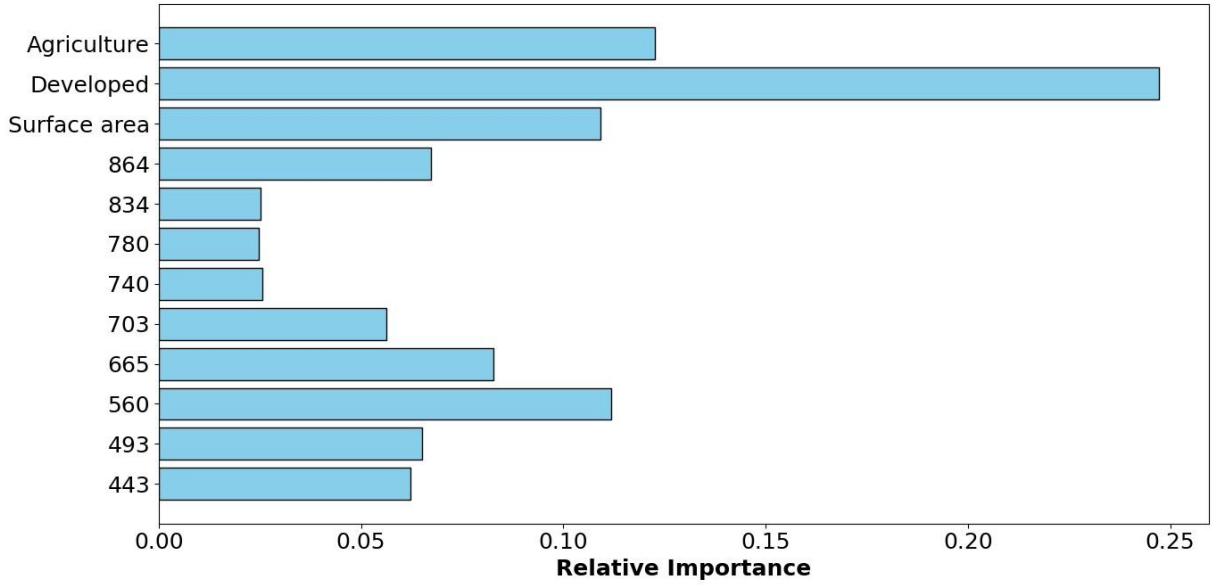

Figure 14. Permutation importance analysis plot for the best performing ETR model with five spectral bands from Landsat 8 & 9, Sentinel 2, morphology, and NLCD (agriculture and developed land) variables.

Next steps

This pilot study established a foundation for more extensive future study. The findings from this research demonstrate the effectiveness of satellite data for long-term monitoring of lake temperature and chlorophyll-*a* dynamics and inform broader ecological and climate studies in the region.

There are several next steps for remote sensing of lake temperatures. First, to understand temperature trends across the Adirondack region it is important to expand the scope of study. Building on the pilot analysis of 135 lakes, it will be important to incorporate the more than 1,200 additional lakes in the Adirondacks that currently lack consistent field

measurements. Since it is not practical to collect field data for every waterbody, the next step is to develop and refine models that can accurately extrapolate temperature conditions across this broader set of lakes using remote sensing observations. Additionally, it is important to expand the scope of this work beyond average surface temperature trends, to understand within-lake temperature gradients and how they vary spatially. Understanding these finer-scale differences can reveal important ecological patterns and identify areas of rapid change.

New data sources will improve remote sensing algorithms. First, data from Landsat 8 and 9, as well as other emerging sensors with higher temporal and spatial resolutions, can be used to obtain more remote sensing imagery. This will expand capacity to track rapid changes and fill any observation gaps in the existing Landsat record. Next, enhancing the validation of satellite products with new ground observations during the SCALE field sampling effort will improve algorithms. Deployment of infrared imaging technology to capture near-surface water temperature measurements will improve temperature algorithms and further quantify the accuracy and reliability of satellite-derived estimates. It will also be important to incorporate remote sensing techniques to analyze the timing of ice-on and ice-off events, as well as explore how changing freeze-thaw cycles influence overall lake stratification and warming rates. This will provide insights into broader ecological shifts tied to climate change.

There are several next steps for remote sensing of lake chlorophyll concentrations. First, a comprehensive model has yet to be established. Building on our initial statewide modeling, SCALE field work can help provide targeted validation efforts specifically for Adirondack lakes. This will help refine our model parameters to ensure accuracy in optically complex water bodies typical of the region. Once validated, the best-performing model will be run for all lakes in the Adirondacks. This effort will provide a comprehensive snapshot of Chl-a concentrations across the region, laying the groundwork for long-term monitoring and trend analysis.

Once a successful model is well validated it is possible to understand how chl-a concentrations have changed over time. This involves examining historical satellite data to detect potential trends—such as increasing or decreasing chl-a—over the period of satellite records. Additionally, once chlorophyll estimates are available it may be possible to evaluate environmental and anthropogenic variables—such as land use, watershed characteristics, and climate drivers—to identify factors that may contribute to elevated chl-a levels. Next, remote sensing can be used to assess spatial variability in chl-a estimates across larger Adirondack lakes by mapping and analyzing pixel-by-pixel results. This qualitative evaluation will help us understand within-lake heterogeneity, identify potential hot spots of higher Chl-a, and determine how effectively our model captures these variations.

Another key next step to increase accessibility and transparency of the SCALE project would be to create an interactive web map that visualizes lake temperature trends, lake chlorophyll concentrations, and other key findings. Users will be able to explore individual lakes,

view time-series data, and compare trends across the Adirondack region. Users will be able to visualize spatiotemporal patterns, query individual lakes, and download relevant data.

Data availability

Data used for remote sensing research includes satellite products and in situ data. Both satellite data and the in-situ data used in this study are publicly available. Data outputs from this study will be publicly available following review for publication (Azarderakhsh et al., Under Review), (Greene et al., under preparation).

Data mining

Overview and motivation

We conducted a thorough examination of historical data to understand the variation in lake water quality attributes across Adirondack lakes. This work was undertaken as a key step in the lake selection process for SCALE. Because only a small subset of Adirondack lakes can be sampled in a survey it is critical that we first understand patterns in water quality attributes so that survey teams avoid potential bias during field data collections. The data mining process is a critical step in the lake selection process for SCALE field operations.

Data mining process

The data mining work proceeded in several stages. First, we obtained data on the surface area, location, and total number of lakes using the (U.S. Geological Survey n.d.; Viger et al. 2016). The NHD provides information on rivers, streams, lakes, ponds, and more throughout the United States. In that dataset there are over 160,000 waterbodies in New York or adjacent watersheds draining into New York. Within the Adirondack State Park there are 11,200 lakes and ponds of varying shapes and sizes (**Figure 15**). We next accessed and compiled data from historical datasets. Lakes in the Adirondack State Park have been the subject of numerous studies over the past 45 years.

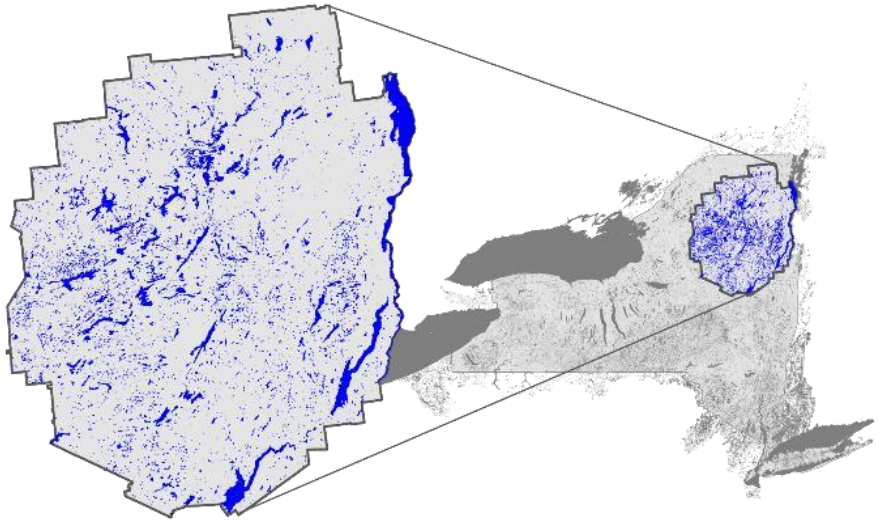

Figure 15: A map of lakes and ponds in the Adirondack State Park based on the National Hydrography Dataset.

Historical data review

The wealth of historical data available for Adirondack lakes provides a valuable baseline for comparison to present-day values and insight into the distribution of water quality variables throughout the Park. We identified nine large scale surveys of lakes and ponds in the park covering different periods of time (**Table 3**). Each survey has good spatial coverage of the park (**Figure 16**), except for the Adirondack Effects Assessment Program (AEAP) which focused on the Southwest side of the Park thought to be most heavily impacted by acid rain.

Table 3: Number of lakes sampled by different programs in the Adirondack State Park

Sampling program	Number of lakes sampled	Years
Adirondack Lake Survey (ALS)	1469	1984-1987
Adirondack Effects Assessment Program (AEAP)	28	1994-2012
EPA Temporally Integrated Monitoring of Ecosystems (TIME)	41	1991-2010
NY DEC Citizens Statewide Lake Assessment Program (CSLAP)	51	1986-2012
Eastern Lake Survey (ELS)	173	1984-1986
EPA Environmental Monitoring and Assessment Program (EMAP)	70	1991-1994
NY DEC Lake Classification Inventory (LCI)	86	1981-2010
Adirondack Long Term Monitoring (ALTM)	54	1992-2012
Adirondack Lake Assessment Program (ALAP)	228	1997-2024

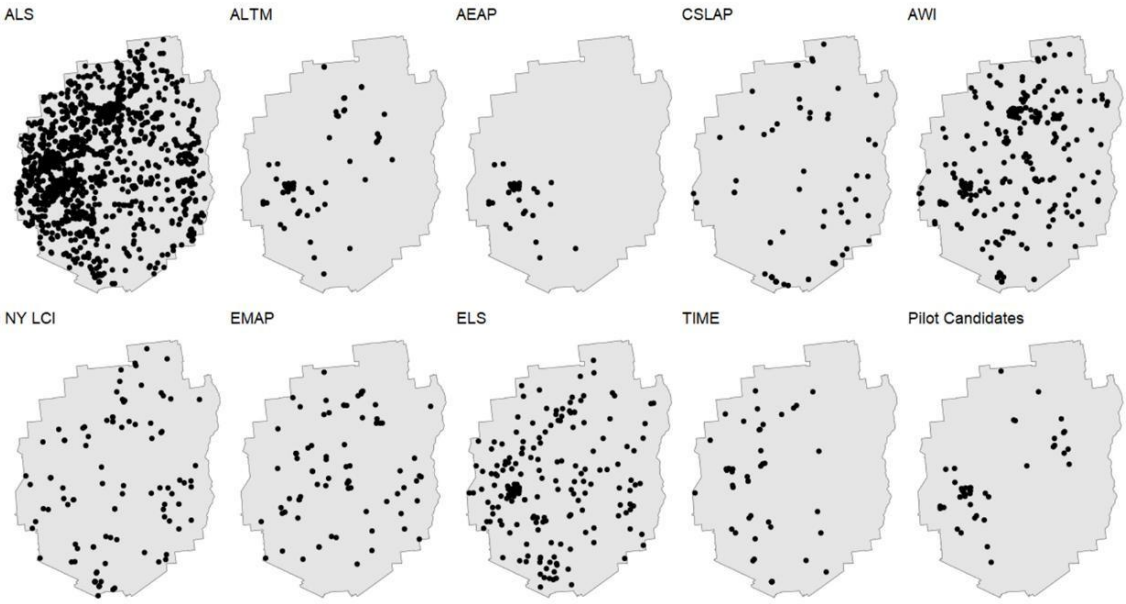

Figure 16: Lake locations within the Adirondack State Park sampled by various monitoring programs as well as those sampled in the SCALE Pilot study.

In total we found 1,721 lakes and ponds that have been previously sampled in the Adirondack State Park. However, due to idiosyncrasies in naming conventions this number becomes 1,598 unique waterbodies in the NHD. For example, several larger lakes have unique identifiers from the 1980s survey for different subbasins.

Much of the available data from the Adirondack sampling programs were compiled as part of LAGOS-NE-LIMNO (Soranno et al. 2015; Soranno et al. 2017). Other data were available from the Adirondack Lake Survey Company (Kretzer et al https://doi.org/10.6084/m9.figshare.22312732.v1). Data from ALTM and the 1980s ALS survey were also available from EDI repositories (Roy and Dukett, 2017a; Roy and Dukett, 2017b). We obtained additional information from reports published by the Adirondack Watershed Institute for the Adirondack Lake Assessment Program (Laxson et al. 2018). All the data used in our analyses are already publicly available, so no new data release is required to make the data public.

Clustering

The 1980s Adirondack Lake Survey showed that lakes and ponds in the Adirondacks come in many shapes and sizes and can have a large range in water quality. One of our primary goals was to discover if lakes could be grouped together based on their water quality, watershed, and morphometric characteristics. This step was undertaken so that we could later ensure that all types (clusters) of lakes were sampled during SCALE field visits. To begin, we conducted a Principal Components Analysis (PCA) using data from the 1980s lake survey.

Variables included in the PCA covered water chemistry, lake shape (e.g., depth, area, volume), and watershed characteristics (land cover). All variables were centered and scaled to units of standard deviation prior to analysis.

The first two principal components explained about 25% of the total variation across the lakes (14.5 and 11.7% respectively; **Figure 17**). Dissolved organic carbon (DOC), color, and total phosphorus (TP) all correlated with wetland area in the watershed and wetland area adjacent to the lake, as well as with watershed slope. Larger, deeper lakes were inversely correlated with DOC and TP. Some lakes also had very high conductivity, acid neutralizing capacity (ANC), dissolved inorganic carbon (DIC), and calcium. These higher conductivity lakes were largely independent of the variation in DOC and TP.

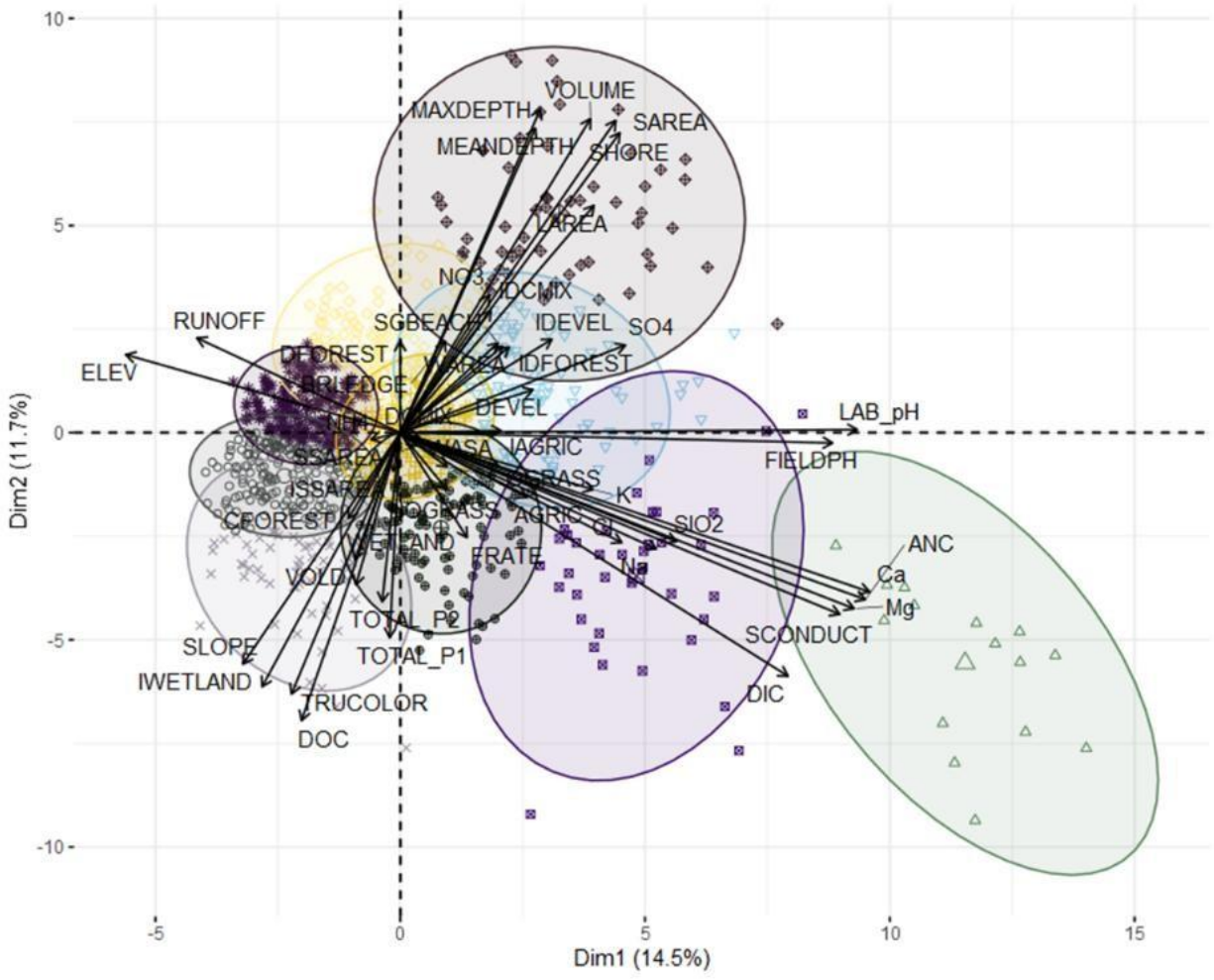

Figure 17: PCA biplot of lake characteristics in the Adirondacks. Colored circles and point shapes indicate clusters identified through k-means. Large points show cluster centroids.

We next assessed the clustering of lake properties using k-means (**Figure 17**). Using the elbow method, identifying the point where the slope changes in a scree plot indicated that ten was the optimal number of clusters. The number of lakes in each cluster ranged from 15 – 250 (**Figure 18**). Visual inspection of the spatial distribution of clusters indicated that the lakes in each cluster were well-distributed across the park.

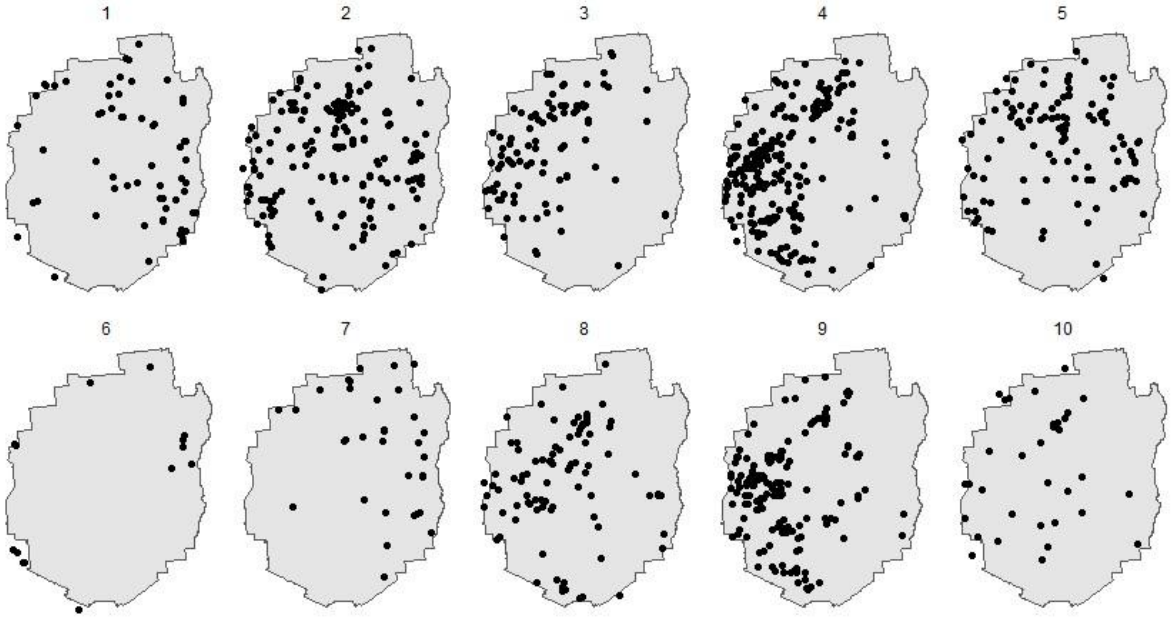

Figure 18: The distribution of lakes in each cluster identified following PCA of lake chemistry, morphometry, geography, and watershed characteristics throughout the Adirondack State Park.

The spatial clustering results raised the question of whether there are spatial relationships among lakes in terms of their water chemistry. We sought to determine if lakes that are closer together geographically are more similar in water chemistry, or if similarity in lake shape or watershed characteristics could explain similarities in chemistry. For each pair of lakes, we computed the environmental, geographic, morphometric, and watershed distance.

Data mining results

Our goal was to select lakes at three levels or categories. The first category of lakes is those that will be sampled approximately every three weeks throughout the open water season for three years and have sensors installed for high-frequency monitoring. It is anticipated there will be 10 lakes in this category. The second category of lakes are those that will be sampled

approximately every three weeks throughout the open water season for a single season and have sensors installed for high-frequency monitoring, for a total of about 30 lakes over three years. In total between categories one and two we anticipate there will be a total of 40 lakes that will have seasonally resolved data over the duration of SCALE. The third category of lakes are single visit lakes. These lakes will be visited once over the duration of SCALE, with approximately 75-100 lakes sampled each year and 250-300 over the three years anticipated for the survey. In addition to these three categories of lakes there will be a small number of additional lakes added to the survey as resources and collaborations permit. These include lakes that are sampled routinely by other organizations where the sampling programs align sufficiently with SCALE to permit them being added to SCALE (e.g., Lake George, Mirror Lake, Cranberry Lake, and Upper Saranac Lake) with minimal additional resource investments.

Given the higher investment required for category one and two lake monitoring, we sought to prioritize lakes for these categories that had a wealth of existing data available. Many lakes in the Park have been studied for more than a decade and building on these datasets could be valuable to better understand long-term trends and variability. We also sought to identify representative category two and three lakes that were relatively easily accessible, given the number of repeated visits that would be required for frequent sampling.

Selection for category two and three lakes began by creating a list of 78 lakes that have been well-studied as part of the AEAP, ALTM, and/or ALAP, and have either long-term biological data or relatively distinct characteristics based on clustering and lake types. We also included in our list those lakes with some significance to the public, with some preference for lakes that also had a history of sampling. There are 15 HUC8 watersheds in the park, and these 78 lakes are spread across 13 of them. The two watersheds with no high-intensity lake candidates (Hudson-Hoosic and Mettawee River) only have a small portion of their area within the park boundary.

Given the spatial distribution of high intensity sample candidates, we chose to select four lakes for the multi-year intensive sampling effort from a regional cluster, and the remaining six spread throughout the park (**Figure 19**). Using this approach, we expect to distinguish the responses of different kinds of lakes to similar regional drivers (e.g., weather) as well as spatial differences. The cluster is in the western part of the park and includes: Seventh, Sagamore, Limekiln, Big Moose, Queer, Dart, Moss, Rondaxe, Cascade, Windfall, Squash, West, Constable, and Lower Sister.

Many of these lakes were also part of the AEAP program, which means they have a lot of biological data associated with them, in addition to the chemical and physical data from the ALTM. We selected four lakes from this cluster: Sagamore, Queer, Dart, Squash. These four lakes represent different clusters for trends in DOC and Color as well as covering most of the range for DOC and TP and have distinct plankton communities. They also range from small to large, and remote sensing data are available for all but Squash. The remaining six lakes include Little Echo

Pond, Arbutus Lake, G Lake, West Caroga Lake, Garnet Lake, and Upper Ausable Lake. G, West Caroga, Little Echo and Arbutus were a part of the ALTM, and Garnet Lake has also been sampled as part of ALAP. These lakes range from 0.8 to 133 ha in area with maximum depths from 4.6 to >22 m.

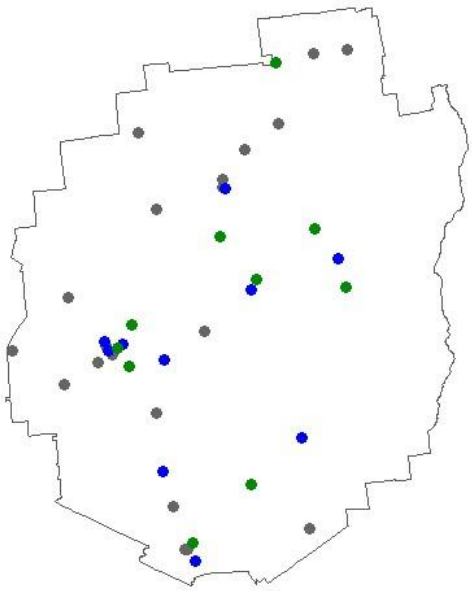

Figure 19: Map of lakes where seasonally resolved measurements will occur, with blue for multiyear, green for a single year.

For the single year seasonally sampled lakes (category two) we chose from the well studied lakes to represent the distribution of lakes around the park. We first split the list into each of the 13 HUC8 watersheds. Watersheds with more well-studied lakes had more lakes included in the list of high intensity candidates. Lakes were chosen based on their position in the distributions of watershed area, surface area, maximum depth, mean measured total phosphorus, and mean measured DOC.

Table 4: List of lakes selected for the first year of SCALE sampling (indicated by an "X" in the column "yr1"). Here, "grp" indicates the group or category of lake, whether the lake will be sampled every year of the survey (grp 1) or one year (grp 2). Grp 3 are those lakes that will be monitored for a single year in years two and three. Grp 4 indicates those lakes where external monitoring programs we are aware of may enable inclusion of this lake in SCALE with minimal additional resource investment. Additional columns indicate the National Hydrography dataset permanent identifier (NHDID), latitude (LAT), longitude (LONG), name (PONDNAME), elevation (ELEV), watershed area (WAREA), surface area (SAREA), max depth (DEPTH), and 8 digit hydrologic unit watershed name (HU8name).

yr1	grp	NHDID	LAT	LONG	PONDNAME	ELEV (m)	WAREA (ha)	SAREA (ha)	DEPTH (m)	HU8name
X	1	115353991	44.084	-73.862	UPPER AUSABLE LAKE	607	4119	61.7	14.6	Ausable River
X	1	131843739	43.826	-74.886	SQUASH POND	648	41	3.3	5.8	Black
X	1	131844150	43.793	-74.871	DART LAKE	536	10757	51.8	17.7	Black
X	1	53540671	43.414	-74.633	G LAKE	619	413	32.2	9.8	Mohawk
X	1	53542311	43.132	-74.491	WEST CAROGA LAKE	443	1413	129.1	22.6	Mohawk
X	1	132437639	43.814	-74.807	QUEER LAKE	597	155	54.5	21.3	Raquette
X	1	132437679	43.766	-74.628	SAGAMORE LAKE	580	4946	68	22.9	Raquette
X	1	129691062	44.309	-74.356	LITTLE ECHO POND	479	7	0.8	4.6	Saranac River
X	1	89365829	43.519	-74.022	GARNET LAKE	448	2121	133	NA	Upper Hudson
X	1	89362525	43.988	-74.242	ARBUTUS LAKE	513	365	48.2	7.9	Upper Hudson
X	2	115353949	44.18	-73.967	HEART LAKE	661	63	10.7	16.8	Ausable River
X	2	131844009	43.805	-74.831	WINDFALL POND	601	44	2.4	6.1	Black
X	2	131842438	43.879	-74.769	UPPER SISTER LAKE	588	1409	32	3.7	Black
X	2	131844637	43.745	-74.782	SIXTH LAKE FULTON CHAIN	544	4837	43.6	11.6	Black
X	2	53542015	43.189	-74.499	OTTER LAKE	503	361	14.8	4	Mohawk
X	2	150679608	44.157	-74.378	FOLLENSBY POND	471	NA	393	31.1	Raquette
X	2	47723283	43.371	-74.246	WILLIS LAKE	397	139	14.6	2.7	Sacandaga
X	2	132876321	44.705	-74.136	MOUNTAIN VIEW LAKE	453	11474	97.1	2.7	Salmon
X	2	89362297	44.021	-74.22	WOLF LAKE	556	673	56	NA	Upper Hudson
X	2	89362411	43.994	-73.827	CLEAR POND	583	601	70.4	24.4	Upper Hudson
	3	131845587	43.69	-75.065	GRASS POND	546	237	5.3	5.2	Black
	3	131844924	43.794	-75.291	PAYNE LAKE	375	42	7	6.7	Black
	3	131844064	43.811	-74.883	WEST POND	585	108	10.4	5.2	Black
	3	131845828	43.6	-74.662	BROOK TROUT LAKE	722	177	28.7	23.2	Black
	3	131844377	43.781	-74.853	MOSS LAKE	536	1315	45.7	15.2	Black
	3	131844719	43.756	-74.916	LAKE RONDAXE	524	14283	90.5	10.1	Black
	3	132876172	44.733	-73.97	UPPER CHATEAUGAY LAKE	399	20856	1038	21.9	ChateaugayEnglish
	3	132859255	44.24	-74.658	BOOTTREE POND	463	24	6.2	15.2	Grass
	3	92081293	44.747	-73.824	CHAZY LAKE	470	6896	746.6	21	Lake Champlain
	3	53542293	43.169	-74.534	WEST LAKE	470	5146	78.2	8.5	Mohawk

	3	53542293	43.168	-74.523	CANADA LAKE	472	9040	343	45.7	Mohawk
	3	133099412	43.961	-75.045	LOON HOLLOW POND	607	60	5.7	11.6	Oswegatchie
	3	132433418	44.483	-74.74	JOE INDIAN POND	394	5312	138.1	3.4	Raquette
	3	132437266	43.858	-74.45	BLUE MOUNTAIN LAKE	546	2972	697	30.5	Raquette
	3	47726211	43.236	-73.989	MINER MILL VLY	477	558	3.3	1.8	Sacandaga
	3	47724773	43.302	-74.585	JOCKEYBUSH LAKE	599	149	17.3	11.3	Sacandaga
	3	129691051	44.312	-74.372	EAST COPPERAS POND	479	15	3.6	6.4	Saranac River
	3	129690808	44.512	-74.125	BIG HOPE POND	522	194	8.9	11.5	Saranac River
	3	129691004	44.337	-74.372	MIDDLE POND	484	182	24.3	3.3	Saranac River
	3	135271335	44.432	-74.27	LOWER ST. REGIS LAKE	494	4427	141.5	11.6	St. Regis
	4	115353807	44.289	-73.982	MIRROR LAKE	566	301	50.5	18.3	Ausable River
	4	92083789	43.843	-73.432	LAKE GEORGE	66	60347	11536.6	60	Lake Champlain
	4	133098825	44.165	-74.803	CRANBERRY LAKE	453	37478	2795.9	11.6	Oswegatchie
	4	150563204	44.324	-74.322	UPPER SARANAC LAKE	482	19580	1912	26	Saranac River

To select potential lakes for inclusion in the single visit survey we began by analyzing unique lakes within each watershed. We grouped lakes by cluster, lake type, and watershed. Among these groups 108 included a single lake, 58 groups were lake pairs, and 143 groups had more than 3 lakes. From the 58 pairs of lakes, if one was on public land and the other on private, we selected the public lake resulting in 23 lakes selected. If both lakes were on public land, we randomly selected one, giving an additional 20 lakes. Similarly, for groups with three or more lakes we selected any public land lakes from groups where there was only one and randomly sampled public lakes when there was more than one. Additionally, we included lakes that represented surface area, watershed area, or depth outliers within clusters. Another 68 lakes were included to represent lakes with either more complex or simple shapes within watersheds. For lakes not included in clustering analysis we assessed lakes within watersheds, selecting a range of depths, mean measured DOC, mean measured chlorophyll *a*, and/or mean measured total phosphorus. We additionally included 57 other well-studied lakes and 39 lakes from the ALTM. Our final list of potential low intensity lakes included 500 lakes (**Appendix A**).

For the first year of sampling, we selected 100 potential lakes. Approximately half the lakes recommended for the single visit survey list were not included in the clustering analysis, so we chose 50 lakes from clusters and 50 from the non-clustered lakes. We randomly sampled lakes from each of 5 larger clusters based on the relative number of lakes in each group. From the non-clustered lakes, we randomly selected 50.

Next steps

The data mining process has been completed with the conclusion of the SCALE pilot program. However, the lakes actually sampled during SCALE field operations may not exactly

match the list of recommended lakes due to logistical challenges that may arise during field work, such as the inability to access selected lakes. The data mining process recommended back up/alternative lakes in case some lakes cannot be accessed.

Data availability

All data used in the historical data mining and lake selection process were publicly available. Code and intermediate data used to generate the lake lists are available on GitHub at: https://github.com/ADK-SCALE/lake_selection.

Carbon characterization

Overview and motivation

Widespread browning of surface waters in boreal and temperate regions of the Northern Hemisphere has been documented through long-term monitoring of color and/or dissolved organic carbon (DOC) over recent decades (Monteith et al. 2007; de Wit et al. 2021; Blanchet et al. 2022). Lake browning has received growing attention for its effects on ecosystem function, but the ways in which it alters carbon quality remain less well defined. Optical properties such as UV absorbance and fluorescence are often used to infer Dissolved Organinc Material (DOM) characteristics like molecular weight, aromaticity, and chromophore content, but their variation across Adirondack lakes and influence on lake processes are not well understood. Moreover, the relationship between these DOM attributes and photochemical reactivity, particularly the formation of photooxidants like singlet oxygen ($^1O_2$), remains unclear, despite its relevance to biogeochemical cycling and contaminant transformation in sunlit surface waters.

Developing and implementing SCALE to understand lake browning requires improved methods for characterizing carbon and assessing how variations in carbon quality influence key processes. To address this need, we examined DOM characteristics and $^1O_2$ production in 37 lakes within the Adirondack Long-Term Monitoring (ALTM) program sampled during three periods: October-November 2022, May-June 2023, and September 2023.

Carbon characterization approaches

Carbon quality can be inferred from optical properties such as UV-visible absorbance and fluorescence. For example, absorbance at specific wavelengths, normalized to DOC concentration, yields specific UV absorbance (SUVA) that serves as an indicator of aromatic content (Weishaar et al. 2003). Fluorescence measurements typically involve collecting excitation-emission matrices (EEMs), which record the intensity of emitted light across a range of excitation and emission wavelengths. Such fluorescence matrices can then be analyzed to identify fluorescence components indicative of DOM sources and compositional features (Fellman, Hood and Spencer 2010).

In this work, EEMs were measured on water samples from 37 ALTM lakes using a Horiba Scientific Aqualog spectrofluorometer. EEMs were recorded across an excitation wavelength range of 240 to 650 nm in 1-nm increments and an emission wavelength range of 248 to 830 nm in 2.33-nm increments. Optical indices, such as Napierian absorption coefficients (Cuthbert and del Giorgio 1992), $SUVA_{254}$ (the specific UV absorbance at 254 nm; indicating DOM aromaticity) (Weishaar et al. 2003), *E2*:*E3* (the ratio of Napierian absorption coefficients at 250 and 365 nm; indicating DOM molecular size) (De Haan and De Boer 1987), fluorescence index (indicating the relative abundance of microbially versus terrestrially derived DOM) (McKnight et al. 2001), humification index (indicating the degree of humification) (Zsolnay et al. 1999), and freshness index (indicating the presence of freshly produced DOM) (Wilson and Xenopoulos 2008), were extracted from the absorbance and EEM fluorescence data using *MATLAB*.

Concurrently, we characterized the spatiotemporal patterns of apparent quantum yields of singlet oxygen ($^1O_2$) for whole water samples collected from these lakes. $^1O_2$ is a reactive oxygen species ubiquitous in sunlit aquatic environments and plays a central role in the sunlight-driven oxidation of DOM, as well as transformation of organic micropollutants (e.g., pesticides) and biomolecules (e.g., cyanobacterial metabolites), among other processes (Ossola et al. 2021). The $^1O_2$ apparent quantum yield represents the number of moles of $^1O_2$ produced per mole of photons absorbed by the chromophoric fraction of DOM and serves as a key input parameter for photochemical modeling (Partanen et al. 2021). Importantly, apparent quantum yields capture changes in the intrinsic photoreactivity of DOM, which is governed by variations in its composition rather than its concentration (i.e., DOC). Measurements of apparent quantum yields offer a quantitative basis for predictive modeling of pollutant lifetimes in the sunlit euphotic zone of lakes. To this end, we combined the apparent quantum yields of $^1O_2$ with site-specific solar irradiance modeled by the *Simple Model of the Atmospheric Radiative Transfer of Sunshine* (Gueymard 1995; Gueymard 2001; Gueymard 2019) to estimate depthaveraged steady-state concentrations of $^1O_2$ in the euphotic zone for each ALTM lake. Our data will be valuable to practitioners interested in estimating the environmental half-lives of $^1O_2$reactive pollutants as well as to investigators assessing the natural attenuation capacity of ALTM lakes and similar aquatic ecosystems.

Carbon characterization and photochemistry results

Characteristics of DOM quality varied across ALTM lakes and seasons, with higher DOC concentrations generally associated with more processed, terrestrially sourced DOM of higher molecular weight and greater aromaticity (**Figure 20**). Hydrogeological conditions of lake watersheds (e.g., hydrologic connectivity and surficial geology) and seasonal variations in DOM quality jointly shaped the spatiotemporal patterns of the apparent quantum yields of $^1O^2$. Overall, the apparent quantum yields of $^1O_2$ for headwater and chain drainage lakes were higher than for seepage lakes, which is attributable to enhanced $^1O_2$ production by DOM with a greater proportion of microbially derived components and smaller molecular sizes in drainage lakes.

Furthermore, the apparent quantum yields of $^1O_2$ for thin till drainage lakes were higher than for both medium till and thick till drainage lakes, as can be rationalized by the greater contribution of upland runoff with shorter transit times (e.g., less DOM processing along the terrestrial-aquatic continuum) over deep groundwater inflow into thin till lakes. Within the euphotic zone of ALTM lakes, the depth-averaged steady-state concentrations of $^1O_2$ varied from 3.6×10^{-16} to 9.3×10^{-15} M (median 2.0×10^{-15} M) and fell on the upper end of the range of depthaveraged values (e.g., 6×10^{-17} to 5×10^{-15} M) predicted for the epilimnia of lakes globally (Partanen et al. 2021). While $^1O_2$ concentrations were less sensitive to watershed hydrologic connectivity and surficial geology than the apparent quantum yields, they followed a similar seasonal trend: May/June > September > October/November. Consistently across seasons, $^1O_2$ concentrations were highest in lakes undergoing intense browning, intermediate in those experiencing moderate browning, and lowest in those exhibiting mild browning (**Figure 21**). For compounds with second-order reaction rate constants with $^1O_2$ on the order of 10^7 M^{-1} s^{-1} (e.g., herbicides and cyanopeptides), median half-lives attributable to $^1O_2$ were predicted to range from 6 to 23 months in the euphotic zone of lakes with intense browning, 9 to 38 months in those with moderate browning, and 13 to 56 months in those with mild browning.

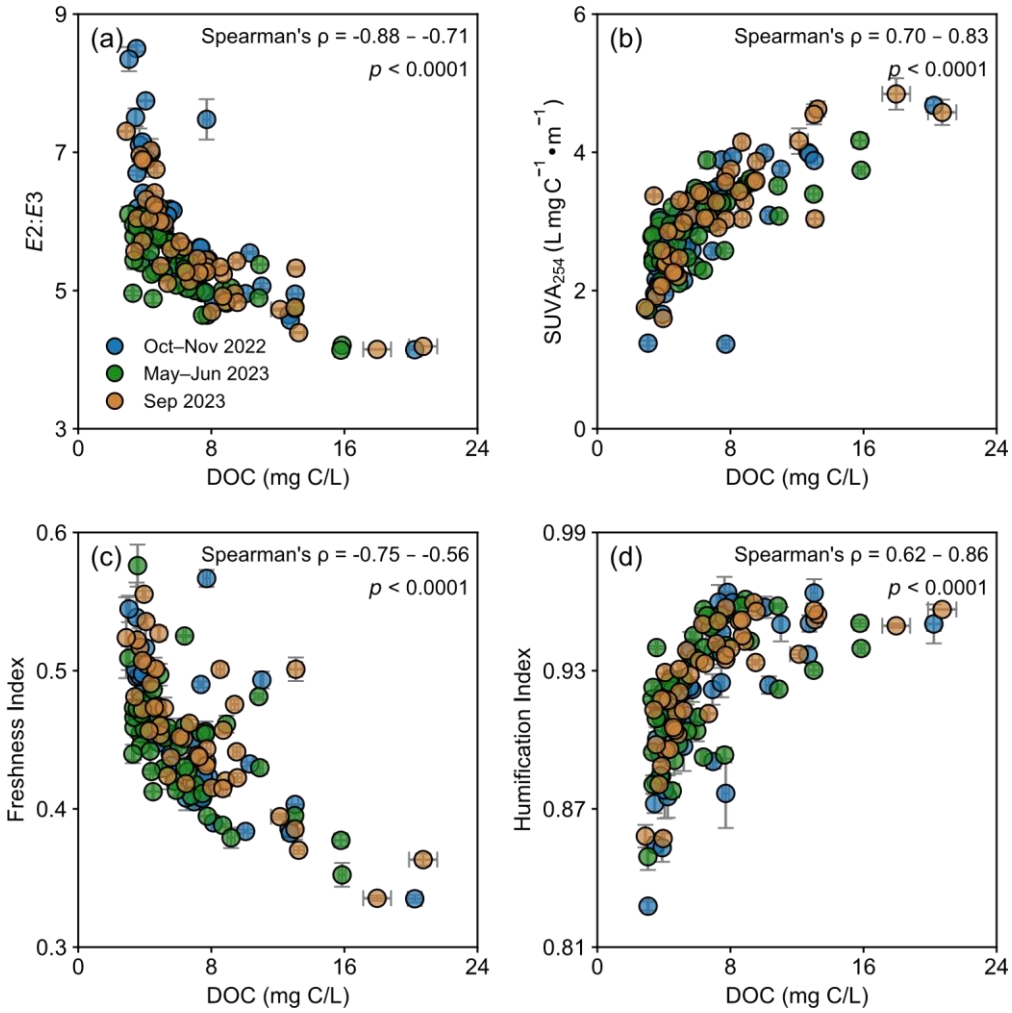

Figure 20. Spearman's correlation between dissolved organic carbon (DOC) and selected DOM quality indicators measured in ALTM lakes sampled during the pilot study: (a) E2:E3, which is an indicator of DOM molecular size; (b) SUVA254 (specific UV absorbance at 254 nm), which is an indicator of DOM aromaticity; (c) freshness index, which is an indicator of the relative contribution of recently produced DOM; (d) humification index, which is an indicator of the degree of DOM humification. Error bars denote standard deviations from duplicate measurements; if not visible, they fall within the markers.

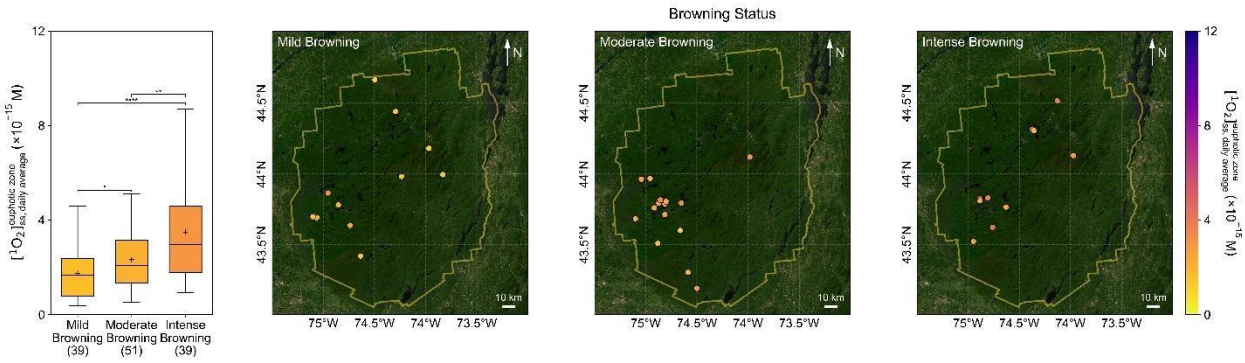

Figure 21. Multiple comparison of the estimated depth-averaged steady-state concentrations of 1O2 in the euphotic zone of ALTM lakes with varying degrees of browning. In the boxplot, each box spans the 25th to 75th percentiles, with whiskers extending to 1.5 times the interquartile range below the 25th and above the 75th percentiles. The centerline and "+" mark indicate the median and mean, respectively. The gray circles represent outliers. The numbers in parentheses represent the number of samples in each group. Box colors correspond to their respective median values referenced against the color bar. A Kruskal-Wallis test was first performed to determine whether statistically significant differences existed among groups. If significant, pairwise Mann-Whitney U tests were performed, with significant differences marked by asterisks as "" (p<0.05), "**" (p<0.01), "***" (p<0.001), or "****" (p<0.0001). For the maps, the solid yellow line delineates the boundary of Adirondack Park.*

Next steps

Since DOM is a key regulator of physical, chemical, and biological processes in lakes, it is valuable to characterize both its quantity (i.e., DOC) and its quality (e.g., optical properties and photoreactivity) as part of SCALE framework. This component of research would expand understanding of spatial and temporal patterns of DOM attributes in Adirondack lakes and the lake-watershed characteristics that drive this variation, as well as the water quality parameters that are related to shifts in DOM quantity and quality. Optical properties of DOM can also inform other SCALE components, including the influence of browning on epilimnetic warming, thermal stratification, hypolimnetic oxygen depletion and associated biological responses; inlake carbon processing; nutrient and metal cycling (e.g., mercury); acid-base chemistry; and the interpretation of remotely sensed data. Our $^1O_2$ measurements provide a baseline for assessing DOM photoreactivity in the ALTM lakes; however, generalizing $^1O_2$ production in response to browning remains challenging given the limited scope of sampling during this pilot phase.

Measuring $^1O_2$ production within the SCALE framework will increase the spatial coverage and temporal resolution of data beyond what we learned from the SCALE pilot study. In addition, several other aspects of this work would benefit from SCALE. For example, *in situ* measurements of diffuse attenuation coefficients would improve estimates of light availability in the water column, and high-resolution temperature profiling would refine depth-specific correction factors for $^1O_2$ production. Together, these efforts will allow for a more complete

assessment of the role of $^1O_2$, and potentially other photooxidants (e.g., hydroxyl radicals), in carbon cycling and contaminant attenuation in Adirondack lakes.

Data availability

Data for this study are summarized in a manuscript which has been submitted for review and publication. Oz, B., P. K. Snyder, C. T. Driscoll, T. Zeng in review. Browning and Singlet Oxygen Production in Adirondack Long-Term Monitoring Lakes, *Environmental Science and Technology*.

The data will be submitted for public access in the U.S. Environmental Protection Agency Water Quality Exchange https://www.epa.gov/waterdata/water-quality-data

Environmental DNA

Overview and motivation

A key goal of SCALE pilot work was to evaluate whether environmental DNA (eDNA) can be used as a robust tool for evaluating the fauna of Adirondack lakes. Specifically, we evaluated the potential for eDNA to provide an efficient and sensitive way of profiling the species composition of aquatic communities. Previous surveys, including the Adirondack Lake Survey (ALS) from 1984-87, were performed using labor-intensive collection methods such as gillnets and minnow traps. These conventional approaches require significant time and effort to capture, identify, and document the species that are present, and are prone to overlooking rare, cryptic, and small-bodied species. In contrast, eDNA methods hold promise for detecting and identifying species of multiple major taxa from water samples, thereby providing a rapid, noninvasive, and comprehensive snapshot of biodiversity. This approach can streamline both broad surveys and long-term monitoring, enabling researchers and resource managers to efficiently track species distributions, assess ecosystem health, and detect invasive species or endangered taxa.

The SCALE pilot work involved sampling and analyzing eDNA from 12 lakes across the Adirondack Park. We filtered water samples from replicate sites in shallow nearshore, deep offshore, shallow offshore, and outlet habitats. DNA from fish, insects, and mussels was amplified and analyzed, producing a table of unique sequences with their inferred taxonomic identities. Sampling for this pilot study was designed to resolve four major uncertainties about achieving adequate field sampling of small temperate lakes, thereby guiding design of field sampling protocols for future sampling efforts. These uncertainties were: how much water should be collected per sample to ensure strong species representation in every sample; how many replicate samples should be collected per major habitat type in a lake; how many discrete

habitat types should be sampled to fully represent the fauna of a lake; and whether the month of sampling between May and September affects the inferred faunal inventory from a lake. In addition, the laboratory analysis and bioinformatics steps to complete the dataset were expected to offer lessons on primer selection, taxa that can be assessed most cost-efficiently, and sensitivity to invasive and rare species.

Sample collection

Twelve lakes were included in this pilot study, and each was sampled to capture a range of habitats and seasonal variations (**Figure 22**). From each lake, five samples were collected from the surface nearshore habitat, five from the offshore habitat within the hypolimnion layer, five from the offshore habitat near the surface, and one from the outlet stream flow. For the ALTM lakes (n=8), we collected these 16 samples twice per year — once in spring (late May-June) and once in fall (late August-early October) to test for seasonal differences in species presence and detectability.

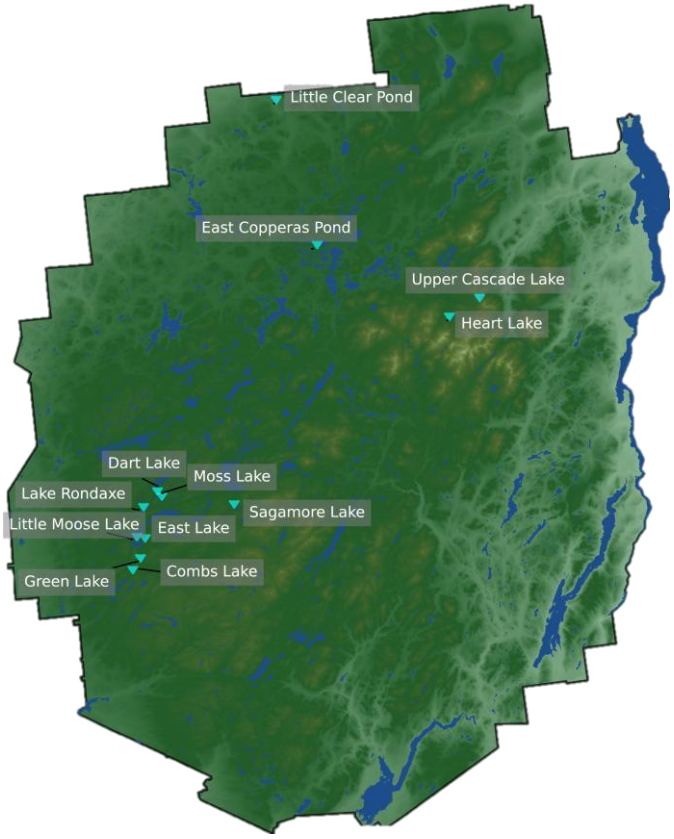

Figure 22. Lakes and ponds sampled for environmental DNA within the Adirondack Park for this pilot study.

Two of the ALTM lakes, Dart Lake and Sagamore Lake, were sampled at twice as many sites per habitat in the fall to provide stronger inferences about the accumulation of species detections with sampling effort. Four additional, non-ALTM lakes (Combs Lake, East Lake, Little Moose Lake, Green Lake) were only sampled in the fall. These non-ALTM lakes were chosen to represent a wide range of fish and mussel assemblage richness that has been documented by Cornell's Adirondack Fishery Research Program. These lakes offered the best-known faunal composition for comparison to eDNA results.

eDNA data generation and reference database

The Environmental DNA and Genomics Core Facility (EGCF) at Cornell University performed phenol-chloroform organic DNA extractions on a total of 376 field eDNA samples collected during pilot field collections. Of these 376 samples, 361 were lake samples and 15 were field blanks collected to estimate levels of contamination during the sampling process. In addition to lake samples and field blanks, 18 extraction blanks were generated in the lab to monitor contamination during the extraction process. Additionally, two PCR blanks were included to confirm the absence of contamination during amplification. To target the amplification of barcodes associated with fish species, the MiFish region was amplified from all samples following the protocol by Miya et al. (2015). To target amplification of mussels across all lakes, COI primers based on Dokai et al. (2023) were used.

The focus of the pilot project was fish and mussel eDNA, and all samples were sequenced using the NextSeq 500 platform with 2x150bp chemistry. The same eDNA extracts can be analyzed for other taxa by sequencing other genes, and we tested two other barcoding loci on an exploratory basis to inform future SCALE work. First, we analyzed samples from Moss Lake only for insects using COI primers as described by Leese et al. (2021). Given the smaller number of samples, insects in Moss Lake were sequenced on the MiSeq platform, also using 2x150bp chemistry. Second, we analyzed the full set of 376 samples using a universal set of 18S rRNA primers intended to target all metazoan organisms by Hadziavdic et al. (2014). An initial screening of the dataset suggested high rates of non-target amplification (i.e., non-metazoans) with limited applicability to the goals of this study. This dataset will continue to be analyzed but is not being further addressed in this report due to its unexpected complexity.

The EGCF processed the sequencing data using a pipeline that included Trimmomatic (Bolger, Lohse and Usadel 2014) for read trimming, DADA2 for error modelling and amplicon sequence variant (ASV) inference (Callahan et al. 2016), and BLAST for taxonomic assignment (Camacho et al. 2009). The resulting output was a detailed table of unique sequences (amplicon sequence variants, or ASVs) detected in each sample for each barcoding locus.

To convert ASVs into a list of species whose barcodes were detected in each sample, the sequences are compared to a reference database that serves as an identification key. We drew upon existing reference databases from the National Institute of Health National Center for Biotechnology Information (NIH NCBI) for these taxonomic classifications. The nucleotide database (GenBank) contains over 250 million sequences across all metazoans and serves as the most commonly used and taxonomically comprehensive reference database for environmental DNA sequence classification. To ensure the applicability of the GenBank dataset to Adirondack ecosystems, the database was screened by the EGCF to ensure that reference sequences were available for all fish species known to be present in the region. Although the GenBank database is comprehensive for fish species of the Adirondacks, several gaps were identified in regard to mussel species native to the region (as highlighted below in "Synthesis and Next Steps").

Comparing fish eDNA results with SCALE pilot study catches

For stable isotope analyses conducted under the SCALE pilot study, a modest number of fish were captured from eight of our twelve study lakes (Combs Lake, Dart Lake, East Lake, Green Lake, Heart Lake, Moss Lake, Sagamore Lake, and Upper Cascade Lake). All but one species captured in each lake for isotopic analyses were also detected using eDNA. The exception was the northern redbelly dace (*Chrosomus eos*) population in Moss Lake. Only two northern redbelly dace were captured near the Moss Lake inlet using minnow traps, and historical survey data indicate that northern redbelly dace represented ~0.1% of individual fishes in Moss Lake and are most abundant at the inlet (~3% of fishes). It is possible that eDNA sampling missed this species because it moves into and out of Moss Lake seasonally from the inlet stream.

Comparing fish eDNA results with historical catch data

Nearly a century of historical fish catch data is available for three of the ALTM lakes in this pilot study (Lake Rondaxe, **Figure 23**, Moss Lake, **Figure 24**, and Dart Lake, **Figure 25,** Daniels et al. 2011), with 4-5 visits per lake since 1931. For these three lakes, we compared species list between historical catches and eDNA results to assess the thoroughness of eDNA-based fish species inventories. For the other ALTM lakes in this pilot study, we have only a single historical time point to compare against (Adirondack Lake Survey in the 1980s), so these three lakes represent a rare opportunity to investigate community changes over longer time scales.

Most eDNA results agreed with knowledge from historical surveys by traditional methods. However, we also inferred three distinct patterns of species changes in the three lakes relative to previous records: population resurgences, recent losses, and recent gains. 1) Population resurgences were evident in cases where species last recorded in catch data from the 1930s were not observed again until our 2023 eDNA analysis (e.g., northern redbelly dace, *Chrosomus eos* and finescale dace, *C. neogaeus* in Lake Rondaxe). These detections may reflect

populations recovering after environmental stressors, such as acidification, or could represent rare community members that are not consistently detected by traditional sampling methods. 2) Species losses were
represented by species that were historically present in catch data but were not detected in the 2023 eDNA samples. These were often prey species, such as the common shiner (*Luxilus cornutus*) which was historically common in Lake Rondaxe, Moss Lake, and Dart Lake but was not detected in any of the three lakes using eDNA in 2023. If real, the lack of detection in 2023 may be linked to the introduction of invasive predators (i.e., *Micropterus* bass species), which could have pushed populations too low to be reliably detected by limited eDNA sampling. 3) Species gains refer to new species detected in the eDNA dataset that had never been previously documented in these lakes. Some of these species may have been present at low abundance during previous surveys but can be detected more effectively by sensitive eDNA methods. Other apparent species gains may be new migrants or invasive species. A notable example is the margined madtom (*Noturus insignis*), a species not native to the Adirondacks but known to be expanding its range into this watershed. *N. insignis* was detected in multiple samples from both Lake Rondaxe and Dart Lake, highlighting the utility of eDNA for tracking community changes.

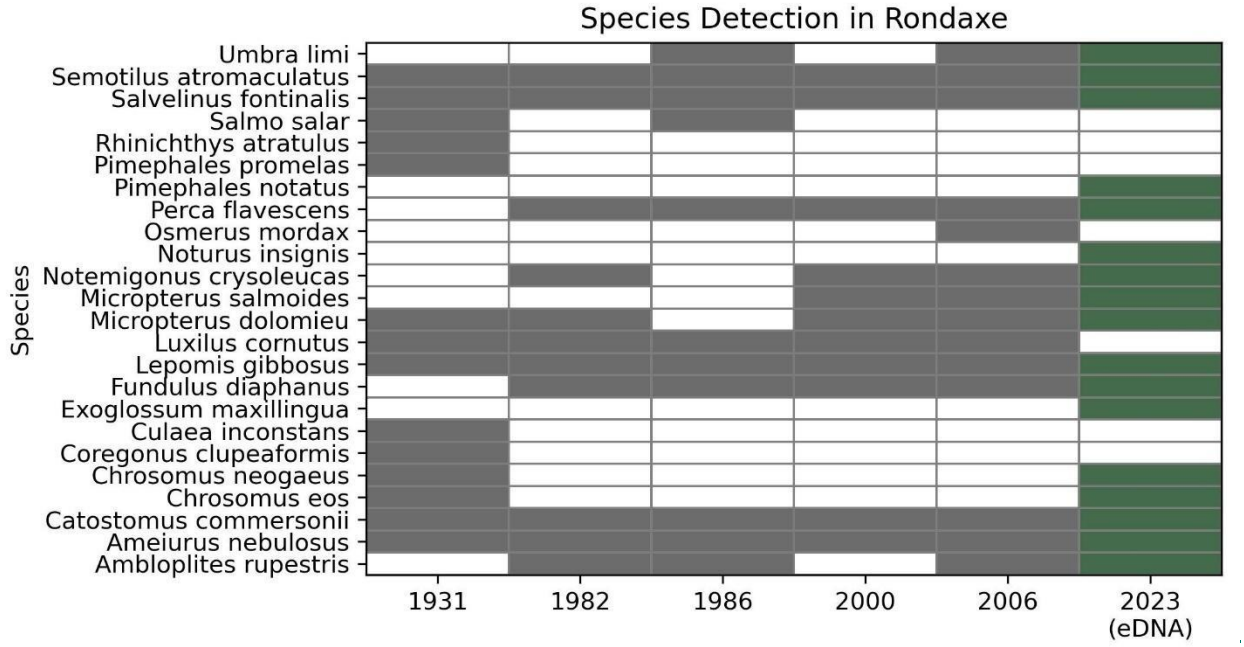

Figure 23. Presence-absence data for species in Lake Rondaxe. Filled, grey cells represent the presence of species determined by catch data and filled, green cells represent the presence of species determined by eDNA pilot samples.

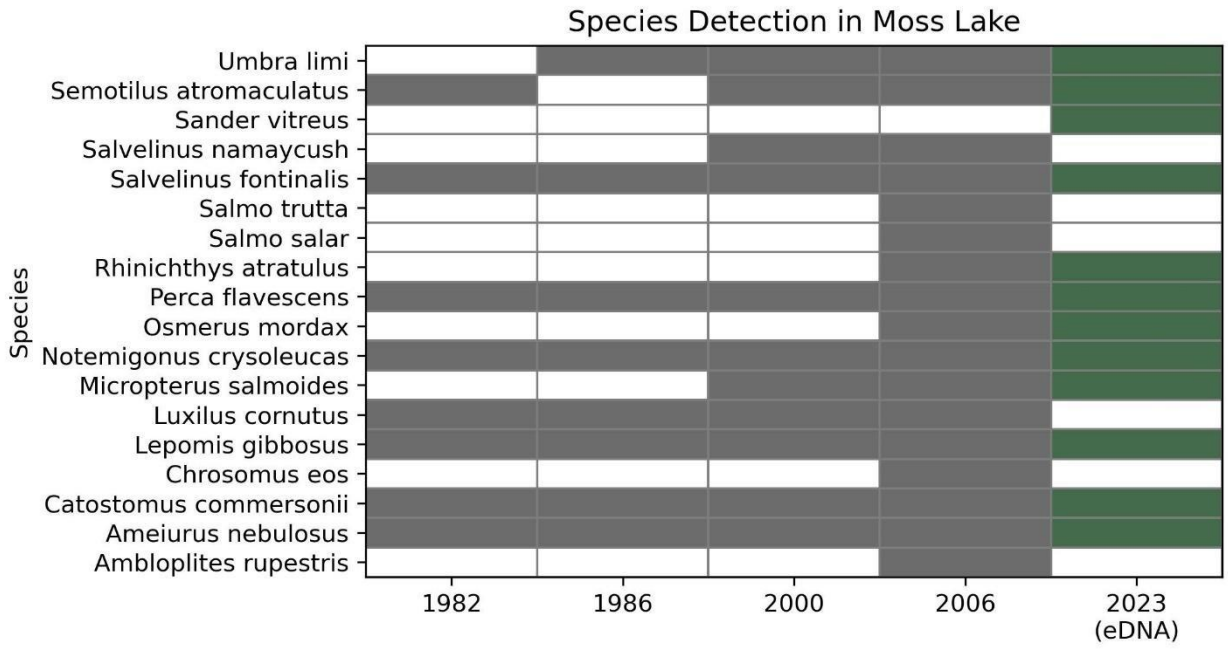

Figure 24. Presence-absence data for species in Moss Lake. Filled, grey cells represent the presence of species determined by catch data and filled, green cells represent the presence of species determined by eDNA pilot samples.

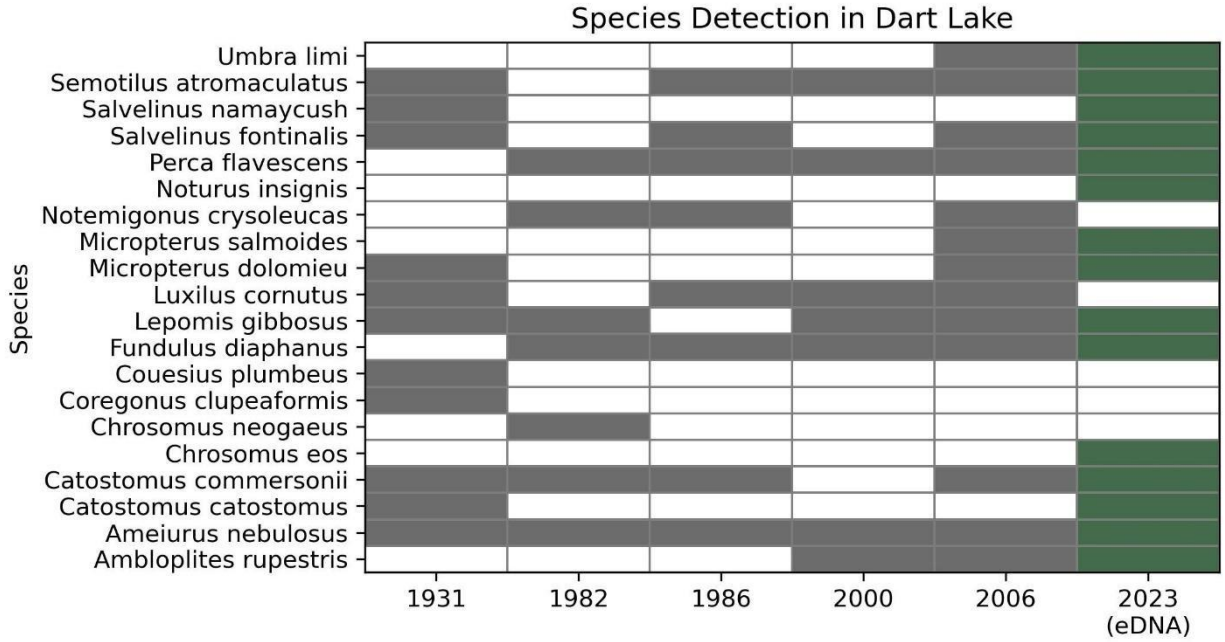

Figure 25. Presence-absence data for species in Dart Lake. Filled, grey cells represent the presence of species determined by catch data and filled, green cells represent the presence of species determined by eDNA pilot samples.

Fish species accumulation curves with eDNA sampling effort

eDNA samples collected for this pilot study produced species lists that closely resemble those from historical catch data, yet did not indicate a plateau in fitted species accumulation curves (**Figure 26**). We conclude that the majority of species are successfully detected in eDNA sampling using our pilot methodology (n=16 samples per lake; 150mL filtered per sample), but that a combination of low abundance and ephemeral presence in lake habitats allowed some species to be overlooked. As highlighted by previous literature, lakes in the Adirondacks are highly connected (Daniels et al. 2008) and fish readily move back and forth between fluvial and lacustrine ecosystems. Highly connected lakes that have communities influenced by dispersal often do not conform to the accumulation patterns of closed systems, hence accumulation curves may not achieve their expected asymptote (Dove and Cribb 2006). For instance, in spring samples, species accumulation curves for our results from Sagamore Lake and Moss Lake suggest an asymptote at a similar number of species, but the curve of Moss Lake accumulates more gradually (**Figure 26**). Previous literature (Daniels et al. 2008) has suggested that Moss Lake is highly connected with Dart Lake and Lake Rondaxe, and exchanges of species among these lakes may drive the apparent low species accumulation rate in Moss Lake.

Seasonal differences in species accumulation were observed in some lakes. In general, lakes tended to accumulate higher numbers of species in the spring, though this trend was not consistent across lakes. These patterns may be influenced by spring snowmelt and seasonal fish movements, such as adult migrations for spawning or movement of juveniles from streams into lakes. Notably, Lake Rondaxe exhibited the highest species richness in the spring, with fitted accumulation curves approaching 25 species. Located at the intersection of several lakes and with a known history of species introductions, Lake Rondaxe may function as a hub for fish movement within the region.

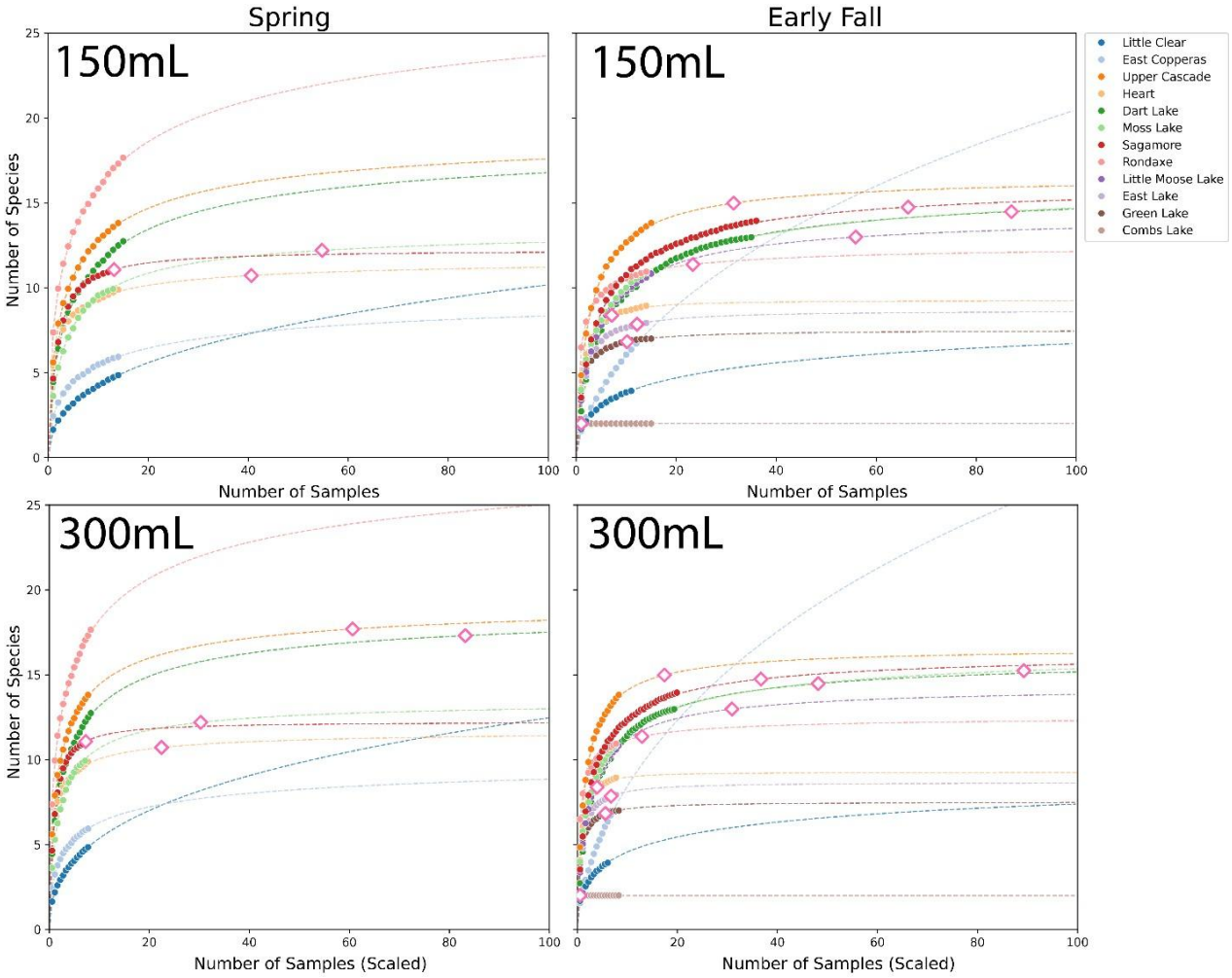

Figure 26. Species accumulation curves from eDNA sampling of SCALE pilot lakes. The left column represents spring sampling events, and the right column represents fall sampling events. The upper row presents results from individual 150mL field samples; the bottom row illustrates simulated 300mL samples (pooled results from two 150mL replicates collected at the same time and location). Pink diamonds represent the number of samples at which 90% of the projected number of species would be recorded.

To evaluate the potential effect of larger sample volumes on species accumulation, we combined sequence data from replicate samples taken at the same time and location, effectively creating 300 mL composite samples from two 150 mL replicates (**Figure 26, bottom row**). These larger volume samples demonstrated, on average, a 1.8X increase in species information content, meaning they detected far more species per sample but were somewhat less efficient per unit volume than additional small-volume samples from other locations. Species accumulation curves suggest that even with 300 mL volumes, a very large number of samples would be required to fully profile community diversity. This finding has motivated the SCALE eDNA team to plan future sampling around 2 L samples collected from a broader zone within a

sampling site. Shifting to larger volumes and less-fine filters is becoming more standard practice in eDNA surveys, with the goal of improving detection of rare or low-abundance taxa while also minimizing the total number of samples required.

Some lakes, particularly small systems like East Copperas and Little Clear Pond, displayed unexpected accumulation patterns. For example, Little Clear Pond is known from historical data to support only brook trout and brown bullhead, yet eDNA sampling yielded up to five species. Contamination is unlikely, as negative controls (blanks) were clean. Index hopping (GuenayGreunke et al. 2021), a sequencing artifact that can occur when highly similar barcodes lead to incorrect assignment of reads to samples, could be a possible explanation for observed patterns in small lakes. To address this, future sequencing will adopt higher-accuracy platforms (e.g., MiSeq rather than NextSeq) and revised library preparation protocols. Additionally, replacing dual indexing with matching forward and reverse barcodes may reduce or eliminate index hopping during demultiplexing, although this would reduce the number of samples that can be multiplexed in a single sequencing run (i.e., a non-trivial efficiency cost). Index hopping is a more problematic issue in samples with low species diversity and low data yield, where even minor index hopping during demultiplexing can have a disproportionate effect and overwhelm true signal. This pilot study has helped our team to identify this suite of technical issues to be addressed in future eDNA sampling and laboratory analyses.

Seasonal and habitat detection heterogeneity

Most detected species (68%, on average) were present in samples from both seasons, whereas 16% were detected only in the fall and 16% were detected only in the spring. The lake with the highest percentage of species detected in both seasons was Upper Cascade Lake (87.5%), which had one of the richest fish faunas among our pilot lakes.

Both spring and fall were similar in their detection variability across habitats. The category of species that was most different in detection between spring and fall was those detected only in the nearshore environment. In spring, the average percentage of species only detected in the nearshore environment was 15.49% while the same category for fall was 7.21%. It is possible that juvenile fish aggregating in the shallows or seasonal movement of adult fish for spawning in the spring are being captured by our eDNA sampling, but seasonal differences in physical mixing of lake waters could also be involved. Thus, we are unable to resolve the explanation for this pattern.

Species commonly associated with shallow water environments (e.g. golden shiner) were typically found in both nearshore and offshore surface water sampling. Similarly, species commonly associated with deepwater environments (e.g. round whitefish in Upper Cascade), were detected primarily in offshore habitats (both deep and shallow) across both seasons.

Taken together, these results suggest that spring and fall eDNA sampling each capture a modest number of unique species records, potentially due to seasonal movement patterns. However, we conclude that sampling in both seasons is not necessary to capture the dominant species in the fish community of Adirondack lakes, especially if we enhance the volume of water filtered and integrate a broader sampling area per sample. In contrast, in any season, sampling distinct habitats is necessary to detect a variety of species that are habitat specialists, including certain species of special conservation concern in the State of New York (e.g., brook trout and round whitefish). Thus, we recommend continuing collection of both nearshore and offshore samples, but the team should consider vertical integration of offshore samples to reduce the number of habitat classes from three to two.

Detection of insects and mussels by eDNA

eDNA samples were also analyzed to evaluate the detectability of mussels and insects, which lack historical survey data for comparison. These efforts were exploratory and relied upon barcoding loci that were drawn from recent literature on each group. For the insect eDNA survey at Moss Lake, non-biting midges (*Chironomidae*) were by far the most highly detected arthropod family, representing 72.1% of the 1,701,260 reads sequenced across the dataset. This accords well with previous uses of this barcoding locus, which is highly sensitive to dipterans. The second and fourth most common families were both terrestrial insects: Lauxaniidae flies (9.7%) and Caeciliusid barklice (1.5%), which presumably fell into the water. The top 10 families detected in Moss Lake samples are shown in **Table 5**, which includes two families of water fleas (microcrustaceans). We find these results intriguing and recommend that the SCALE team consider expanding the use of insect eDNA primers given the long history of using aquatic insects as bioindicators of environmental condition. Unlike fish, there is no existing data on differences in insect assemblages among Adirondack lakes, but eDNA findings could establish a baseline for interpreting future faunal changes.

Table 5. eDNA sequence assignments to arthropod families from Moss Lake samples.

Order	Family	Number of Reads	Percent of Reads (%)
Diptera	Chironomidae	1226808	72.1117
Diptera	Lauxaniidae	165379	9.721
Diptera	Chaoboridae	96201	5.6547
Psocodea	Caeciliusidae	25850	1.5195
Trichoptera	Sericostomatidae	23061	1.3555
Ephemeroptera	Ephemeridae	23006	1.3523
Anomopoda	Chydoridae	14879	0.8746
Anomopoda	Macrotrichidae	14617	0.8592
Diptera	Ceratopogonidae	18518	1.0885
Diptera	Simuliidae	16891	0.9929

Mussel primers amplified DNA from all lakes. Across all the pilot lakes, four taxonomic groups were identified: *Utterbackia imbecillis, Elliptio complanata, Elliptio hopetonensis*, and a set of similar sequences belonging to the genus *Elliptio* that did not match any particular species in the reference database. *Elliptio hopetonensis* is narrowly endemic in Georgia, while *Elliptio complanata* is wide ranging across the entire east coast of the United States, including Georgia. As *Elliptio hopetonensis* was only detected in one of our samples, it could be the result of sequencing error. However, the taxonomic assignment of some of our samples to *Elliptio hopetonensis* could also arise from taxonomic misidentifications within the reference database, which includes other *Elliptio* species whose geographic range overlaps with that of *E. Hopetonensis*. To tackle these challenges in mussels, a group with poor representation in the genetic databases, we will be generating Adirondack-specific mussel databases (described further below in “Synthesis and next steps”). *Utterbackia imbecillis* was only detected at the outlet of Moss Lake and is known to be a riverine species native to the region. The full, habitat-level breakdown of where each taxonomic group was observed is shown above in **Table 6**. In all lakes, mussels were most frequently detected in the near-shore environment, although mussel eDNA was also detected in some offshore sites, with more offshore detections being from surface samples than from deep samples.

Table 6. eDNA detections of unionid mussels in SCALE pilot samples.

Lake	Habitat	Sites with detections	Taxon
East Lake	Nearshore	4/5	*Elliptio sp.*
	Offshore surface	2/5	
Heart	Offshore deep	1/10	
	Nearshore	1/10	
Moss Lake	Offshore deep	3/10	
	Nearshore	10/10	
	Offshore surface	10/12	
Rondaxe	Offshore deep	6/9	
	Nearshore	7/10	
	Surface	8/12	
Sagamore	Offshore deep	5/14	
	Nearshore	7/14	
	Offshore surface	8/16	
Sagamore	Offshore deep	3/14	*Elliptio complanata*
	Nearshore	12/14	
	Offshore surface	4/16	
Moss Lake	Nearshore	1/10	*Elliptio hopetonensis*
Moss Lake	Offshore surface	1/12	*Utterbackia imbecillis*

During this pilot study, we did not sample for the physical presence of mussels. Previous sampling efforts of the Adirondack Fishery Research Program have found populations of *Elliptio complanata* in East Lake, suggesting that eDNA is successfully capturing true, known populations. Unfortunately, that is our only check on inferences regarding mussels in this pilot study.

Synthesis and next steps

Overall, our results indicate that most fish species were detected in both seasons, with some additional species detections were season specific. Similarly, most species were detected across all habitat types (nearshore, offshore shallow, offshore deep), but some important species were unique to specific habitats (e.g., round whitefish in deep habitats of Upper Cascade Lake). eDNA detections aligned well with both contemporary and historical catch data

in most cases. Insect detections were dominated by chironomid midges and suggested that many taxa were present. Mussels were detected in five lakes, most commonly in nearshore habitats. We conclude that eDNA is highly promising as a scalable and cost-effective component of future surveys, offering unique power to inventory present-day aquatic biodiversity across multiple taxa. We also conclude that eDNA surveys are suitable for revealing changes in the fauna of Adirondack lakes relative to historical baselines.

The lessons from this pilot study are guiding refinement of our plans for future field sampling and lab analysis protocols for eDNA, particularly regarding the number and spatial distribution of samples. The pilot clearly demonstrated the importance of sampling both nearshore and offshore habitats to adequately capture fish community diversity. Additionally, the majority of species are reliably detected across seasons, indicating that a single site visit between May-September will suffice for community characterization. However, more intensive sampling across multiple seasons might be necessary to detect rare and ephemeral species that move in and out of lake systems. Thus, we recommend delving further into temporal stability of eDNA detections by collecting seasonal samples in future sampling efforts. Performing monthly sampling of that modest number of lakes may also offer compelling insights into the seasonal dynamics of species composition in Adirondack lakes, providing an important phenological baseline for future evaluations of climate change impacts.

Although the species lists detected by eDNA captured major community members historically present in the pilot lakes, current species accumulation curves based on 150 mL and 300 mL samples suggest that a prohibitively high number of samples would be required to fully characterize communities under the existing protocols. Simulations of collecting larger sample volumes (300 mL) indicate potential to gather more information per sample processed, hence we recommend that future surveys be based on filtering 2.0 L of lake water per sample, which is becoming more common in eDNA research. We will continue to explore simulation approaches to refine the recommended sample volume and identify the number of samples required to meet or exceed the detection probabilities evident from this pilot work.

Another key issue is the size of the lake: pilot eDNA data suggest that sampling intensity should be adjusted with lake size. For instance, small systems such as Combs Lake exhibited low fish diversity (just two fish species in recent catch data as well as every eDNA sample), suggesting that minimal sampling is sufficient in these systems. In contrast, large lakes like Little Moose Lake showed high species richness and habitat heterogeneity, but our pilot eDNA sampling overlooked a number of fish species documented by the Adirondack Fishery Research Program. Many of the species expected in Little Moose Lake were not detected in fall-only eDNA sampling, indicating that both increased sample volume and spatial coverage might be needed for adequate biodiversity assessment of such a large lake.

For genetic analyses of eDNA samples, our experience from this pilot study indicates that future eDNA surveys should utilize single index barcodes that are incorporated into both sides of reads. This would require identical index sequences to be present on both ends of the reads, which reduces the possibility of index hopping during the demultiplexing process. Unexpected species detections in small lakes during the pilot study may be attributed to this sequencing artifact, which occurs when sequencing reads are misassigned to incorrect samples during demultiplexing (Guenay-Greunke et al. 2021). By using unique, matching indices on both the forward and reverse reads rather than combinatorial indexing, a revised protocol can minimize false positives and improve community characterization across all sampled lakes.

Due to the success of the Moss Lake aquatic macroinvertebrate eDNA exploration, we recommend expanding sampling efforts to characterize macroinvertebrate communities using eDNA. The literature suggests that dipterans are sensitive to environmental change and should be quite useful in eDNA biomonitoring efforts (Keck, Brantschen and Altermatt 2023). The inherent difficulty in taxonomically identifying aquatic dipterans (especially chironomids) to genus or species level via microscopy has excluded them from being a significant part of traditional bioindices, which instead focus on Ephemeroptera, Trichoptera, and Plecoptera (EPT, e.g., (Zweig and Rabeni 2001). However, the sensitivity of the widely used aquatic macroinvertebrate primers to amplification of Chironomidae have revealed greater biodiversity and community sensitivity to change than previously understood. The primers used here amplified dipteran DNA effectively but are biased against Trichoptera and Odonata (Leese et al. 2021), two groups that were demonstrated to be present in most lakes by pilot sampling for stable isotope analyses of macroinvertebrates. To reduce these biases and increase our ability to compare eDNA data with traditional macroinvertebrate surveys, we recommend testing additional macroinvertebrate primers that focus on EPT amplification, which could be paired with the primers used in our pilot analysis of Moss Lake samples. Future sampling efforts should include paired eDNA and aquatic macroinvertebrate surveys on a subset of lakes to enable confirmation of detected taxa.

Based on the low detection and poor taxonomic identification of our mussel samples, we recommend producing a customized freshwater mussel mitochondrial genome reference database for the Adirondack Park. In support of that goal, we have already collected both voucher specimens and tissue samples from Adirondack waters in 2024. To account for genetic variation found across isolated populations of freshwater mussels, we sought to collect tissues from every species in each of the 5 major drainage basins within the park. Our pilot work also made us aware of a major complication with freshwater mussel eDNA. Freshwater mussels exhibit heteroplasmy; in addition to the standard matrilineal mitochondrial inheritance, male mussels also inherit male-type mitochondria patrilineally (e.g., Wen et al. 2017). The sequence

divergence between the male- and female-type mitochondrial haplotypes of a single individual can be greater than the divergence between two male-type or female-type mitochondria of

different species. This unique life history trait may have also led to the poor taxonomic matches that characterized some of our results. To accommodate this revelation, we plan to extract and sequence DNA from the gonads of the male voucher specimens in addition to the mantle tissue. After we produce an updated reference database, we will evaluate the Dokai et al (2023) freshwater mussel primers to confirm their efficacy for Adirondack freshwater mussel species. Future sampling efforts should incorporate searches for mussels into standard macroinvertebrate surveys to provide confirmatory manual sampling. It remains unclear whether mussel eDNA can be effectively integrated into plans for future analyses, but we recommend that the team continue to seek an effective way to address this vulnerable taxon for which traditional field surveys are challenging and time-consuming.

Data availability

All sampling metadata has been deposited in the EPA Water Quality eXchange (WQX) database with notes in the "Result Comment" header mentioning that the sampled water was stored as an eDNA filter and that the raw sequence data is hosted by the National Institutes of Health National Center for Biotechnology Information (NIH NCBI) short read archive (SRA) under BioProject PRJNA1246971, as is typical for sequence data. All SCALE pilot eDNA samples are uploaded on the WQX platform by the organization ID "CORNELLSCALE" under project "SCALE".

Stable Isotopes

Overview and motivation

This pilot study was designed to address a set of four sampling uncertainties to guide future SCALE research. First, we wanted to test whether stable isotope compositions of benthic macroinvertebrate taxa are consistent within the same lake across seasons, despite potential shifts in benthic macroinvertebrate community composition and trophic ecology. Second, we wanted to identify which macroinvertebrate taxa are commonly observed across most lakes, and test whether stable isotope analysis of benthic macroinvertebrate tissues can reveal food web patterns in Adirondack lakes. Third, we wanted to explore whether hydrogen and sulfur isotopes could help refine understanding of the contribution of terrestrial energy sources and deep-water deoxygenation, respectively, to the food web. Finally, we wished to resolve how many different sites within a lake should be sampled to obtain a representative isotopic baseline from macroinvertebrates. To address all these issues, we sampled four lakes during one season and eight lakes during two seasons for both benthic macroinvertebrates and their potential food

resources (i.e. periphyton, leaves, and zooplankton). When possible, we also collected fishes to represent higher trophic levels.

The characterization of food webs through stable isotope analysis requires an appropriate lake-specific baseline to enable comparisons across different ecosystems (Post 2002). We surveyed benthic macroinvertebrates to determine the most appropriate taxa to use as isotopic baselines during surveys of Adirondack lakes. This work is a key step in preparing for food web sampling and analysis for SCALE, including interpretation of results from fishes. Invertebrate taxa used to establish isotopic baselines for ecosystem comparisons should be commonly found across the landscape, and should include primary consumers (i.e., algae grazers or filter feeders). Mollusks are commonly used in this context (Post 2002), but the low calcium availability of Adirondack waters—especially following a century of acid precipitation—makes them challenging to find.

Sample collection process

We conducted three tiers of lake sampling intensity for stable isotope analyses of animal tissues: "seasonal with site intensity", "seasonal", and "fall only" (**Table 7**). This series of sampling approaches was designed to balance sampling intensity within a lake against the number of lakes included in comparisons. Taken together, the datasets were intended to address all four study design questions indicated earlier by informing the amount of variance attributable to sites within lakes, seasonal variation, and between-lake differences.

At each site, we conducted traditional sampling of benthic macroinvertebrates with either D-Frame net sweeps or searches, both of which are frequently used in isotopic baseline surveys (Post 2002; Jardine, Kidd and Cunjak 2009). We conducted three, thirty-second sweeps using a D-Frame net and combined all samples to form a composite sample of benthic macroinvertebrates for each site. Additionally, ten-minute searches were conducted by manually searching woody debris and rocks for clinging macroinvertebrates that would be missed in D-Frame net sweeps. We also sampled leaves and periphyton from each lake through manual grabs and scrapes. We sampled zooplankton from each lake with a 64µm zooplankton tow taken vertically from the thermocline to the surface. Finally, we collected fish, when possible, to verify that the sampled invertebrates provide a robust basis for interpreting the isotopic composition of fishes in the same lake. After collection, benthic macroinvertebrates and zooplankton were placed in clean water and were held for at least 12 hours in order to evacuate their gut contents. After collection and gut evacuation, tissue samples from each taxon were frozen for later processing in the lab at Cornell.

Table 7. Sampling strategies that describe the seasonal and site intensity used within each lake.

		Sites Sampled	
Category	Water	Spring	Fall
Seasonal with site intensity	Dart Lake	4	2
	Moss Lake	4	2
Seasonal	Sagamore Lake	2	2
	Rondaxe Lake	2	2
	Upper Cascade Lake	2	2
	Little Clear Pond	2	2
	East Copperas Pond	2	2
	Heart Lake	2	2
Fall only	Little Moose Lake	0	2
	East Lake	0	2
	Combs Lake	0	2
	Green Lake	0	2

Laboratory processing

In the lab, all benthic macroinvertebrates were identified to the lowest possible taxonomic unit using Freshwater Macroinvertebrates of Northeastern North America (Peckarsky et al. 1990) and enumerated. For stable isotope analysis, we analyzed whole invertebrates. Each invertebrate was inspected to determine if the gut tract was empty. If the gut tract had not evacuated during the overnight holding period mentioned above, we removed it. However, if the gut tract had evacuated, we left invertebrates whole. Periphyton and zooplankton samples were processed as bulk samples and were not identified past assemblage type. Leaves were attributed to a tree species based on their shape, and we sampled only leaf material (no woody petiole or veins). Fishes were identified to species, and dorsal white muscle was dissected out for analysis (no skin, scales, or bones).

We oven-dried all samples (60C, 48 hours), then ground them into a fine powder using a spatula inside their glass storage vial. We analyzed all samples for $\delta^{13}C$ and $\delta^{15}N$, then processed ~ 25% of samples for $\delta^{34}S$ and $\delta^{2}H$.

Benthic macroinvertebrate distributions

We identified a broad variety of macroinvertebrate taxa in the surveyed Adirondack lakes. The most commonly observed taxa included Odonata, Ephemeroptera, Amphipoda, and

Trichoptera (**Table 8**). We calculated three metrics to determine how common each taxon was across lakes, sites, and seasons. First, we quantified lake-level occurrence as the proportion of lakes in which a taxon was present in at least one sample (N = 12). Second, we calculated site-level occurrence by averaging, across lakes and seasons, the proportion of sites within each lake where the taxon was detected. Finally, we assessed seasonality using only lakes sampled in both seasons, calculating the proportion of those lakes where the taxon occurred in both spring and summer.

We did not find any single species of macroinvertebrate across all lakes, indicating that we will likely need to obtain a range of taxa in order to be confident that we can develop comparable baseline isotope ratios based on an overlapping set of taxa across all waterbodies. Most common taxa were observed from a particular lake during both spring and fall. The within-lake distribution of taxa also varied; some families frequently occurred at all sampled sites (e.g., Heptageniidae), while others (e.g., Polycentropodidae) were typically observed at only a subset of sites within a lake (**Table 8**).

Table 8. Details of the most frequently observed taxa across the twelve surveyed lakes. Values represent how broadly species were distributed across lakes (proportion of lakes), across sites within a lake (proportion of sites within a lake, averaged across lakes), and across seasons within a lake (average across lakes of likelihood of being observed at 1 or more sites in one season [0.5] vs. both seasons [1.0]).

Order	Family	Prop. of Lakes	Avg. Prop. of Sites	Seasonality
odonata	libellulidae	0.92	0.67	0.77
diptera	chironomidae	0.83	0.68	0.80
odonata	aeshnidae	0.83	0.60	0.87
odonata	coenagrionidae	0.75	0.84	0.95
odonata	corduliidae	0.67	0.65	0.87
ephemeroptera	heptageniidae	0.67	0.88	0.93
amphipoda	talitridae	0.58	0.84	0.89
odonata	gomphidae	0.58	0.82	0.94
trichoptera	polycentropodidae	0.58	0.36	0.80

Benthic macroinvertebrate trophic positions and source contributions

We estimated trophic positions by standardizing the $\delta^{15}N$ values of macroinvertebrates against that of basal resources (i.e., zooplankton, periphyton, and leaves) within each lake, accounting for the expected fractionation between trophic positions (3.4 ‰ $\delta^{15}N$) (Post 2002). From the estimated trophic positions, we distilled a list of taxa that could potentially serve as low-trophic position (median <1.5) reference points (“baselines”) across lakes. For these taxa, we further examined their variation within a lake based on sampling season and site (**Figure 27**).

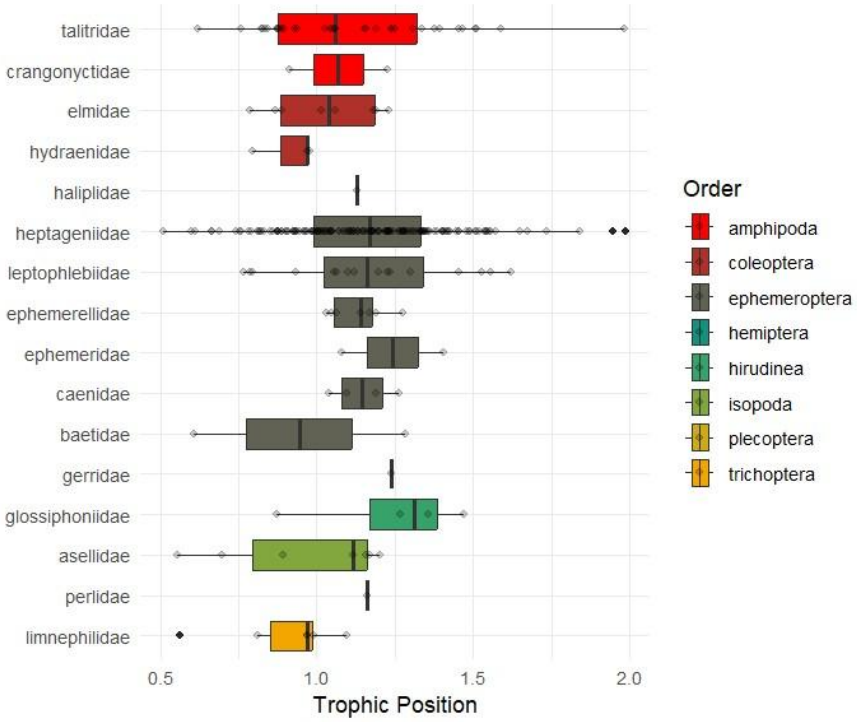

Figure 27. Estimated trophic positions for a subset of the surveyed taxa that had median trophic positions less than 1.5, indicating the taxon's potential to represent a baseline.

It is ideal to identify a suite of animal taxa that provide a baseline for each major energy flow pathway fueling the food web (periphyton, phytoplankton, terrestrial inputs). Thus, we used stable isotope ratios measured from periphyton, zooplankton, and tree leaves as endmembers for estimating energy flow to each macroinvertebrate taxon using three-source mixing models of $\delta^{13}C$ and $\delta^{15}N$ in the R package 'simmr' (version 0.5.1.216; (Parnell et al. 2010). This allowed us to identify which taxa had high proportional contributions from periphyton (to represent the benthic baseline) for comparison to zooplankton (which represents the pelagic baseline; **Figure 28**).

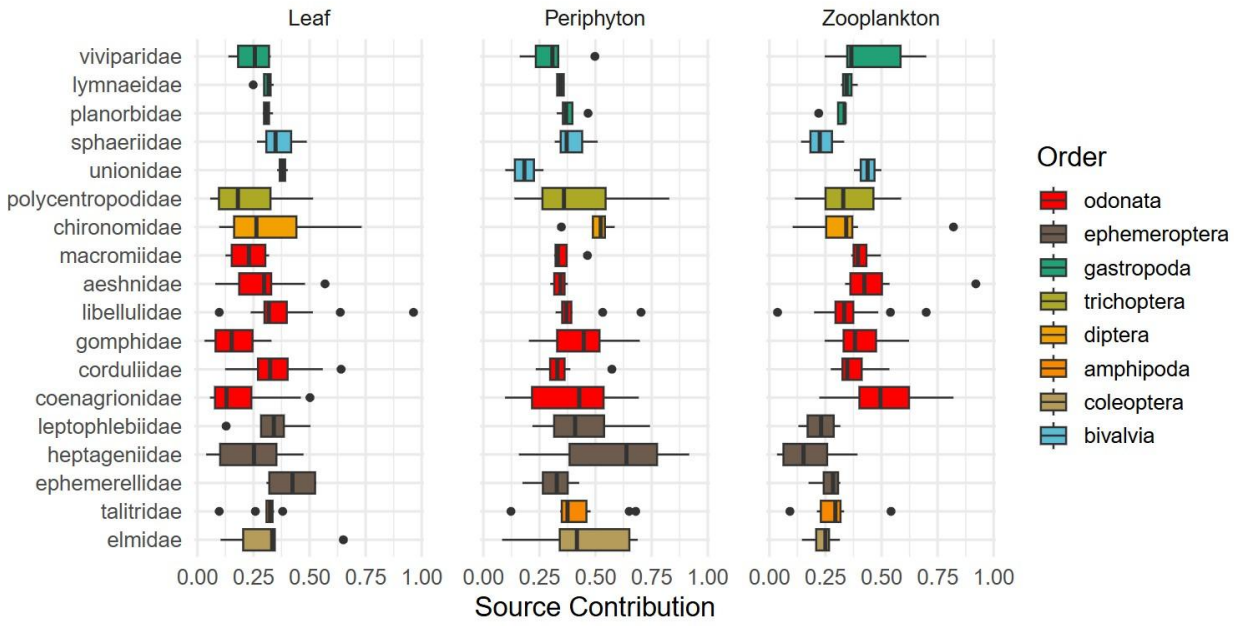

Figure 28. Contribution of isotopic baselines for terrestrial subsidies (e.g. leaves), benthic baselines (e.g. periphyton), and offshore baselines (e.g. zooplankton).

Seasonal effect on trophic position and source contributions

After correcting for baseline variation, we found no consistent differences by season across lake macroinvertebrate taxa, indicated by minimal variation in both their trophic positions and energy source contributions between seasons. This suggests that sampling just once between May and September should be adequate to capture variation in lake-level differences in isotope baselines.

Site-level variation in baselines

If macroinvertebrates used to estimate baseline stable isotope ratios are themselves spatially variable within a lake, it could add substantial uncertainty to all subsequent calculations. Our pilot sampling was designed to resolve the magnitude of variation within a taxon across sites in the same lake, and whether there were systematic spatial differences across all taxa. We quantified the 95% confidence intervals for the entire macroinvertebrate community for $\delta^{15}N$ and $\delta^{13}C$, and found extensive overlap in most cases, indicating little site-specific variation.

Moss Lake (MSL) and Dart Lake (DTL) were sampled in both seasons and with extra sites in Spring. One of the four DTL sites showed minimal overlap with the other three sites during Spring sampling (**Figure 29**). In most other cases, there was sufficient overlap in community isotope space to infer that spatial variation is relatively minor. In addition, to the extent that

there were spatial differences, they arose primarily on the $\delta^{13}C$ axis rather than $\delta^{15}N$. Given that the isotopic composition of macroinvertebrates was occasionally different among sites within each lake, we suggest that future SCALE sampling should include at least two sites per lake to establish isotopic baselines

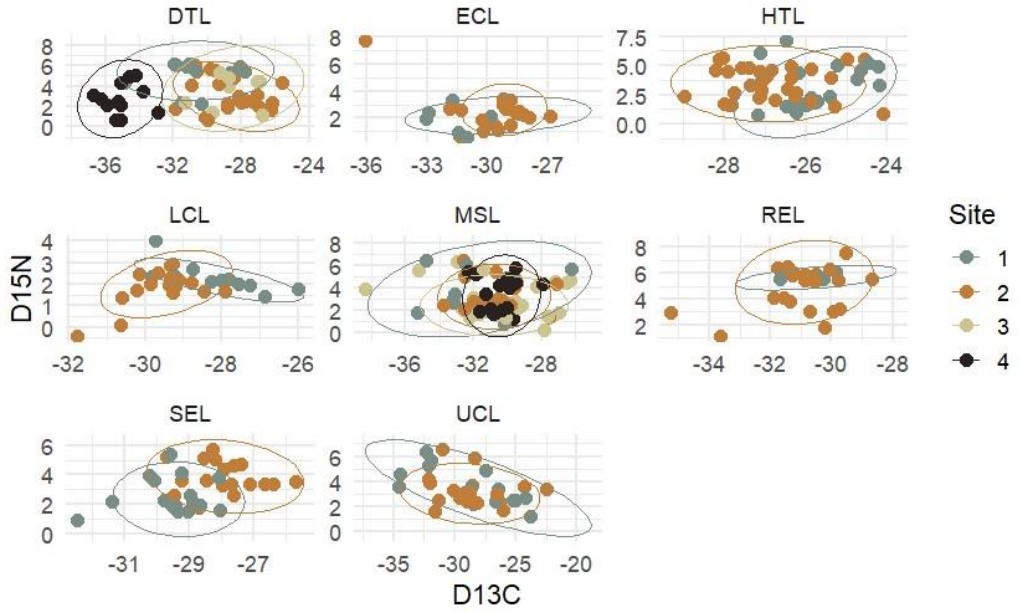

Figure 29. Evaluating inter-site differences in isotopic composition (δ13C and δ15N) of benthic macroinvertebrates from lakes sampled during the spring. Each panel is a lake, and the color indicates the nearshore site within each lake. Points represent raw isotopic compositions for individual samples with 95% confidence intervals around all individuals at each site. The sampled taxa in each lake include 1-12 families of benthic macroinvertebrates representing snails, midges, beetles, mayflies, caddisflies, alderflies, damselflies, and dragonflies.

Isotopic composition of fishes

We analyzed fish from a subset of the sampled lakes to ensure that the results from benthic macroinvertebrates and basal resources were adequate to interpret energy flow and trophic position of fishes, which will be a key objective for SCALE. We found that fishes were consistently higher in $\delta^{15}N$, as expected, than all basal resources. Their $\delta^{13}C$ was also intermediate between tree leaves and periphyton in most lakes and fell within the range of macroinvertebrate taxa in all cases (**Figure 30**). Thus, we have no concern about being able to use basal resource and macroinvertebrate samples to interpret the energy flow and trophic position of fishes in Adirondack Lakes.

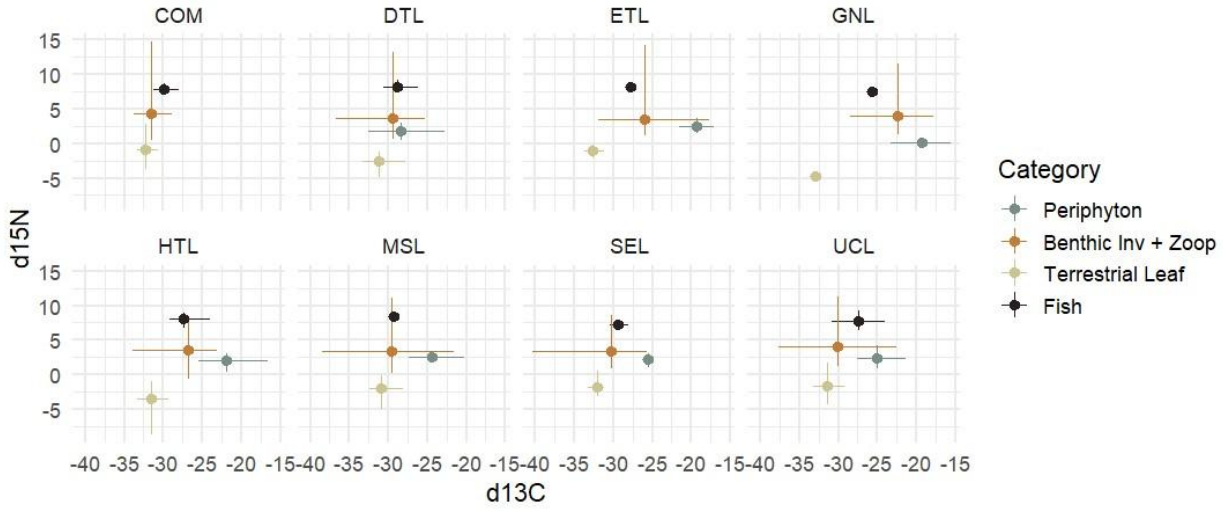

Figure 30. Summary of the isotopic ranges for both δ13C and δ15N for all major biotic groups sampled during the pilot, as represented by color. Each point represents the mean isotopic composition for that group with the range of each isotope represented by the vertical and horizontal lines.

Deuterium and sulfur isotopes

Our goal in quantifying δ^2H and $\delta^{34}S$ for a subset of samples was to determine whether these less-used isotope ratios would be useful for resolving the influence of terrestrial energy subsidies (δ^2H differs sharply between terrestrial and aquatic primary producers) and low oxygen conditions ($\delta^{34}S$ is highly redox sensitive due to fractionation during sulfate reduction) on Adirondack lake food webs. We found a clear positive relationship between δ^2H of benthic macroinvertebrates and the [DOC] across all sampled lakes. There were no consistent seasonal shifts in δ^2H. This suggests that inputs of terrestrial carbon to lakes enhance the δ^2H of the food web (**Figure 31**), hence δ^2H can be used as a broad proxy for terrestrial energy subsidies.

For $\delta^{34}S$, we compared the $\delta^{34}S$ compositions of all benthic macroinvertebrates to the minimum depth (m) at which low oxygen concentrations (< 5 mg/L dissolved oxygen) arise. This depth was unique to each lake and was determined from oxygen profiles collected during each sampling visit. We found no strong relationship between the $\delta^{34}S$ and the depth where oxygen stress began (**Figure 31**). Thus, we recommend further investigation of the causes of differences among lakes in $\delta^{34}S$ before it is integrated deeply into SCALE.

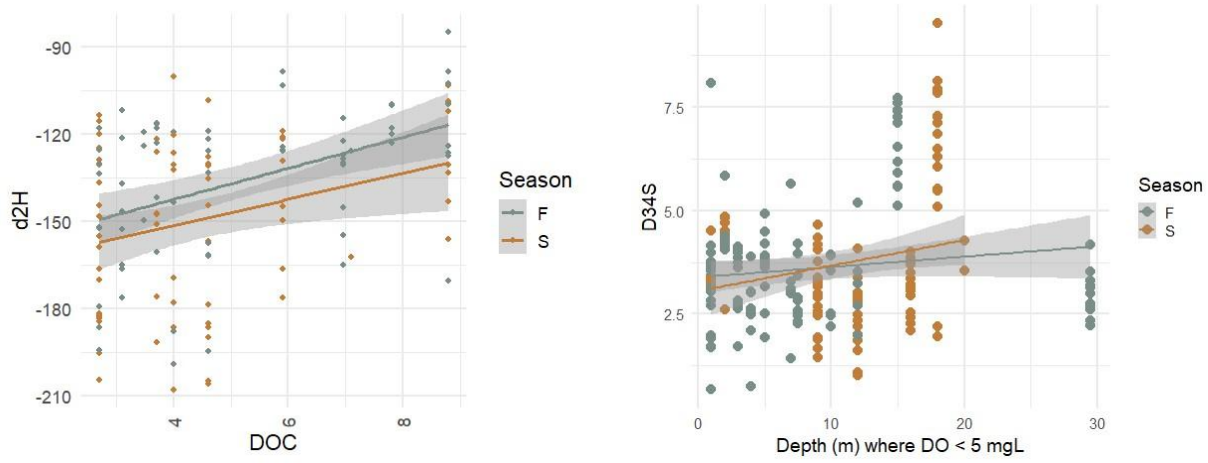

Figure 31. (Left) δ2H of macroinvertebrates increases with dissolved organic carbon (DOC) concentrations, suggesting a positive relationship between dissolved organic carbon and the contribution of terrestrial energy subsidies to lake food webs. (Right) δ34S shows no strong relationship with the depth where oxygen stress begins (5 mg/L).

Baseline candidates

We identified a set of primary consumers (trophic position ~ 1) that can serve as useful indicators of the baseline for major energy inputs to food webs in Adirondack lakes. We have selected the most common of these taxa, Heptageniidae, as the primary taxon to represent periphyton baselines. Given the heterogeneity of benthic macroinvertebrates communities across sites, seasons, and lakes, we also selected a set of secondary taxa that should be collected from sites where Heptageniidae cannot be found. These taxa include other Ephemeroptera and several families of snails (when available). We also recommend that zooplankton samples be taken at multiple locations within the lake as no benthic macroinvertebrates adequately represented the planktonic energy pathway.

Recommendations for future field sampling for SCALE

Our pilot sampling was designed to determine the value of using stable isotope analysis of benthic macroinvertebrates to characterize food webs across Adirondack lakes, and to guide decisions about the number of lakes, sites within lakes, and seasons of the year to target for stable isotope sampling for SCALE. Our analyses of the same macroinvertebrate taxa from the same lake in different seasons suggests that stable isotope composition of benthic macroinvertebrates is quite temporally stable compared to differences among lakes. Nonetheless, we recommend that SCALE sampling be focused on the May-Sept warm season to minimize any minor seasonal effects. The medium- and high-intensity lakes may offer an opportunity to further test for finer-scale seasonality of stable isotope ratios within a lake.

Second, our pilot sampling indicated that benthic macroinvertebrate communities vary widely across lakes, complicating the design of a simple, consistent set of taxa for comparisons across SCALE lakes. Despite this heterogeneity in benthic macroinvertebrate communities, we were able to identify a portfolio of taxa that can be found across most sites and will provide a robust baseline for cross-lake comparisons. Differences in benthic macroinvertebrate communities reflected the availability of various habitat types; large, deep lakes had different nearshore communities compared to shallow, boggy lakes. Additionally, we aimed to determine if the benthic macroinvertebrate communities can reveal food web patterns within Adirondack lakes. We observed that the benthic macroinvertebrate communities adequately represented the range of isotopic composition of fish tissues within lakes where both were sampled. We also observed expected differences in isotopic compositions between the benthic macroinvertebrate functional guilds, suggesting that stable isotope ratios are functioning well to showcase the trophic diversity of benthic macroinvertebrate communities.

For our third objective, we evaluated the usefulness of $\delta^{2}H$ and $\delta^{34}S$ as tracers of terrestrial energy sources and environmental deoxygenation, respectively. We found that $\delta^{2}H$ displayed the expected relationship with terrestrial subsidies (in the form of DOC), suggesting that measuring hydrogen isotopes from a modest subset of samples will be useful to describe differences among lake food webs in terrestrial energy inputs. In contrast, there were no clear patterns of $\delta^{34}S$ with respect to observed deep-water deoxygenation. Further work would be needed to resolve appropriate inferences from $\delta^{34}S$ in Adirondack lakes.

Our fourth and final objective was to determine how many different sites within a lake should be sampled to represent isotopic baselines using benthic macroinvertebrates. We found moderate spatial variation among sites in a few lakes, but most lakes exhibited consistent isotopic composition of benthic macroinvertebrate communities across sites. Therefore, we recommend sampling from multiple sites per lake in order to establish an isotopic baseline against which to interpret results from fish.

This pilot study also provided an opportunity to test and refine methods for rapid collection of invertebrates from lakes of all sizes. For nearshore samples, we conclude that targeted searches of microhabitats favored by specific taxa will be the most efficient way to sample macroinvertebrates for isotopic baselines. If broader collections are needed, timed sweeps with D-frame nets were also effective but yielded large amounts of detritus that must be sorted. Because zooplankton tows are straightforward, and zooplankton are essential as the pelagic endmember for quantifying energy sources for the food web, we recommend collecting samples from multiple offshore locations. Similarly, to represent terrestrial-derived energy inputs, we recommend collecting fresh leaves from three common tree or shrub species in the riparian zone of each lake.

Next steps

The recommendations outlined above will be incorporated into the QAPP and field protocols for Year-1 of full sampling for SCALE in 2025. Our most important findings are that stable isotope samples may be collected any time during the warm season but should be collected from multiple sites within each lake to account for potential spatial variation. To characterize the base of the food web in each waterbody, baseline collections at each lake will be sampled from at least three sites along the perimeter in the littoral zone and three pelagic sites. Fish collections within the lake will occur within 1km of any baseline sampling site. In larger waterbodies, we will sample from a maximum of 5 sampling sites to increase our chances of encountering fish taxa that may partition the potentially more heterogeneous environment. All baseline sampling sites will be no further than 1 mi from another site. We will not specifically target particular habitats. We will continue to assess which macroinvertebrates are most suitable as secondary taxa for quantifying isotopic baselines, thereby ensuring commensurate comparisons across lakes. All these lessons will help to ensure the success of SCALE sampling in Year-1 and beyond.

Data availability

All stable isotope and taxon information were made publicly available through the EPA's Water Quality Exchange (WQX) portal by the organization ID "CORNELLSCALE" under project "SCALE".

References

Blanchet, Clarisse C., Céline Arzel, Aurélie Davranche, Kimmo K. Kahilainen, Jean Secondi, Sami Taipale, Henrik Lindberg, et al. 2022. "Ecology and extent of freshwater browning - What we know and what should be studied next in the context of global change." *Science of the Total Environment* 812: 152420.

Bolger, Anthony M, Marc Lohse, and Bjoern Usadel. 2014. "Trimmomatic: a flexible trimmer for Illumina sequence data." *Bioinformatics* 30 (15): 2114-2120.

Boucher, Julien, Florian Faure, Olivier Pompini, Zara Plummer, Olivier Wieser, and Luiz Felippe de Alencastro. 2019. "(Micro) plastic fluxes and stocks in Lake Geneva basin." *TrAC Trends in Analytical Chemistry* 112: 66-74.

Callahan, Benjamin J, Paul J McMurdie, Michael J Rosen, Andrew W Han, Amy Jo A Johnson, and Susan P Holmes. 2016. "DADA2: High-resolution sample inference from Illumina amplicon data." *Nature Methods* 13 (7): 581-583.

Camacho, Christiam, George Coulouris, Vahram Avagyan, Ning Ma, Jason Papadopoulos, Kevin Bealer, and Thomas L Madden. 2009. "BLAST+: architecture and applications." *BMC Bioinformatics* 10 (421).

Cuthbert, Iain D., and Paul del Giorgio. 1992. "Toward a standard method of measuring color in freshwater." *Limnology and Oceanography* 37 (6): 1319-1326.

Daniels, Robert A, Richard S Morse, James W Sutherland, Robert T Bombard, and Charles W Boylen. 2008. "Fish Movement Among Lakes: Are Lakes Isolated." *Northeastern Naturalist* 15 (4): 577-588.

Daniels, Robert A, Bombard, Robert T, Sutherland, James W, and Charles W Boylen. 2011. “Status of Fishes in Selected Adirondack Lakes: Eight Decades of Changing Assemblage Composition”. *The Open Fish Science Journal* 4:21-39.

De Haan, H., and T. De Boer. 1987. "Applicability of light absorbance and fluorescence as measures of concentration and molecular size of dissolved organic carbon in humic Lake Tjeukemeer." *Water Research* 21 (6): 731-734.

de Wit, Heleen A., John L. Stoddard, Donald T. Monteith, James E. Sample, Kari Austnes, Suzanne Couture, Jens Fölster, et al. 2021. "Cleaner air reveals growing influence of climate on dissolved organic carbon trends in northern headwaters." *Environmental Research Letters* 16 (10): 104009.

Dokai, William K, Patrick D Barry, Dave T Zanatta, Kristen M Gruenthal, Megan V McPhee, Peter B McIntyre, and Wesley A Larson. 2023. "Two for the price of one: eDNA metabarcoding reveals temporal and spatial variability of mussel and fish co-distributions in Michigan riverine systems." *Environmental DNA* 5 (3): 424-437.

Dove, Alistair D. M., and Thomas H Cribb. 2006. "Species accumulation curves and their applications in parasite ecology." *Trends in Parisitology* 22 (12): 568-574.

Dyba, Krzysztof, Sofia Ermida, Mariusz Ptak, Jan Piekarczyk, and Mariusz Sojka. 2022. "Evaluation of Methods for Estimating Lake Surface Water Temperature Using Landsat 8." *Remote Sensing* 14 (15): 3839.

Fellman, Jason B., Eran Hood, and Robert G. M. Spencer. 2010. "Fluorescence spectroscopy opens new windows into dissolved organic matter dynamics in freshwater ecosystems: A review." *Limnology and Oceanography* 55 (6): 2452-2462.

Gaudard, Adrien, Love Råman Vinnå, Fabian Bärenbold, Martin Schmid, and Damien Bouffard.

2019. "Toward an open access to high-frequency lake modeling and statistics data for scientists and practitioners – the case of Swiss lakes using Simstrat v2.1." *Geoscientific Model Development* 12 (9): 3955-3974.

Guenay-Greunke, Yasemin, David A Bohan, Michael Traugott, and Corinna Wallinger. 2021. "Handling of targeted amplicon sequencing data focusing on index hopping and demultiplexing using a nested metabarcoding approach in ecology." *Scientific Reports* 11: 19510.

Gueymard, Christian A. 2001. "Parameterized transmittance model for direct beam and circumsolar spectral irradiance." *Solar Energy* 71 (5): 325-346.

Gueymard, Christian A. 2019. "The SMARTS spectral irradiance model after 25 years: New developments and validation of reference spectra." *Solar Energy* 187: 233-253.

Gueymard, Christian. 1995. *SMARTS2, A Simple Model of the Atmospheric Radiative Transfer of Sunshine: Algorithms and performance assessment.* Florida Solar Energy Center/University of Central Florida.

Hadziavdic, Kenan, Katrine Lekang, Anders Lanzen, Inge Jonassen, Eric M Thompson, and Christofer Troedsson. 2014. "Characterization of the 18S rRNA Gene for Designing Universal Eukaryote Specific Primers." *PLoS ONE* 9 (2): e87624.

Helms, John R., Aron Stubbins, Jason D. Ritchie, Elizabeth C. Minor, David J. Kieber, and Kenneth Mopper. 2008. "Absorption spectral slopes and slope ratios as indicators of molecular weight, source, and photobleaching of chromophoric dissolved organic matter." *Limnology and Oceanography* 53 (3): 955-969.

Hersbach, Hans, Bill Bell, Paul Berrisford, Shoji Hirahara, András Horányi, Joaquín MuñozSabater, Julien Nicolas, et al. 2020. "The ERA5 global reanalysis." *Quarterly Journal of the Royal Meteorological Society* 146 (730): 1999-2049.

Keck, François, Jeanine Brantschen, and Florian Altermatt. 2023. "A combination of machinelearning and eDNA reveals the genetic signature of environmental change at the landscape levels." *Molecular Ecology* 32 (17): 4791-4800.

Laxson, Corey, Elizabeth Yerger, Hunter Favreau, Sean Regalado, and Daniel Kelting. 2018. *Adirondack Lake Assessment Program: 2018 Report.* Adirondack Watershed Institute.

Leach, Taylor H., Luke A. Winslow, Frank W. Acker, Jay A. Bloomfield, Charles W. Boylen, Paul A. Bukaveckas, Donald F. Charles, et al. 2018. "Long-term dataset on aquatic responses to concurrent climate change and recovery from acidification." *Scientific Data* 5: 180059.

Leese, Florian, Mandy Sander, Dominik Buchner, Vasco Elbrecht, Peter Haase, and Vera M. A. Zizka. 2021. "Improved freshwater macroinvertebrate detection from environmental DNA through minimized nontarget amplification." *Environmental DNA* 3 (1): 261-276.

McKnight, Diane M., Elizabeth W. Boyer, Paul K. Westerhoff, Peter T. Doran, Thomas Kulbe, and Dale T. Anderson. 2001. "Spectrofluorometric characterization of dissolved organic matter for indication of precursor organic material and aromaticity." *Limnology and Oceanography* 46 (1): 38-48.

Miya, M, Y Sato, T Fukunaga, T Sado, J Y Poulsen, K Sato, T Minamoto, et al. 2015. "MiFish, a set of universal PCR primers for metabarcoding environmental DNA from fishes: detection of more than 230 subtropical marine species." *Royal Society Open Science* 2 (7): 2:150088.

Monteith, Donald T., John L. Stoddard, Christopher D. Evans, Heleen A. de Wit, Martin Forsius, Tore Høgåsen, Anders Wilander, et al. 2007. "Dissolved organic carbon trends resulting from changes in atmospheric deposition chemistry." *Nature* 450: 537-540.

Moore, Tadhg N., Jorrit P. Mesman, Robert Ladwig, Johannes Feldbauer, Freya Olsson, Rachel M. Pilla, Tom Shatwell, et al. 2021. "LakeEnsemblR: An R package that facilitates ensemble modelling of lakes." *Environmental Modelling and Software* 143: 105101.

Moran, Mary Ann, Wade M. Jr. Sheldon, and Richard G. Zepp. 2000. "Carbon loss and optical property changes during long-term photochemical and biological degradation of estuarine dissolved organic matter." *Limnology and Oceanography* 45 (6): 1254-1264.

National Centers for Environmental Information. n.d. *Air Temperature.*

Ossola, Rachele, Oskar Martin Jönsson, Kyle Moor, and Kristopher McNeill. 2021. "Singlet Oxygen Quantum Yields in Environmental Waters." *Chemical Reviews* 121 (7): 41004146.

Page, Benjamin P., Leif G. Olmanson, and Deepak R. Mishra. 2019. "A harmonized image processing workflow using Sentinel 2/MSI and Landsat 8/OLI for mapping water clarity in optically variable lake systems." *Remote Sensing of Environment* 231 (15): 111284.

Partanen, Sarah B., Jennifer N. Apell, Jianming Lin, and Kristopher McNeill. 2021. "Factors affecting the mixed-layer concentrations of singlet oxygen in sunlit lakes." *Environmental Science: Processes & Impacts* 23 (8): 1130-1145.

Peterson, Britt M., Ann M. McNally, Rose M. Cory, John D. Thoemke, James B. Cotner, and Kristopher McNeill. 2012. "Spatial and Temporal Distribution of Singlet Oxygen in Lake Superior." *Environmental Science & Technology* 46 (13): 7222-7229.

Ritchie, Jerry C., Charles M. Cooper, and Jiang Yongqing. 1987. "Using landsat multispectral scanner data to estimate suspended sediments in Moon Lake, Mississippi." *Remote Sensing of Environment* 23 (1): 65-81.

Roy, Karen, and James Dukett. 2017. *Adirondack Lakes Long Term Monitoring (NY), 1992-2011 ver 1.* 04 11.

Roy, Karen, and James Dukett. 2017. *Adirondack Lakes Survey (NY): summer surface chemistry datat, 1984-1987 ver. 2.* July 07.

Soranno, Patricia A., Edward G. Bissell, Kendra S. Cheruvelil, Samuel T. Christel, Sarah M. Collins, C Emi Fergus, Christopher T. Filstrup, et al. 2015. "Building a multi-scaled geospatial temporal ecology database from disparate data sources: fostering open science and data reuse." *Gigascience* 4: 28.

Soranno, Patricia A., Linda C. Bacon, Michael Beauchene, Karen E. Bednar, Edward G. Bissell, Claire K. Boudreau, Marvin G. Boyer, et al. 2017. "LAGOS-NE: a multi-scaled geospatial and temporal database of lake ecological context and water quality for thousands of US lakes." *Gigascience* 6 (12): 1-22.

Turley, Matt D, Gary S Bilotta, Chris A Extence, and Richard E Brazier. 2014. "Evaluation of a fine sediment biomonitoring tool across a wide range of temperate rivers and streams." *Freshwater Biology* 59 (11): 2268-2277.

Twardowski, Michael S., Emmanuel Boss, James M. Sullivan, and Percy L. Donaghay. 2004. "Modeling the spectral shape of absorption by chromophoric dissolved organic matter." *Marine Chemistry* 89 (1): 69-88.

U.S. Geological Survey. n.d. *National Hydrography Dataset.*

Viger, Roland J., Alan H. Rea, Jeffrey D. Simley, and Karen M. Hanson. 2016. "NHDPlusHR: A national geospatial framework for surface-water information." *American Water Resources Association* 52 (4): 901-905.

Wan, Z., S. Hook, and G. Hulley. 2015. "MODIS/Terra Land Surface Temperature/Emissivity 8-Day L3 Global 1km SIN Grid V061." *NASA EOSDIS Land Processes Distributed Active Archive Center.* Vol. 10.

Weishaar, James L., George R. Aiken, Brian A. Bergamaschi, Miranda S. Fram, Roger Fujii, and Kenneth Mopper. 2003. "Evaluation of specific ultraviolet absorbance as an indicator of the chemical composition and reactivity of dissolved organic carbon." *Environmental Science & Technology* 37 (20): 4702-4708.

Wen, Hai B, Zhe M Cao, Dan Hua, Pao Xu, Xue Y Ma, Xin H Yuan, and Ruo B Gu. 2017. "The Complete Maternally and Paternally Inherited Mitochondrial Genomes of a Freshwater Mussel Potamilus alatus (Bivalvia: Unionidae)." *PloS One* 12 (1): e0169749.

Wilson, Henry F., and Marguerite A. Xenopoulos. 2008. "Effects of agricultural land use on the composition of fluvial dissolved organic matter." *Nature Geoscience* 2: 37-41.

Winslow, Luke, Jordan Read, Richard Woolway, Jennifer Brentrup, Taylor Leach, Jake Zwart, Sam Albers, and Doug Collinge. 2019. *rLakeAnalyzer: Lake Physics Tools.* June 9.

Woolway, R. Iestyn. 2023. "The pace of shifting seasons in lakes." *Nature Communications* 14: 2101.

Zhang, Hongbo, Fan Zhang, Guoqing Zhang, Yaoming Ma, Kun Yang, and Ming Ye. 2018. "Daily air temperature estimation on glacier surfaces in the Tibetan Plateau using MODIS LST data." *Journal of Glaciology* 64 (243): 132-147.

Zsolnay, Adam, Erik Baigar, Miguel Jimenez, Bernd Steinweg, and Flavia Saccomandi. 1999. "Differentiating with fluorescence spectroscopy the sources of dissolved organic matter in soils subjected to drying." *Chemosphere* 38 (1): 45-50.

Zweig, Leanna D, and Charles F Rabeni. 2001. "Biomonitoring for deposited sediment using benthic invertebrates: a test on 4 Missouri streams." *Journal of the North American Benthological Society* 20 (4): 643-657.

Appendix

Appendix A: List of Potential Low Intensity Lakes

NHDID	LAT	LONG	PONDNAME	ELEV	WAREA	SAREA	DEPTH	HU8name
92080871	44.850319	-73.850703	MOON POND	411	687	2	2	Lake Champlain
129690692	44.567544	-73.817367	WHISTLE POND	431	40	4	3	Saranac River
92081613	44.590878	-73.770697	MUD POND	359	385	7	1	Lake Champlain
129690712	44.563381	-73.913478	MUD POND	418	946	44	2	NA
129690762	44.543939	-74.079872	LINE POND	511	10	2	11	NA
129690817	44.527550	-74.103206	LAKE KUSHAQUA	509	7387	153	28	Saranac River
129690806	44.515883	-74.124875	LITTLE HOPE POND	521	38	3	6	NA
129690808	44.511994	-74.124597	BIG HOPE POND	522	194	9	12	NA
129690813	44.505883	-74.114319	BUCK POND	507	388	53	4	Saranac River
129690823	44.488661	-74.134319	RAINBOW LAKE	508	1707	144	18	Saranac River
129690850	44.470608	-74.176544	RAINBOW LAKE INLET	508	980	35	3	Saranac River
129690852	44.476442	-74.177378	UNNAMED POND	512	10	1	8	Saranac River
129690838	44.487553	-74.166819	LOON POND	513	128	8	5	Saranac River
129690868	44.436158	-73.974036	FRANKLIN FALLS FLOW	446	76491	184	6	Saranac River
129690895	44.365883	-74.065986	MOOSE POND	472	1862	57	21	Saranac River
129690928	44.324217	-74.074597	MCKENZIE POND	506	702	97	16	Saranac River
129691038	44.260047	-74.038208	ALFORD POND	596	96	14	1	Saranac River
129691088	44.259775	-74.150992	LITTLE PINE POND	488	105	2	2	Saranac River
129691035	44.283386	-74.171269	SECOND POND	468	33362	33	3	NA
129691035	44.288664	-74.183492	FIRST POND	468	33172	29	6	NA
129690922	44.333942	-74.153489	LAKE COLBY	474	920	110	14	Saranac River
129690924	44.351167	-74.209047	MCCAULEY POND	476	159	31	4	Saranac River
129691110	44.250058	-74.282942	BARTLETT POND	475	11	1	2	Saranac River
129691099	44.284781	-74.359053	BRANDY POND	488	128	2	3	Saranac River
129691020	44.310614	-74.345442	FOLLENSBY CLEAR POND	480	1029	196	18	Saranac River
129691003	44.326447	-74.355719	POLLIWOG POND	486	332	84	24	Saranac River
129691008	44.336725	-74.367108	WEST POLLIWOG POND	486	7	1	6	NA
129691154	44.302836	-74.364608	SQUARE POND	480	427	58	17	Saranac River
129691056	44.308600	-74.355730	LITTLE ECHO POND	479	7	1	5	Saranac River
129691083	44.300892	-74.397667	LITTLE EGG POND	487	4	0	10	NA
129691085	44.299503	-74.389889	DUMP POND	485	223	12	4	NA

129691061	44.307281	-74.368497	S-W AMPHITHEATER POND	480	2	0	7	NA
129691051	44.312003	-74.371831	EAST COPPERAS POND	479	15	4	6	NA
129691055	44.313947	-74.383778	NORTH WHEY POND	488	9	1	8	NA
129691046	44.316169	-74.382944	LITTLE NORTH WHEY	488	9	1	5	NA
129691004	44.337003	-74.371553	MIDDLE POND	484	182	24	3	NA
129691011	44.337558	-74.394333	UNNAMED POND	485	53	3	5	Saranac River
129691001	44.343392	-74.397111	MARSH POND	494	12	2	7	NA

129691017	44.339781	-74.411833	EAST PINE POND	484	115	26	10	Saranac River
129690990	44.353114	-74.413222	PINK POND	492	221	5	4	Saranac River
129690981	44.355614	-74.416000	NORTH PINK POND	489	41	2	3	Saranac River
129690942	44.368947	-74.392664	LONG POND #3	494	22	1	1	Saranac River
129690952	44.365614	-74.383219	SLANG POND	491	1013	20	7	Saranac River
129690949	44.358114	-74.359053	HOEL POND	493	652	182	24	Saranac River
129690964	44.347836	-74.336275	CHURCH POND	492	52	11	18	NA
129691034	44.326447	-74.411278	UNNAMED POND	480	4	1	3	Saranac River
129691090	44.323669	-74.409611	ROLLINS POND	480	2996	180	24	Saranac River
129691053	44.317281	-74.424611	UNNAMED POND LOWER	482	221	4	4	NA
129691060	44.304225	-74.398778	WHEY POND	481	133	43	6	Saranac River
129691107	44.276169	-74.387667	DEER POND	490	174	47	20	Saranac River
129690983	44.338114	-74.343219	GREEN POND	481	135	26	18	Saranac River
129690946	44.352833	-74.311272	RAT POND	492	79	12	9	Saranac River
129690961	44.344778	-74.300161	SUNDAY POND	485	109	4	11	NA
129690930	44.355333	-74.285439	LITTLE CLEAR POND	487	631	142	24	Saranac River
129690936	44.358667	-74.297383	LITTLE GREEN POND	488	69	28	12	NA
129690919	44.372278	-74.289328	GRASS POND	492	39	8	10	Saranac River
129690945	44.352278	-74.294328	SOCHIA POND	500	10	2	6	NA
129690937	44.348389	-74.276828	LAKE CLEAR OUTLET	491	2803	47	3	Saranac River
129690937	44.348389	-74.276828	LAKE CLEAR OUTLET	491	2803	47	3	Saranac River
129690910	44.379500	-74.261269	ST. GERMAIN POND	497	47	5	5	Saranac River
129690921	44.368944	-74.277383	CONLEY LINE POND	497	24	1	5	Saranac River
129691103	44.267558	-74.290997	TAMARACK POND	472	222	6	3	Saranac River

115353579	44.480881	-73.716253	UNNAMED POND	375	15	2	2	Ausable River
115353631	44.424214	-73.849311	MORGAN(COOPER KILL) POND	922	26	1	1	Ausable River
115353747	44.330881	-73.917092	WARREN POND	561	70	2	4	Ausable River
115353767	44.323103	-73.902922	OWEN POND	515	1139	8	9	Ausable River
115353749	44.329214	-73.881533	MARSH POND	558	263	4	1	Ausable River
115353811	44.294214	-73.942647	BIG CHERRYPATCH POND	504	230	5	5	Ausable River
115353787	44.307825	-73.942092	TOM PECK POND	521	122	4	5	Ausable River
115353799	44.295881	-73.965425	ECHO LAKE	570	61	7	2	Ausable River
115353875	44.242269	-73.883756	UNNAMED POND	685	40	0	2	Ausable River
115353967	44.148664	-74.037650	SCOTT POND	972	94	1	2	Ausable River
115353949	44.179772	-73.967092	HEART LAKE	661	63	11	17	NA
115353777	44.316158	-73.760694	CLEMENTS POND	503	60	2	6	Ausable River
115353869	44.247547	-73.879589	UNNAMED POND	678	22	1	1	Ausable River
115353879	44.237825	-73.860144	LOWER CASCADE LAKE	618	505	10	13	Ausable River
115353909	44.224492	-73.874033	UPPER CASCADE LAKE	620	231	10	19	Ausable River
115353849	44.256992	-73.712639	LOST POND	863	38	1	1	Ausable River
115353975	44.143939	-73.738469	GIANT WASHBOWL	695	46	1	7	Ausable River
92082313	44.284772	-73.556244	BIG POND	188	1115	22	2	NA
115353641	44.399492	-73.651528	DOYLE POND	262	336	4	4	Ausable River

92083097	44.116164	-73.559853	RUSSET POND	454	555	9	11	Lake Champlain
92083105	44.109775	-73.549850	TANAHER POND	461	93	5	4	Lake Champlain
92083099	44.112553	-73.541239	FIFTH POND	465	10	1	6	Lake Champlain
92083133	44.123108	-73.723189	BULLET POND	469	17	0	1	Lake Champlain
92083129	44.123942	-73.732081	ROUND POND	527	132	9	11	Lake Champlain
92083177	44.100608	-73.723744	LILYPAD POND	465	40	1	1	Lake Champlain
92083153	44.106164	-73.708467	CRANBERRY POND	482	9	1	1	Lake Champlain
92083329	43.867003	-73.575403	BEAR POND	430	122	5	4	Lake Champlain
92083363	43.821172	-73.547900	LOST POND	479	56	11	10	Lake Champlain
92083367	43.839228	-73.571792	PUTNAM POND	399	1933	70	10	Lake Champlain
92083355	43.837839	-73.594014	CLEAR POND	432	65	11	18	Lake Champlain

92083365	43.834228	-73.591236	MUD POND	457	267	1	2	Lake Champlain
92083367	43.837561	-73.582347	NORTH POND	399	148	42	5	Lake Champlain
92083573	43.598400	-73.534561	LOWER BLACK MTN POND	518	135	2	4	Lake Champlain
92083569	43.597844	-73.525117	UPPER BLACK MTN POND	518	39	1	4	NA
92083521	43.657842	-73.578175	BROWN POND	277	27	1	4	Lake Champlain
92083515	43.682842	-73.644289	LONG POND	399	114	13	12	Lake Champlain
165902470	43.708397	-73.616233	UNNAMED POND	451	47	3	2	Lake Champlain
92083457	43.710342	-73.530675	JABE POND	400	230	60	23	Lake Champlain
92083451	43.712564	-73.537064	LITTLE JABE POND	419	20	2	7	Lake Champlain
92083575	43.593122	-73.516228	LAPLAND POND	524	169	4	5	Lake Champlain
92083583	43.592844	-73.521783	UNNAMED POND	524	110	0	2	Lake Champlain
92083601	43.588400	-73.527339	MILLMAN POND	571	41	2	7	Lake Champlain
92083613	43.573678	-73.536228	FISHBROOK POND	559	167	14	17	Lake Champlain
165902469	43.560622	-73.550950	BUMPS POND	582	31	2	6	NA
92083725	43.497292	-73.578725	CROSSET POND	446	147	41	32	Lake Champlain
52532837	43.430625	-73.557892	COPELAND POND	137	343	23	8	Mettawee River
52532673	43.465625	-73.602339	THIRD POND	381	108	3	15	Mettawee River
52532909	43.414514	-73.577058	HADLOCK LAKE	138	2269	84	13	Mettawee River
52532543	43.493681	-73.585669	INMAN POND	411	44	3	9	Mettawee River
52532659	43.473125	-73.550669	LAKE NEBO	255	374	50	23	Mettawee River
52533243	43.352847	-73.755119	WILKIE RESERVOIR	395	64	10	6	Mettawee River
132876070	44.753375	-73.893200	BRADLEY POND	501	1656	44	3	Chateaugay-English
132876232	44.691711	-73.958478	UNNAMED POND	489	1997	1	2	Chateaugay-English
132876274	44.675322	-73.962089	NORTH TWIN POND	532	104	10	2	Chateaugay-English
132876286	44.671433	-73.966256	SOUTH TWIN POND	532	57	5	2	Chateaugay-English
132876194	44.723100	-74.040425	MOUNTAIN POND	594	163	4	1	Chateaugay-English
132876139	44.764494	-74.190992	PETER POND	393	264	5	2	Chateaugay-English
132876182	44.750050	-74.187658	OWLSHEAD POND	423	2	0	2	Salmon
132876179	44.748939	-74.185436	CHILDS POND	442	30	1	2	Salmon
132876224	44.738383	-74.181267	FISHPOLE POND	450	45	2	2	Salmon
132876478	44.630050	-74.199600	DEBAR POND	477	747	35	9	Salmon

132876501	44.597550	-74.137653	DUCK POND	500	230	24	4	Salmon

132876492	44.601439	-74.126819	RAZORBACK POND	504	9	1	4	Salmon
132876128	44.769492	-74.110708	INGRAHAM POND	501	523	54	5	Salmon
132876321	44.705325	-74.136264	MOUNTAIN VIEW LAKE	453	11474	97	3	NA
167435690	44.690881	-74.107931	DEERFLY POND	459	103	0	2	Salmon
132876535	44.707544	-74.066539	RAGGED LAKE	528	3109	110	15	Salmon
132876536	44.744489	-74.065147	LOWER LILYPAD POND	532	980	6	2	NA
132876340	44.680325	-74.099039	GRASS POND	456	8	3	3	Salmon
135270648	44.657831	-74.319886	DEER RIVER FLOW	444	7166	160	4	St. Regis
135270641	44.650608	-74.278772	SPRING POND	449	16	1	2	St. Regis
135270613	44.660331	-74.289328	HORSESHOE POND	444	1736	21	3	NA
135271176	44.558394	-74.772136	CLEAR POND	396	52	14	7	Raquette
135271593	44.357836	-74.430722	OTTER POND	518	27	5	16	NA
135271580	44.382283	-74.437389	EAST POND	527	295	28	3	St. Regis
135271558	44.380892	-74.386831	BESSIE POND	496	205	7	15	St. Regis
135271488	44.397281	-74.378775	SKY POND	512	27	3	3	St. Regis
135271547	44.377003	-74.346831	GRASS POND	503	222	9	4	St. Regis
135271498	44.381722	-74.300439	GREEN POND	493	44	9	9	St. Regis
135271564	44.366722	-74.311550	SOUTH OTTER POND	491	168	3	3	St. Regis
135271555	44.370611	-74.313494	NORTH OTTER POND	494	102	1	3	St. Regis
135270908	44.590894	-74.574619	EAST POND	410	45	4	2	St. Regis
135270708	44.661447	-74.500447	MUD POND	395	16	3	1	St. Regis
135270716	44.657281	-74.495447	GRASS POND	384	36	2	7	St. Regis
135270711	44.660614	-74.497669	LITTLE CLEAR POND	384	36	2	14	NA
135270885	44.545886	-74.266825	NORTHERN STAR MTN. POND	510	56	1	1	St. Regis
135271022	44.518944	-74.298769	WARD POND	486	49	1	2	St. Regis
135271076	44.502833	-74.292658	UNNAMED POND	476	11	0	7	St. Regis
135271236	44.462000	-74.283492	LOST POND	518	27	2	4	NA
135271075	44.492278	-74.254047	BEAVER VALLEY POND	503	64	4	2	St. Regis
135271223	44.450331	-74.200156	JONES POND	504	1132	57	3	St. Regis

167401934	44.620336	-74.482392	UNNAMED POND	442	27	1	4	St. Regis
135271288	44.446444	-74.293494	UNNAMED POND	515	51	1	3	NA
135271322	44.436722	-74.300994	BLACK POND	498	344	29	14	NA
135271335	44.431722	-74.270436	LOWER ST. REGIS LAKE	494	4427	142	12	St. Regis
135271484	44.384500	-74.282939	ROILEY POND	499	355	6	4	St. Regis
135271461	44.389778	-74.292106	LITTLE LONG POND	504	243	33	18	St. Regis
135271439	44.391167	-74.276828	MIKES POND	497	2	1	10	NA
135271422	44.394500	-74.282383	HUMDINGER POND	506	9	1	9	St. Regis
132858821	44.412006	-75.043811	HORSESHOE POND	308	73	7	13	Grass
132859738	44.445342	-74.984919	CRANBERRY POND	302	300	8	1	Grass
132858629	44.465342	-74.961308	TWIN POND UPPER	332	12	2	4	Grass
132858799	44.379786	-74.769631	CHURCH POND	472	120	10	3	Grass
132858801	44.391175	-74.871858	BLUE POND	395	39	2	20	Grass
132858934	44.337006	-74.809356	CLEAR POND	445	53	12	3	Grass

132859654	44.231728	-74.820742	SILVER LAKE	452	145	45	6	NA
132859257	44.271450	-74.762131	SAMPSON POND	457	372	27	2	Grass
132859261	44.263672	-74.768797	EGG POND	466	5	0	1	Grass
132859085	44.282839	-74.691569	CARTRIDGE HILLS POND 3	472	4	1	7	Grass
132859280	44.255061	-74.744350	GRASS RIVER FLOW	460	11763	14	2	NA
132859126	44.267561	-74.639622	CATAMOUNT POND	462	536	41	3	NA
132859339	44.227006	-74.665178	TOWNLINE POND	466	40	16	15	Grass
132859255	44.240061	-74.657956	BOOTTREE POND	463	24	6	15	NA
132859648	44.212283	-74.709069	BURNTBRIDGE POND	490	345	22	2	Grass
133098522	44.223117	-75.204369	PORTAFERRY LAKE	262	244	32	24	Oswegatchie
133098794	44.160342	-75.204644	LONG LAKE	331	134	9	6	Oswegatchie
133098835	44.146731	-75.155753	DRY TIMBER LAKE	424	520	9	8	Oswegatchie
133099091	44.080064	-75.203528	LITTLE SILVER DAWN LAKE	378	106	3	2	NA
133099100	44.065619	-75.128803	UNNAMED POND	445	1515	2	1	NA
133099412	43.961453	-75.044908	LOON HOLLOW POND	607	60	6	12	NA
133099268	43.995342	-75.049908	BRINDLE POND	539	16	1	2	Oswegatchie

133099411	43.958675	-75.009908	BEAR POND	623	238	32	29	Oswegatchie
133099321	43.972286	-74.955183	WILLYS LAKE (HORSESHOE)	630	156	24	14	NA
133099276	43.979508	-74.952961	UNNAMED POND	625	40	0	1	Oswegatchie
133099361	43.995344	-75.200189	ROCK POND	411	6822	8	10	NA
133098391	44.263117	-75.130203	PARTLOW POND	298	359	7	9	Oswegatchie
133098458	44.242006	-75.154369	TITUS POND	302	14	1	4	NA
133098403	44.253117	-75.109089	DODGE POND	307	101	6	7	Oswegatchie
133098764	44.151453	-75.050750	READWAY POND	424	1	1	2	Oswegatchie
133098898	44.110897	-75.071025	STREETER LAKE	453	339	28	5	Oswegatchie
133098933	44.101731	-75.054358	UNNAMED POND	454	1475	4	1	Oswegatchie
133098922	44.100897	-75.068247	CRYSTAL LAKE	453	22	6	8	Oswegatchie
133098502	44.189783	-74.925192	UNNAMED POND	456	173	4	2	NA
167248139	44.214228	-74.986306	UNNAMED(NEWTON FALLS)RES	433	43686	78	10	NA
167248139	44.214228	-74.986306	UNNAMED(NEWTON FALLS)RES	433	43686	78	10	NA
133098575	44.195617	-75.001583	BEAVER POND	454	106	11	5	Oswegatchie
133098510	44.159506	-74.721847	LITTLE DOG POND	556	58	2	1	Oswegatchie
133098759	44.112839	-74.797961	FISHPOLE POND	524	482	6	6	Oswegatchie
133098754	44.122283	-74.849631	SIMMONS POND	521	64	7	19	Oswegatchie
133098761	44.128394	-74.924911	UNNAMED POND (MILL POND)	456	432	3	1	Oswegatchie
133099041	44.052564	-74.949908	BIG SHALLOW POND	510	177	3	1	Oswegatchie
133099058	44.048675	-74.952686	LITTLE SHALLOW POND	512	141	3	2	Oswegatchie
133098913	44.066450	-74.840461	BIG DEER POND	533	160	23	2	Oswegatchie
133099147	44.026175	-74.904906	OVEN LAKE	611	590	21	12	NA
133099147	44.026175	-74.904906	OVEN LAKE	611	590	21	12	NA
133099147	44.017286	-74.904906	GRASSY POND	611	411	12	8	NA
133099147	44.017286	-74.904906	GRASSY POND	611	411	12	8	NA
133099140	44.008117	-74.859350	JENKINS POND	549	12	1	6	Oswegatchie

131843092	43.918678	-75.223519	SOFT MAPLE RESERVOIR	392	61268	128	18	NA
131843830	43.882567	-75.161294	BEAVER LAKE	435	50350	95	9	NA
131844118	43.858956	-75.170739	FRANCIS LAKE	440	533	55	7	NA

131843550	43.871733	-75.093239	UNNAMED POND	500	66	1	2	Black
131843906	43.853678	-75.098239	UNNAMED POND	512	17	1	2	Black
131843874	43.854233	-75.093794	UNNAMED POND	500	52	2	2	Black
131843281	43.886456	-75.108517	MOSHIER RESERVOIR	500	47141	114	23	Black
131841894	43.932011	-75.053797	SUNSHINE POND	589	215	27	15	NA
131841662	43.947286	-74.995186	UNNAMED POND	625	47	9	6	Black
131841569	43.953119	-74.983239	DISMAL POND	621	204	22	5	Black
131841526	43.944508	-74.888236	UNNAMED POND	515	147	9	2	NA
131842175	43.893953	-74.817678	TERROR LAKE	618	418	25	4	NA
131843078	43.870380	-74.952250	WOODS LAKE	607	204	25	10	NA
131843653	43.834233	-74.917122	SNAKE POND	588	1452	7	7	Black
131843383	43.841175	-74.892956	TWITCHELL LAKE	625	732	58	10	Black
131843116	43.854231	-74.870733	LILYPAD POND LOWER	628	88	9	5	Black
131844565	43.839792	-75.280183	CRYSTAL LAKE	378	207	31	14	Black
131845121	43.772292	-75.266847	MAHAN POND	387	12	1	4	NA
131844966	43.780347	-75.222958	NORTH POND	407	184	2	2	Black
131844924	43.793958	-75.291017	PAYNE LAKE	375	42	7	7	Black
131844590	43.832292	-75.262406	GOURD POND	357	90	1	1	Black
131844627	43.815344	-75.181847	MIKES POND	472	59	1	5	Black
131845681	43.720903	-75.286289	PITCHER POND	364	19	2	8	Black
131845110	43.733678	-75.017678	UNNAMED POND	559	508	4	1	Black
131845875	43.684792	-75.275456	BRANTINGHAM LAKE	376	1232	132	23	Black
131846204	43.639792	-75.262397	GARRIT LAKE	376	156	2	5	Black
131845717	43.683958	-75.099619	MIDDLE SETTLEMENT LAKE	526	98	16	11	NA
131845625	43.693403	-75.084342	CEDAR POND	518	702	3	6	Black
131845587	43.690347	-75.064619	GRASS POND	546	237	5	5	NA
131845583	43.697847	-75.101842	MIDDLE BRANCH LAKE	494	363	17	5	Black
131846283	43.624792	-75.246286	UNNAMED POND	376	217	9	2	Black
131845488	43.694789	-75.007953	WINDFALL POND	522	34288	16	5	Black
131844983	43.737011	-74.972397	ROUND POND	528	12	4	7	NA
131844538	43.788956	-74.949622	BIG DIAMOND POND	613	84	3	8	NA

131844719	43.756456	-74.916008	LAKE RONDAXE	524	14283	91	10	NA
131844809	43.749233	-74.901286	FLY POND	565	208	2	3	Black
131844377	43.781178	-74.852675	MOSS LAKE	536	1315	46	15	Black
131844130	43.789231	-74.812394	CASCADE LAKE	553	475	40	6	Black
131844532	43.774789	-74.846561	BUBB LAKE	553	186	18	4	NA
131844150	43.793400	-74.870731	DART LAKE	536	10757	52	18	NA
131844009	43.805064	-74.831008	WINDFALL POND	601	44	2	6	Black
131843856	43.828064	-74.854500	BIG MOOSE LAKE	556	9585	513	21	NA
131844064	43.811456	-74.882953	WEST POND	585	108	10	5	NA

131843739	43.825622	-74.886011	SQUASH POND	648	41	3	6	NA
131842612	43.855342	-74.725728	OTTER POND	649	118	5	3	Black
131842438	43.871731	-74.777397	LOWER SISTER LAKE	588	1598	34	3	NA
131842438	43.878953	-74.768508	UPPER SISTER LAKE	588	1409	32	4	NA
131843304	43.830619	-74.807119	CONSTABLE POND	582	945	21	4	NA
131844592	43.765067	-74.842117	SURPRISE POND	526	15	2	2	Black
131844242	43.763675	-74.729336	BUG LAKE	614	132	32	24	Black
131843989	43.770064	-74.712947	EIGHTH LAKE FULTON CHAIN	546	823	123	25	Black
131845967	43.641736	-75.021281	BLOODSUCKER POND	582	204	3	6	Black
131845700	43.671456	-74.995450	NICKS LAKE	519	1053	84	5	Black
131845700	43.673122	-74.986283	UNNAMED POND	519	441	2	2	Black
131846085	43.620903	-75.029892	UNNAMED POND	493	194	1	2	Black
131844984	43.713400	-74.812669	LIMEKILN LAKE	576	1393	187	22	NA
131845383	43.676733	-74.814056	UNNAMED POND	643	33	2	2	NA
131845343	43.673956	-74.819056	UNNAMED (KETTLE) POND	646	21	3	13	NA
131845523	43.651178	-74.751833	BEAVER LAKE	559	916	55	5	NA
131845641	43.636178	-74.738497	SQUAW LAKE	645	177	36	7	NA
131845751	43.628400	-74.747386	UNNAMED POND	637	36	1	4	Black
131845836	43.623400	-74.761831	INDIAN LAKE	654	1061	33	11	NA
131846180	43.566733	-74.792383	UNNAMED POND	722	376	3	1	Black
131846215	43.562567	-74.812939	TWIN LAKE LOWER	739	75	1	2	NA

131846215	43.562567	-74.812383	TWIN LAKE UPPER	740	66	2	5	NA
131846038	43.582289	-74.750439	CARTER MUDHOLE	674	67	1	3	Black
131845673	43.618122	-74.641828	TWIN LAKES WEST	810	302	1	1	NA
131845673	43.617567	-74.641272	TWIN LAKE WEST	810	287	8	7	NA
131845673	43.620344	-74.635161	TWIN LAKE EAST	811	139	8	3	NA
131845828	43.600067	-74.662106	BROOK TROUT LAKE	722	177	29	23	NA
131845255	43.666178	-74.703219	ICEHOUSE POND	566	27	3	13	NA
131845216	43.669511	-74.699608	HELLDIVER POND	566	85	7	3	Black
131844990	43.688122	-74.665719	LOST POND	584	2426	9	2	NA
131845210	43.646733	-74.557936	LOST POND	584	138	4	1	NA
131846683	43.536736	-75.170444	DEER POND	430	25	4	4	Black
131846452	43.588403	-75.132947	LOST POND	473	31	1	6	Black
131846419	43.587014	-75.126003	OTTER LAKE	462	598	56	3	Black
131846566	43.551458	-75.067667	GULL LAKE	540	212	50	3	NA
131846593	43.512090	-74.890750	SOUTH LAKE	615	1644	197	18	NA
131846580	43.522847	-74.947661	NORTH LAKE	555	8126	177	18	NA
131846146	43.573678	-74.821275	MONUMENT LAKE	759	33	6	2	Black
50520955	43.233961	-73.848456	BULLHEAD POND	186	28	2	4	Hudson-Hoosic
47725669	43.270072	-73.949847	UNNAMED POND	314	54	1	1	Sacandaga
47725761	43.264239	-73.919014	JENNY LAKE	377	805	36	8	Sacandaga
47726211	43.235628	-73.989294	MINER MILL VLY	477	558	3	2	Sacandaga
47726908	43.188961	-73.947347	LITTLE LAKE	552	21	1	1	Sacandaga

47723995	43.332847	-74.210411	MIDDLE LAKE	456	66	12	7	Sacandaga
47723267	43.355347	-74.097353	TENANT LAKE	507	686	28	6	Sacandaga
47722741	43.399792	-74.156800	WILCOX LAKE	440	281	54	15	Sacandaga
47724701	43.298403	-74.078742	UNNAMED POND	399	280	8	2	Sacandaga
47723283	43.371458	-74.245969	WILLIS LAKE	397	139	15	3	NA
47722841	43.390625	-74.519036	SPY LAKE	505	904	151	9	Sacandaga
47721675	43.477014	-74.553486	DEER POND	710	59	1	1	Sacandaga
47721563	43.479792	-74.504875	FALL LAKE	512	4241	10	4	Sacandaga

47722273	43.432292	-74.509872	SILVER POND	512	22	1	5	Sacandaga
47724773	43.302292	-74.585425	JOCKEYBUSH LAKE	599	149	17	11	NA
47725511	43.273681	-74.544867	TROUT LAKE	503	465	8	4	Sacandaga
47725595	43.274236	-74.482642	ROSS LAKE	549	28	1	3	Sacandaga
47720751	43.538678	-74.117356	EAGLE POND	503	156	2	9	Sacandaga
47719461	43.671453	-74.169308	TWIN POND (LOWER)	638	222	6	1	Sacandaga
47719523	43.659786	-74.085414	SECOND POND	683	476	18	4	Sacandaga
47719269	43.689231	-74.074581	THE VLY POND	617	408	9	2	Sacandaga
47721246	43.507289	-74.419592	SOUND LAKE	527	70	8	3	Sacandaga
89363837	43.826453	-73.910689	OLIVER POND	455	140	17	4	Upper Hudson
89363491	43.866175	-73.972361	HEWITT POND	517	751	67	17	Upper Hudson
89364221	43.785619	-73.818464	MARSH POND	332	115	4	5	NA
89363585	43.855061	-73.817078	BIG POND	390	639	25	6	Upper Hudson
89363847	43.825339	-73.710406	HARRISON MARSH POND	314	276	2	3	NA
89363979	43.812839	-73.704294	SPECTACLE POND (UPPER)	354	164	7	6	Upper Hudson
89364311	43.775342	-73.659569	CRAB POND	320	130	5	10	Upper Hudson
89363721	43.843672	-73.677906	GOOSE POND	359	116	27	31	Upper Hudson
89363549	43.855617	-73.640403	UNNAMED POND	331	764	9	2	NA
89362641	43.972833	-73.563736	MUD POND	354	35	3	2	NA
89362411	43.993947	-73.827358	CLEAR POND	583	601	70	24	NA
167103332	44.065056	-73.811247	DIX POND	680	481	2	1	Upper Hudson
89362515	43.986167	-73.706797	GERO POND	280	5756	7	3	Upper Hudson
89362319	44.016722	-73.638186	HOWARD POND	374	58	5	9	Upper Hudson
89362289	44.019778	-73.632353	BROTHERS POND (LOWER)	381	71	3	6	Upper Hudson
167100585	43.970611	-73.611517	BLACK BROOK POND (LOWER)	338	316	1	2	NA
89362321	44.018111	-73.705131	JUG POND	600	45	3	1	Upper Hudson
89365911	43.491178	-73.912347	BEAR POND	390	215	16	4	Upper Hudson
89364705	43.722286	-73.936242	BIRD POND	334	951	8	9	NA
89364879	43.717842	-74.117361	THIRTEENTH LAKE	510	2849	133	15	Upper Hudson
89363765	43.840897	-74.019028	RANKIN POND	579	142	6	5	Upper Hudson
89363743	43.844231	-74.024861	LITTLE RANKIN POND	611	265	1	1	Upper Hudson

89363785	43.838675	-73.985136	STONY POND	633	298	24	7	NA
89362763	43.957839	-73.932361	WOLF POND	557	1558	24	5	Upper Hudson
89363569	43.859231	-74.092922	NATE POND	614	116	8	6	NA
89364195	43.781175	-74.255428	LAKE ADIRONDACK	506	378	80	6	NA

89365099	43.677008	-74.246256	ROUND POND	566	519	57	3	NA
89364351	43.771453	-74.212369	LAKE SNOW	515	2814	30	3	Upper Hudson
{CE57E4DF-187C-4AFB-95231D0345861DE0}	43.649511	-74.389872	LEWEY LAKE	503	6900	149	18	NA
89365087	43.683675	-74.296258	CROTCHED POND	555	534	26	9	NA
89365939	43.495069	-74.565986	JESSUP LAKE	735	83	4	6	NA
89365529	43.592289	-74.427372	MASON LAKE	547	195	37	6	Upper Hudson
89363601	43.855342	-74.315708	UNNAMED POND	534	35	4	3	Upper Hudson
89363677	43.853397	-74.329600	BARKER POND	562	34	3	4	Upper Hudson
89363899	43.829508	-74.436269	CASCADE POND	650	638	14	7	Upper Hudson
89363813	43.837564	-74.480161	LONG POND	570	26	2	4	NA
89363781	43.840342	-74.471272	GRASSY POND	564	22	3	1	Upper Hudson
89365069	43.681733	-74.488767	CARRY POND	649	20	3	5	Upper Hudson
120023791	43.629233	-74.536269	CEDAR LAKE	744	976	149	12	NA
120023791	43.627289	-74.551547	BEAVER POND	744	325	35	1	NA
89363049	43.930619	-74.214319	BATES POND	515	46	2	2	Upper Hudson
89362727	43.970064	-74.129594	HARRIS LAKE	473	9133	116	12	Upper Hudson
89362525	43.987920	-74.241820	ARBUTUS LAKE	513	365	48	8	Upper Hudson
89362643	43.977564	-74.270156	COUNTY LINE FLOW	505	6671	25	2	NA
89361879	44.111444	-73.988203	LIVINGSTON POND	846	27	1	7	Upper Hudson
89361867	44.119219	-73.982647	LAKE COLDEN	842	645	15	7	Upper Hudson
89361863	44.130886	-73.969867	AVALANCHE LAKE	873	115	4	7	NA
132433284	44.547561	-74.792136	ROCK POND	405	125	7	8	Raquette
132433360	44.529786	-74.843525	FIVE FALLS RESERVOIR	328	241396	59	12	NA
132433312	44.538953	-74.768244	LONG POND	405	110	9	6	Raquette
132433418	44.482842	-74.739911	JOE INDIAN POND	394	5312	138	3	NA
132433489	44.435064	-74.626011	KETTLE POND	460	21	3	11	NA
132433630	44.368672	-74.554339	ROCK POND	467	369	17	2	NA
132433673	44.345894	-74.506558	UNNAMED POND	478	7	1	8	NA
132433730	44.317006	-74.515447	SUNSET POND	466	352	3	2	Raquette
132433819	44.310894	-74.721294	UNNAMED POND	444	11	0	3	Raquette
132433779	44.278114	-74.418778	LEAD POND	483	289	34	4	NA
132433789	44.278392	-74.424056	UNNAMED POND	488	13	2	2	NA
132433786	44.292283	-74.488503	NORTH SPECTACLE POND	484	44	3	4	Raquette

132435716	44.080339	-74.652953	BEAR POND	568	543	61	8	Raquette
132435382	44.083950	-74.526558	UNNAMED POND	539	24	0	6	NA
132435146	44.130617	-74.629064	HORSESHOE LAKE	526	1254	161	5	Raquette
132435590	44.088672	-74.657675	TROUT POND	542	239	63	25	Raquette
132435630	44.085339	-74.659064	HIGH POND	573	47	16	17	Raquette
132436462	44.092561	-74.738236	SECOND POND	531	7158	15	15	NA
132435369	44.120617	-74.717403	LAKE MARION	607	519	83	47	NA
132436462	44.065339	-74.803236	TOMAR POND	531	78	2	6	NA
132436462	44.085339	-74.799628	GRASS POND	531	449	49	11	NA

132434585	44.161728	-74.442944	LITTLE SIMON POND	545	737	58	32	NA
132433915	44.228392	-74.338497	PANTHER POND	524	45	5	6	Raquette
132434170	44.206169	-74.344053	ROLL BANK POND	472	30	2	4	Raquette
132434021	44.217836	-74.317942	UNNAMED (CALKINS) POND	475	20	1	3	NA
132434641	44.125617	-74.311828	MIDDLE COUNTY LINE POND	518	51	1	5	Raquette
132434592	44.128394	-74.311828	UPPER COUNTY LINE POND	518	29	1	3	Raquette
132434565	44.127561	-74.250714	SEWARD POND	625	119	2	2	Raquette
132434483	44.128947	-74.136819	ROCK POND	710	84	2	1	Raquette
132433964	44.181164	-74.074042	MOOSE POND	685	975	10	5	NA
132436516	43.970617	-74.404050	SHAW POND	533	839	10	2	Raquette
132436973	43.928672	-74.454328	SOUTH POND	538	5445	173	17	Raquette
132435874	44.029506	-74.451275	MOSQUITO POND	564	46	3	1	Raquette
132437323	43.861175	-74.556831	MIDDLE SARGENT POND	556	48	5	3	Raquette
150679585	43.838953	-74.627667	ELDON LAKE	537	208	48	4	Raquette
132437375	43.834786	-74.543219	UTOWANA LAKE	545	5829	122	7	Raquette
132437273	43.862008	-74.493772	PINE POND	564	207	2	2	Raquette
132437129	43.877008	-74.455439	CHUB POND	586	130	5	4	Raquette
132437679	43.765897	-74.628219	SAGAMORE LAKE	580	4946	68	23	NA
132437600	43.795064	-74.651000	RAQUETTE LAKE RESERVOIR	570	186	2	3	Raquette
132437583	43.804786	-74.700447	LOWER BROWNS TRACT POND	538	1236	65	10	Raquette
132437533	43.813119	-74.666281	FOX POND	537	40	1	10	Raquette
132437546	43.816731	-74.744061	SHALLOW LAKE	551	1539	108	9	Raquette
132437639	43.813675	-74.806561	QUEER LAKE	597	155	55	21	NA

132437564	43.820342	-74.776839	UNNAMED POND	639	33	4	2	Raquette
47727871	43.122572	-74.339303	WOODWORTH POND	509	175	14	19	Mohawk
53542311	43.131739	-74.490697	WEST CAROGA LAKE	443	1413	129	23	Mohawk
53541987	43.192847	-74.542644	NINE CORNER LAKE	570	205	45	15	Mohawk
53542099	43.173958	-74.510419	GREEN LAKE	472	636	18	16	Mohawk
53542015	43.188537	-74.498546	OTTER LAKE	503	361	15	4	NA
53541567	43.268681	-74.723761	MUD POND	613	34	2	5	Mohawk
53541203	43.300347	-74.633206	FERRIS LAKE	525	578	48	7	NA
53541195	43.312014	-74.611536	IRON LAKE	613	74	10	11	NA
53540805	43.368125	-75.048494	FINCH POND(LK MARGARITE)	419	106	2	2	Mohawk
53540971	43.342569	-74.965158	TOMKETTLE POND	419	51	4	4	Mohawk
53541023	43.334792	-74.959047	CURTIS LAKE	393	89	5	11	Mohawk
53541141	43.322014	-74.783208	UNNAMED POND	564	266	2	1	Mohawk
53540621	43.426458	-74.725711	WILMURT LAKE	752	273	39	11	Mohawk
53540671	43.414162	-74.632888	G LAKE	619	413	32	10	NA
53540537	43.453403	-74.578764	UNNAMED POND	753	61	3	10	NA
53540327	43.482847	-74.682656	PEA POND	736	17	2	8	Mohawk
53540525	43.457847	-74.680711	FARMERS VLY	698	71	3	1	Mohawk
53539965	43.576178	-74.575433	SAMPSON POND	731	155	25	10	Mohawk
53539963	43.580344	-74.605436	LAURENCE POND	707	100	2	1	Mohawk

135271226	44.459733	-74.259578	BARNUM POND	504	NA	38	3	NA
132437266	43.857621	-74.449544	BLUE MOUNTAIN LAKE	546	2972	697	31	NA
132437183	43.918026	-74.704405	BRANDRETH LAKE	573	2298	362	54	NA
50520473	43.328701	-73.757797	KEENAN RESERVOIR	365	NA	NA	NA	Hudson-Hoosic
89365509	43.596668	-73.795345	TRIPP LAKE	292	668	20	8	NA
132876387	44.646400	-74.059998	WOLF POND	460	NA	21	15	Salmon
53542311	43.124953	-74.480637	EAST CAROGA LAKE	442	1490	94	12	Mohawk
92083789	43.843056	-73.431944	LAKE GEORGE	66	60347	11537	60	NA
131844637	43.744534	-74.743195	SEVENTH LAKE	544	NA	385	26	Black
132876172	44.732592	-73.969758	UPPER CHATEAUGAY LAKE	399	20856	1038	22	Chateaugay-English
89364961	43.686667	-73.741111	BRANT LAKE	243	NA	616	18	Upper Hudson
92081293	44.747103	-73.824032	CHAZY LAKE	470	6896	747	21	Lake Champlain
135270812	44.587254	-74.285718	CLEAR LAKE (DUANE)	475	NA	34	18	St. Regis
89363335	43.889301	-74.232597	FIFTH LAKE ESSEX CHAIN	489	NA	NA	NA	Upper Hudson

129691021	44.333848	-74.403747	FLOODWOOD POND	480	NA	NA	NA	Saranac River
150679608	44.156502	-74.377998	FOLLENSBY POND	471	NA	393	31	NA
150679605	43.899994	-74.583313	FORKED LAKE	531	NA	362	23	Raquette
89366265	43.357700	-73.824402	FOURTH LAKE	192	NA	20	12	Upper Hudson
131844766	43.758514	-74.840676	FOURTH LAKE	520	NA	831	20	Black
89365829	43.518681	-74.022278	GARNET LAKE	448	2121	133	NA	Upper Hudson
47721841	43.464199	-74.315300	GILMAN LAKE	509	NA	19	18	Sacandaga
89364487	43.765767	-74.254214	LAKE ABANAKEE	487	49953	208	NA	Upper Hudson
89363797	43.844442	-74.414764	LAKE DURANT	540	6044	117	6	Upper Hudson
132436556	43.977576	-74.465563	LAKE EATON	523	NA	232	16	Raquette
131841110	44.002998	-74.763000	LAKE LILA	523	NA	NA	NA	Black
89366321	43.321389	-73.838333	LAKE LUZERNE	190	NA	42	17	Upper Hudson
89364839	43.704163	-73.670776	LILY POND	363	NA	NA	NA	Upper Hudson
92083087	44.165833	-73.566667	LINCOLN POND	314	NA	262	8	Lake Champlain
150679607	44.070080	-74.330226	LONG LAKE	496	76376	1687	14	Raquette
89365151	43.680422	-73.860392	LOON LAKE	264	3363	212	11	Upper Hudson
150563206	44.315412	-74.179529	LOWER SARANAC LAKE	468	32160	870	15	Saranac River
135270871	44.561601	-74.285843	MEACHAM LAKE	473	NA	NA	NA	St. Regis
89363811	43.832199	-73.887901	MULLER POND	447	NA	NA	NA	Upper Hudson
135271203	44.451070	-74.228505	OSGOOD POND	503	1871	209	3	St. Regis
53542005	43.197327	-74.512693	PINE LAKE	476	1129	67	NA	Mohawk
120023153	43.413146	-74.546060	PISECO LAKE	506	NA	1153	24	Sacandaga
131844847	43.737630	-74.871435	QUIVER	530	NA	NA	NA	Black
150679585	43.852318	-74.651214	RAQUETTE LAKE	537	33147	2183	29	Raquette
89363797	43.845299	-74.438500	ROCK POND	540	NA	NA	NA	Upper Hudson
47721625	43.484061	-74.423762	SACANDAGA LAKE	526	NA	651	19	Sacandaga
47721625	43.483890	-74.366110	SACANDAGA LAKE	526	NA	651	19	Sacandaga
131843435	43.901120	-75.002096	STILLWATER RESERVOIR	512	NA	2523	10	Black
133098699	44.179600	-75.119698	SUCKER LAKE	427	NA	NA	NA	Oswegatchie
115353585	44.484254	-73.863495	TAYLOR POND	424	2892	358	29	Ausable River
150679595	44.167843	-74.540089	TUPPER LAKE	471	178856	2132	26	Raquette
150563204	44.324340	-74.321925	UPPER SARANAC LAKE	482	19580	1912	26	Saranac River
89364607	43.739601	-74.467697	WAKELY POND	639	NA	NA	NA	Upper Hudson
131846298	43.591999	-74.984703	WOODHULL LAKE	571	NA	440	27	Black
89363413	43.877690	-74.162300	CHENEY POND	501	NA	7	4	NA
47725927	43.258760	-74.529390	CHUB LAKE	501	NA	6	6	NA
115353633	44.414360	-73.719590	EATON POND	295	NA	8	4	NA
89364599	43.734750	-73.877920	HIDDEN LAKE	387	NA	12	2	NA
133098740	44.112470	-74.764950	JOHN POND	544	NA	6	8	NA
129691002	44.294740	-74.158960	KIWASSA LAKE	466	NA	114	13	NA
131841714	43.911160	-74.774240	LITTLE LILLY POND	596	NA	7	3	NA

89364173	43.793560	-73.974440	MINERVA LAKE	370	NA	32	NA	NA
131842296	43.930980	-75.073250	MOSHER PONDS	568	NA	9	11	NA
132434537	44.187130	-74.600130	MT ARAB LAKE	506	NA	50	17	NA
129691039	44.282440	-74.135880	OSEETAH LAKE	466	NA	306	5	NA
47725041	43.294300	-74.429060	SILVER LAKE	632	NA	32	10	NA
47722049	43.442970	-74.060560	ST. JOHN LAKE	675	NA	14	11	NA
53539935	43.589210	-74.563440	WHITNEY LAKE	752	NA	45	12	NA
47725937	43.254530	-74.314380	WOODS LAKE	417	NA	29	12	NA
89363021	43.932760	-74.184330	ZACK POND	568	NA	37	10	NA
53542293	43.161610	-74.537850	CANADA LAKE	472	NA	361	38	NA
132436462	44.049311	-74.767257	BOG POND	531	NA	NA	NA	NA
133098825	44.167970	-74.839530	CRANBERRY LAKE	453	NA	2796	10	NA
89363405	43.880380	-73.586240	EAGLE LAKE	288	NA	171	12	NA
{CE57E4DF-187C-4AFB-9523-1D0345861DE0}	43.680820	-74.338750	INDIAN LAKE	503	NA	1893	16	NA
115353775	44.322330	-73.973780	LAKE PLACID	566	NA	797	50	NA
132436509	44.031990	-74.609790	LITTLE TUPPER LAKE	524	NA	926	11	NA
132436462	44.073120	-74.763700	LOWS LAKE	531	NA	1136	17	NA
150563205	44.261980	-74.266760	MIDDLE SARANAC LAKE	469	NA	573	17	NA
115353807	44.290500	-73.980160	MIRROR LAKE	566	NA	51	17	NA
89363377	43.886050	-73.692780	PARADOX LAKE	249	NA	378	19	NA
89364675	43.788270	-73.772980	SCHROON LAKE	246	NA	1723	44	NA